INSTITUTO SUPERIOR DE ENGENHARIA DO PORTO
MESTRADO EM ENGENHARIA MECÂNICA




Simulation approach in Matlab/Simulink for the main components of a positioning unit in a closed-loop hydraulic circuit

BENJAMIN WOLF
Setembro de 2016

POLITÉCNICO
DO PORTO

Instituto Superior de Engenharia do Porto

“Simulation approach in Matlab/Simulink for the main components of a positioning unit in a closed-loop hydraulic circuit”

Master’s Thesis

by

Benjamin Wolf

born: 18th August 1987

in

Halle/Saale

Student Number: 1150120

Supervisor: Prof. Doutor Antonio Ferreira da Silva

afs@isep.ipp.pt

Porto, December 2015 – September 2016

Statement of Authorship

I truthfully assure that I prepared this master's thesis on my own independently. I quoted all used tools completely and accurately and I marked everything what was taken unchanged or with modifications from the work of others.

Porto, 26th September 16 ……..…….

(Benjamin Wolf)

Danksagung

Ich möchte meinen Eltern danken, die mich während meiner gesamten studentischen Ausbildung stets unterstützt haben, sowohl in moralischer wie auch finanzieller Hinsicht. Ohne euch wäre das nicht möglich gewesen.
Ein besonderer Dank gilt meiner Freundin Susann. Du hast mich auch in schweren Zeiten immer aufgerichtet und warst immer ein positiver Einfluss, der mir neue Kraft gegeben hat.

Table of Content

Formula Symbols

Latin Symbols

A	[-]	amplitude
A_1, A_2	[m²]	piston's cab and rob end area
A_N,A_P,A_{s1},A_{s2},A_{2t},A_{1t}	[l/min · bar$^{-0.5}$]	pseudo-section function
C	[m³/Pa]	hydraulic capacity
c	[kg/s²]	spring constant
d	[kg/s]	damping constant
d_m	[m]	mean diameter
F	[N]	force
f	[s^{-1}]	frequency
F_{global}	[dB]	global error function
F_{local}	[dB]	local error function
G_g	$\left[\frac{m^3/s}{\sqrt{Pa}}\right]$	conductance value for laminar cylinder leakage
j	[-]	imaginary unit
K	[-]	gain factor
K_b	[bar]	bulk modulus
$\overline{K}_{q,0}$	[l/min]	relative flow gain at middle spool position
$\overline{K}_{p,0}$	[-]	relative pressure gain at middle spool position
k	[kg/s]	coefficient of viscous friction
k_{dr1}, k_{dr2}	$\left[\sqrt{\frac{m^3}{kg}}\right]$	throttling coefficients for cylinder in- and outflow
L_a	[m/s²]	saturation limit for acceleration
L_v	[m/s]	saturation limit for velocity
l	[m]	length
P	[bar]	pressure (proportional valve)
p	[Pa]	pressure (hydraulic cylinder, pressure relief valve)
Q	[m³/s]	leakage flowrate
q	[l/min]	partial volumetric flowrate
T_V	[m/s]	decay constant
t	[s]	time; step size
u	[N]	input variable

$\bar{u}$	[-1,1]	normalized input variable
V	[m³]	volume
v	[m/s]	velocity
x	[m]	displacement
$\bar{x}$	[-1,1]	normalized output variable

Greek Symbols

$\alpha, \beta, \gamma, k, x_t$	[-]	pseudo-section parameters
β_b	[Pa^{-1}]	press number (reciprocal bulk modulus)
Δ	[-]	difference
ε	[°]	deflection angle
ζ	[-]	damping factor
η	[Pa·s]	dynamic viscosity
θ	[°C]	temperature
λ	[various]	solution of the characteristic equation
μ	[-]	friction coefficient
ν	[m²/s]	kinematic viscosity
ρ	[kg/m³]	density
τ	[s]	integration variable in convolution integral
φ	[rad]	phase shift angle
ω	[rad/s]	angular frequency
ω_d	[rad/s]	angular frequency of the damped oscillation
ω_n	[rad/s]	natural frequency

Abbreviations and Indices

Indices

acc	acceleration
df	dynamic friction
dr	drain
ef	effective
ff	flow force
hom	homogeneous
in	incoming
L	load
li	leakage flowrate (hydraulic cylinder)
lk	leakage
lk,0	leakage at middle position (proportional valve)
max	maximum
neg	negative
out	outcome
P	pump
part	particulate
pos	positive
S	supply
s	sampling
sf	static friction
sp	spring
stor	stored
t	transition point
V1, V2	cap and rod end volume (hydraulic cylinder)

Abbreviations

eqn.	equation
FFT	Fast Fourier Transform
FIR	Finite Impulse Response
LTI	linear time invariant
LVDT	Linear Variable Differential Transformer

List of Figures

List of Tables

Abstract

The replacement of on-off solenoids with solenoids which can adjust the spool position of a directional valve proportionally to their input voltage was the groundwork for the development of proportional valve technology. Due to their robustness and well-priced properties, proportional valves are a good alternative to conventional servo-solenoid valves. Indeed, servo-solenoid valves are highly precise but that makes them highly expensive as well. Additionally, they place great demands on maintenance and industrial surroundings. Hence proportional valves are widely-used in automation engineering. A common application is the positioning of actuators. Thus, a closed-loop circuit is necessary. In doing so, the proportional valve's input voltage is the manipulated value which enables a certain area for the oil to pass through the valve. Therefore the flow rate to the actuator can be changed to control the actuator position with high precision. In this thesis the main components of a hydraulic positioning unit shall be modelled and simulated using the software Matlab/Simulink. That includes the actuator, the pressure relief valve, connecting pipes and of course the proportional directional control valve. With this model the positioning unit can be tested under different conditions to make predictions on how the system is going to react.

Due to the fact that it was not possible to collect measured data from the several components, measured data from the datasheets have been used to verify the models. For the actuator was no datasheet available. Consequently only a general model could be created. The dynamic behavior of the pressure relief valve could be obtained by using the dimensions given in the datasheet. However, the datasheet does not provide any curves related to dynamic behavior. Therefore only the static behavior was verifiable. The simulation of the proportional directional control valve was divided into a static and a dynamic part. Based on flow, pressure and leakage curves given by the manufacturer, pseudo-section functions have been created. These functions characterize the relationship between normalized spool position and flow rate. For simulating the dynamic behavior, a nonlinear Simulink model was created. The model was fitted to nonlinear frequency response data points by using a Nelder-Mead simplex optimization algorithm. Methodologies and models were subsequently tested with used data from the manufacturer. The good quality of the results seems to support the approach. Nevertheless, the Simulink model has to be adjusted more properly to the measurement curves.

All important components of a hydraulic positioning unit have been modelled. It is recommended to make further improvements to adjust the Simulink model more properly to the given curves in the datasheet. Subsequently, all components can be connected together to implement the closed-loop circuit.

1 Introduction

Hydraulic positioning units are widely-used in technical applications. In general, the positioning unit consists of an actuator, a pressure relief valve, a proportional directional control valve, connecting pipes and the pump. Due to the complex friction influence at the piston of a hydraulic cylinder, the positioning unit has to be implemented as a closed-loop circuit. In this thesis the named components of a hydraulic positioning unit shall be modelled and simulated with Matlab/Simulink. A deeper understanding about the dynamic behavior for each component is needed to be able to connect them and to develop an appropriate control law. Therefore it is possible to make predictions about the system's reaction under different conditions.
To describe the dynamic behavior of a technical system, it is important to determine its state variables and energy storages. For this reason, typical energy storages and state variables shall be determined with regard to hydraulic systems. Valves are used to control hydraulic systems. Depending on their spool position they uncover a certain area the oil can pass through. When the valve opens, a force acts on the spool. That can cause oscillations. Being able to analyze the dynamic characteristics, forces oscillations of mechanical systems shall be enlarged. Especially for proportional valves, manufacturers provide frequency response curves in their datasheet to give information about the dynamic behavior. These amplitude and phase ratio curves are given in frequency domain. Thus, the relationship of time and frequency domain shall be discussed.
For the simulation of a hydraulic circuit, oil is an important factor. That's why the most important properties of the oil shall be enlarged. Furthermore, it has to be discussed how they can be computed and used in the simulation.
Finally, static and dynamic relations have to be found. Based on these relations models shall be created and simulated in Matlab/Simulink. Subsequently, the results will be discussed.

In chapter 2, necessary fundamentals for are covered. It is discussed which energy storages and state variables are common in hydraulic systems, how they can be identified from a simplified in- and output model and why this is important for creating a dynamic simulation in hydraulics. Furthermore the functionality of proportional directional control valves is explained. Their oscillation characteristics can be described with a damped second order system which is also enlarged in this chapter. Due to the fact that valve manufacturers illustrate the dynamical behavior with frequency response plots, the relationship between time and frequency domain is discussed.

In chapter 3, the characteristics and functionality of the whole circuit is explained. It is described which components exist in the circuit and how the work together.

In chapter 4, all important parameters for developing an oil model are presented. Thereby it is discussed which parameters can be assumed constant.

In chapter 5, the pipe system is modelled. The pipes connect all other main components together which makes them important for the circuit. The march of pressure is shown when oil gets pumped into a pipe system with outlet.

In chapter 6, the hydraulic cylinder model is presented. It is shown how the cylinder can be simplified and how energy storages, state variables, balance as well as static equations can be determined from that. Furthermore, the simulation results are presented.

In chapter 7, the pressure relief valve is discussed. It is shown that the pressure relief valve is simulated dynamically based on the given dimensions from the datasheet. As an alternative, a model is presented which describes the static relationship between pressure and flow rate.

In chapter 8, the proportional directional control valve is simulated. It is explained why the simulation had to split up into a dynamic and a static part. To simulate the dynamical behavior, several functions were implemented in Matlab. Furthermore, it is shown how a Nelder-Mead algorithm based optimizing function was used to find the best parameters for a nonlinear Simulink model which characterizes the valve behavior. The static valve behavior when the spool is in fixed position is explained by the static model. Therefore it is shown how the needed parameters can be obtained from the datasheet.

In chapter 9 and 10, the summary and conclusion is presented as well as the recommendations for the future work.

2 Fundamentals

2.1 Dynamic Behavior of Hydraulic Systems

A simulation is an important tool in modern technology and it is particularly used in engineering. What makes them so meaningful is the ability to reproduce a real system and make virtual improvements to examine what the impact would be. The real system can be tested under several conditions to make sure that it works appropriately for a particular application. An immense advantage is that systems can be tested before being built without the strict need of a prototype, which saves time and money. Furthermore, it allows the analysis of variant model setups for the behavior of an individual parameter which clarifies its impact on the final result. Simulations also allow observing the behavior of a system over a very short as well as a very long period of time. Another important factor is that most real systems cannot be analyzed with adequate accuracy due to high complexity.
In this section, the five important steps of creating a simulation model shall be introduced in relation to hydraulic systems. These are:

1) Drawing a schematic with all in- and output signals and coefficients
2) Identifying the energy storages and their state variables
3) Setting up balance equations
4) Complementing missing relations with static equations
5) Drawing a block diagram

As the first point makes clear, the starting step is drawing a schematic with all important signals coming in or going out of the system. In the context of hydraulics, pressures and flow rates are the most common. The schematic provides a good view on the system and points out why the dynamic system is accelerating.
In a second step, the energy storages of the system have to be identified. These indicate where the dynamic system stores the energy contained in the system. A dynamic technical system has one or more energy storages depending on the complexity. Storages can be divided into concentrated and spatially distributed [1]. Dynamic systems with concentrated energy storages are represented by state variables which depend on time. Whereas spatially distributed storages are described by state variables which depends on time and position. Hence concentrated storages are used more often due to less complexity. The state variables are closely connected to the storages because they describe the amount of energy which is contained in the systems storage elements [2, p. 120]. The state parameters are also of high interest because they describe the dynamic behavior of the system and cannot change abruptly. The following table gives an overview of all relevant energy storages used in hydraulics.

Table 2-1 Fluidic Energy Storages and State Variables [2, p. 121]

Process	***Type of Energy***	***Typical Storage***	***State Variable***	***Energy***	***Function of State Variable***
Mechanical (translational)	Potential Energy	spring constant c (transl. spring)	dis-placement x	$\frac{1}{2}\, c\, x^2$	$x = \int \dot{x} dt$
	Kinetic Energy	mass m	velocity $\dot{x}$	$\frac{1}{2}\, m\, \dot{x}^2$	$\dot{x} = \frac{1}{m} \int F_{acc} dt$
Mechanical (rotational)	Potential Energy	spring constant c_T (rotat. spring)	angle φ	$\frac{1}{2}\, c_T\, \varphi^2$	$\varphi = \int \omega dt$
	Kinetic Energy	mass moment of inertia J	angular fre-quency ω	$\frac{1}{2}\, J\, \omega^2$	$\omega = \frac{1}{J} \int M_{acc} dt$
Fluidic	Pressure-Volume-Energy	capacity C_y of a fluid volume	pressure p	$\frac{1}{2} C_y\, p^2$	$p = \frac{1}{C_y} \int Q_{stor} dt$

The last column in Table 2-1 illustrates the connection between state variables and the energy storages. A state variable is always proportional to the integral of certain input parameters. These input parameters are the inputs for the integration blocks in the simulation and at the same time they are part of balance equations. For this reason it is important to determine the balance equations. Force and momentum balance equations on translational and rotational masses as well as volume flow rate balances in capacities play a major role in hydraulics. It is beneficial to bring them in a specific shape which is shown below.

$$F_{acc} = \sum F_{acting} \tag{2-1}$$

$$M_{acc} = \sum M_{acting} \tag{2-2}$$

F_{acc} is the sum of all forces acting on the mass. That contains i.e. forces generated by pressures, springs, friction or load. These forces can have positive or negative signs depending on their direction. The same considerations can be applied to momentum balance eqn. (2-2). Volumetric flow rate balance equations can be determined as following:

$$Q_{stor} = \sum Q_{in} - \sum Q_{out} \tag{2-3}$$

As eqn. (2-3) indicates, the stored volumetric flow rate is the difference between in- and outflowing oil from a certain capacity. From fluidic state variable computation (Table 2-1) can be concluded that the pressure change dp/dt is proportional to Q_{stor} when capacity is constant.
The fourth step is to complement missing relations with static equations to complete the model. Static equations express the behavior for stabilized conditions. Finally, the block dia-

gram can be drawn based on the shown equations. By the block diagram the simulation model can be created with Matlab/Simulink.

Table 2-2 Block Diagram Notation [2, p. 120]

Name	Function	Block Diagram
Integration	$\dot{x}_{out} = x_{in}; \dot{x}_{out} = \int x_{in} dt$	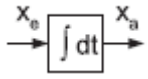
Linear statical transfer element	$\dot{x}_{out} = K_P \cdot x_{in}$	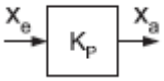
Static non-linearity	$\dot{x}_{out} = x_{in1} \cdot \sin(x_{in2})$	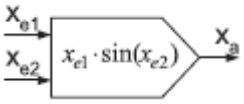
Balance equation	$\dot{x}_{out} = x_{in1} + x_{in2} - x_{in2}$	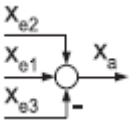

2.2 Functionality of Proportional Direction Control Valves

To master the general requirements of today's hydraulic applications, valves are indispensable. Valves satisfy different tasks in hydraulics. The main function of hydraulic valves is to regulate and control the magnitude of a hydraulic variable. This can be pressure or flow. Also the circuit topology can be controlled by changing the fluid's direction or by blocking it. That's why they are categorized in four different classes. These are pressure valves, flow valves, directional valves and check valves [3, p. 110].

Pressure valves limit or restrict a certain pressure level respectively a pressure difference. Flow-control valves spread or restrict the flow rate as required for the application. Directional valves are used to control the direction of the flow rate. Check valves block the flow rate in one or even both directions and repeal it under some specific circumstances. Each of these four classes is also divided in many more sub types, which won't be discussed further at this point. The last valve group is the electrical operated hydraulic valves. These are directional valves with the improvement of customized control electronics. The control electronics makes sure that the spool can be adjusted continuously and with very high accuracy by an input voltage or current. This characteristic is necessary to have when used in hydraulic control circuits as control element. The electrical operated valves can be divided into directional servo valves and proportional valves. A torque motor is used to control the directional servo valve's spool position by having various amplifying stages. Generally it has two or three of them to use very low input signals to control huge output signals. [4, p. 193]

This type of valve is used in highly-precise applications and creates high demands on the working environment. To get precision in the valve's functionality, the manufacturing has to be precise as well, what makes this type expensive. By contrast, proportional valves are effectively a further development of directional valves with simple switching solenoids. Proportional valves are widely spread in automation engineering because of their robustness and cheapness compared to servo valves. Due to the high precision it is possible when using servo vales to achieve an adjustment of all four control edges around the working point at the same time, whereas proportional valves adjust only one control edge. The others are either closed or opened to ensure that the restricting effect doesn't have an impact compared to the relevant control edge. That allows higher manufacturing tolerances when producing the control edges. The proportional valve technology is used in proportional direction, pressure and flow. However, when using proportional directional control valves it is necessary to have stroke-controlled magnets which are able to adjust the spool position continuously without any problems. Additionally, this permits to have the function of a flow control valve additionally which is important to achieve a correct actuator position in position control applications. In Figure 2:1 below the proportional valve used in the present hydraulic system is illustrated. The parts marked with "a" and "b" are the proportional magnets which are used to move the spool.

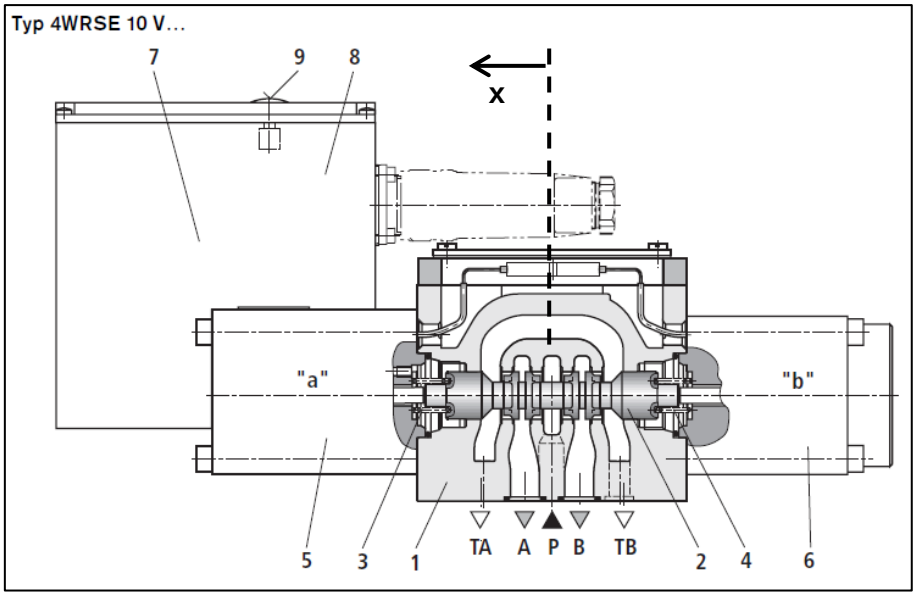

Figure 2:1 Proportional Directional Valve Bosch Rexroth 4WRSE [5]

When both magnets are conducting, their forces are equalized and the springs "3" and "4" center the spool. For positive displacement of x the proportional solenoid "b" has to be active whereas "a" has to be active for the other direction. Inductive displacement measurement detects either a positive or negative spool position and compensates widely the position error caused by friction and spring fatigue.

The applied technology of displacement measurement used in proportional directional valves is LVDT. The LVDT consists of a coil assembly and a core. The coil assembly is typically mounted to a stationary form, while the core is secured to the object whose position is being measured. The coil assembly consists of three coils of wire wound around the hollow form. A core of permeable material can slide freely through the center of the form. The inner coil is the primary, which is excited by an AC source. Magnetic flux produced by the primary is coupled to the two secondary coils, inducing an AC voltage in each coil. The main advantage of the LVDT transducer over other types of displacement transducer is its high degree of robustness. Considering there is no physical contact across the sensing element, there is no wear in the sensing element. Because the device relies on the coupling of magnetic flux, an LVDT can have infinite resolution. Therefore the smallest fraction of movement can be detected by suitable signal conditioning hardware, and the resolution of the transducer is solely determined by the resolution of the data acquisition system. [6]
In Figure 2:2 and Figure 2:3 the measurement system is illustrated. In the left figure the entire inner construction is shown. In Figure 2:3 the LVDT is emphasized with the circle.

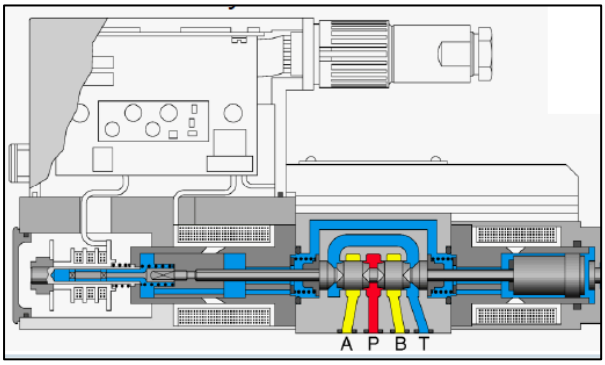

Figure 2:2 LVDT (1) [21]

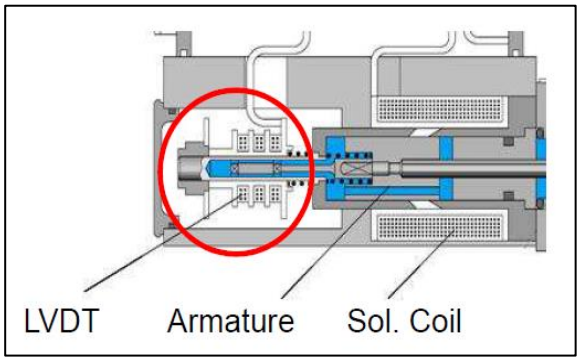

Figure 2:3 LVDT (2) [21]

2.3 Forced Oscillations of a Second Order System

The following section makes clear, what different kind of shapes the output oscillation of a second order system can have if it is getting excited periodically on the input with a certain force and frequency. The mathematical contexts of the waveform shall be described. Firstly, free damped oscillations getting pointed out. Understanding their behavior is highly important to take a closer look to forced oscillations.
The system which shall be analyzed is a spring-mass-damper oscillator (Figure 2:4). The special case of speed-proportional damping will be studied. Damping

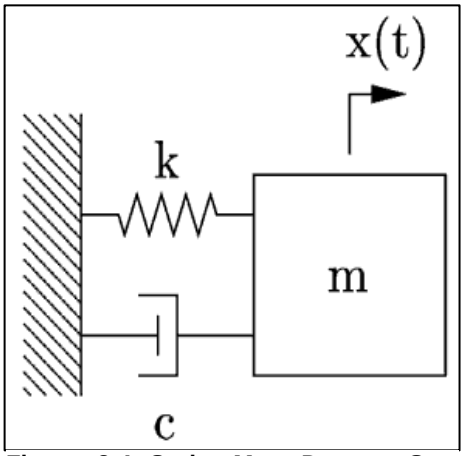

Figure 2:4 Spring-Mass-Damper System [20]

ensures that the amplitudes are decreasing over time. Depending on how big the damping is, this process is faster or slower. To be able to describe the oscillation movement depending on time, differential equations are necessary to build up. Therefore the oscillator is supposed to cut free which makes it possible to apply d'Alemberts law. There are three different forces acting on the mass. These are the damping, the spring resistance and the force of inertia. All of them acting reversed to the movement of the mass. The equations in this section are extracted from [7, pp. 620 - 628]. Making the balance equation from Figure 2:4 leads to the differential equation:

$$m\ddot{x} + d\dot{x} + cx = 0 \tag{2-4}$$

This is a linear homogeneous differential equation with constant factors. The mass is constant anyway, damping has a linear connection to velocity and the spring resistance force has a linear dependency from displacement.

For observations of oscillation analysis, Lehr's law got enforced. Depending on what literature is used, it can be referred to D or ζ. In this thesis the English declaration ζ shall be used. It is a non-dimensional number characterizing the damping of a system. It can be calculated as follows:

$$\zeta = \frac{d}{2 \cdot \sqrt{m\,c}} \tag{2-5}$$

If eqn. (2-5) is replaced in eqn. (2-4) and divided by mass the differential equation can be written in that form:

$$\ddot{x} + 2\zeta\omega_n\dot{x} + {\omega_n}^2 x = 0 \tag{2-6}$$

Eqn. (2-6) is also a differential equation with constant coefficients. The term ω_n is the natural frequency of the undamped system. The solution of eqn. (2-6) can be computed by using the exponential approach $x = C \cdot e^{\lambda t}$. This approach provides the characteristic equation whose results can either have just real values or complex ones.

$$\lambda^2 + 2\zeta\omega_n\lambda + {\omega_n}^2 = 0 \qquad \longrightarrow \lambda_{1,2} = \omega\,(-\zeta \pm \sqrt{\zeta - 1}) \tag{2-7}$$

Eqn. (2-7) shows that ζ dictates whether the solution is just real or complex. Having a damping factor bigger than 1 means there are just real results. If ζ is less than 1, the results are complex.

The solution of the differential equation can be written as follows:

$$x = C_1 e^{\lambda_1 t} + C_2 e^{\lambda_2 t} = e^{-\zeta\omega_0 t} \cdot \left(C_1 e^{\omega_n \sqrt{\zeta^2-1}\, t} + C_2 e^{\omega_n \sqrt{\zeta^2-1}\, t}\right) \tag{2-8}$$

The factor before the brackets provides an asymptotic decay to zero. Having a damping factor of $\zeta = 1$ results in a double solution with real values for λ. This case in particular is referred to a aperiodic limiting case. Under consideration of eqn. (2-8) follows:

$$x = C_1 e^{\lambda t} + C_2 t\, e^{\lambda t} = e^{-\zeta\omega_0 t} \cdot (C_1 + C_2\, t) \tag{2-9}$$

In this case the oscillation is dying out completely after half a period. Only in case $\zeta < 1$ there is going to be an oscillation at all. In boundaries of $0 < \zeta < 1$ exist a low damping which has two conjugate-complex solutions for λ. Therefore Euler's transformation is used:

$$e^{jz} = \cos(z) + j\,\sin(z) \tag{2-10}$$

That means:

$$\begin{aligned} x &= C_1 e^{\lambda_1 t} + C_2 e^{\lambda_2 t} \\ &= e^{-\zeta\omega_n t} \cdot \left(C_1 e^{\omega_n j \sqrt{1-\zeta^2}\, t} + C_2 e^{-\omega_n j \sqrt{1-\zeta^2}\, t}\right) \end{aligned} \tag{2-11}$$

with:

$$\omega_d = \pm\, \omega_n \sqrt{1 - \zeta^2} \tag{2-12}$$

follows:

$$x = e^{-\zeta\omega_n t} \cdot \left(C_1 e^{j\,\omega_d\, t} + C_2 e^{-j\,\omega_n\, t}\right) \tag{2-13}$$

$$= e^{-\zeta\omega_n t} \cdot [C_1(\cos(\omega_d t) + j\, sin(\omega_d t) + C_2(\cos(\omega_d t) - j\, sin(\omega_d t)] \tag{2-14}$$

$$= e^{-\zeta\omega_n t} \cdot [A_1(\cos(\omega_d t) + A_2\, sin(\omega_d t)] \tag{2-15}$$

$$= C \cdot e^{-\zeta\omega_n t} \cdot \cos(\omega_d t - \varphi) \tag{2-16}$$

The qualitative characteristic for a free damped oscillation is illustrated in Figure 2:5 below. Figure 2:5 acknowledges what also can already be read out from eqn. (2-16). The argument of the cosine function characterizes the oscillation's equation of motion depending on time. This is forced to die out exponentially for t ⟶ ∞ with the increase of time due to term $C \cdot e^{-\zeta\omega_n t}$. Thus, this term can be understood as envelopes of the function. These envelopes are illustrated in the figure below as x_o and x_u. These curves touch the function at those points where the cosine function has their extreme values. However these points are not the amplitudes of the damped function.

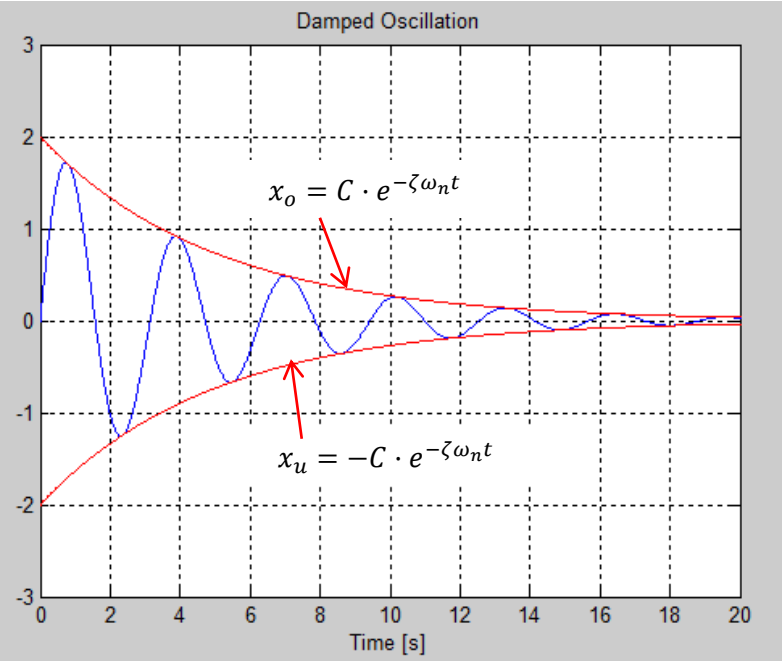

Figure 2:5 Free Damped Oscillation

Being able to oscillate at all, free damped oscillations need to have initial conditions such as a starting displacement or velocity in case of the spring-mass-damper system.

Contrary to that, there are forced oscillations with a harmonic force acting permanently on the system from the outside to make the oscillator move. It's unclear though what impact the dynamic behavior of specific stimulating amplitude and frequency has on the system when applying energy to it.

If a force acts harmonically with a certain intensity and frequency on a system it is referred to a forced oscillation. The differential equation from eqn. (2-4) has to be complemented with a stimulating term:

$$m\ddot{x} + d\dot{x} + cx = F_0 \cdot \cos(\omega_{ef} t) \tag{2-17}$$

There are different ways of stimulation the spring-mass-damper-system. There is a stimulation by the spring or damper, a dynamic unbalance excitation or the excitation of the mass. The mass stimulation is getting pointed out because the simplified model of the proportional valve's spool is similar to that case.

It is possible to convert eqn. (2-18) with the parameters natural angular frequency ω_0 and damping value ζ according to eqn. (2-6) to:

$$\ddot{x} + 2\zeta\omega_n\dot{x} + {\omega_n}^2 x = F_0 \cdot \frac{{\omega_n}^2}{c} \cdot \cos(\omega_{ef} t) \tag{2-18}$$

The solution of this second order inhomogeneous differential equation can be found with following approach:

$$x = x_{hom} + x_{part} \tag{2-19}$$

Therefore the solution of the homogeneous term can be copied from eqn. (2-16) due to the fact that there is no change in the systems setup. But the particulate solution which only refers to excitation term has to be found as well. The following approach can be applied:

$$x_{part} = A\cos(\omega_{ef}t - \varphi) \tag{2-20}$$

and replaced into eqn.(2-18):

$$\begin{aligned}\left(-{F_0\omega_n}^2/_c - A\,\omega_{ef}^2\cos(\varphi) + 2A\zeta\omega_n\omega_{ef}\sin(\varphi) + A\,\omega_n^2\cos(\varphi)\right)cos(\omega_{ef}t)\\ + \left(-A\,\omega_{ef}^2\sin(\varphi) + 2A\zeta\omega_n\omega_{ef}\cos(\varphi) + A\,\omega_n^2\sin(\varphi)\right)sin\left(\omega_{ef}t\right) = 0\end{aligned} \tag{2-21}$$

Eqn. (2-21) is just able to be zero for any value of t if both brackets on the left side get set zero. Therefore, both brackets getting set to zero. Doing so for the second bracket results in the following calculation for φ:

$$tan(\varphi) = {2\zeta\omega_n\omega_{ef}}/{\omega_n^2 - \omega_{ef}^2} = {2\zeta\left(\frac{\omega_{ef}}{\omega_n}\right)}\Big/{1 - \left(\frac{\omega_{ef}}{\omega_n}\right)^2} \tag{2-22}$$

Setting the first bracket to zero leads after some conversions to the last missing value of A:

$$A = {\frac{F_0}{c}}\Big/{\sqrt{\left[1 - \left(\frac{\omega_{ef}}{\omega_n}\right)^2\right] + 4\zeta^2\left(\frac{\omega_{ef}}{\omega_n}\right)^2}} \tag{2-23}$$

With eqn. (2-22) and eqn. (2-23) the solution of the particulate part is complete. Hence, the general solution of the oscillation's differential equation can be described. By looking at the homogeneous and inhomogeneous part of the solution it can be determined that both of them include a cosine function. That's why the overall solution can be understood as a interfering of two oscillations. According to eqn. (2-19), the final function is as follows:

$$x = C \cdot e^{-\zeta\omega_n t} \cdot \cos(\omega_d t - \varphi) + A\cos(\omega_{ef}t - \varphi) \tag{2-24}$$

To maintain a better overview eqn. (2-22) and (2-23) are not inserted in (2-24). But the following figures clarify the impact of the exciting frequency of the oscillation response.

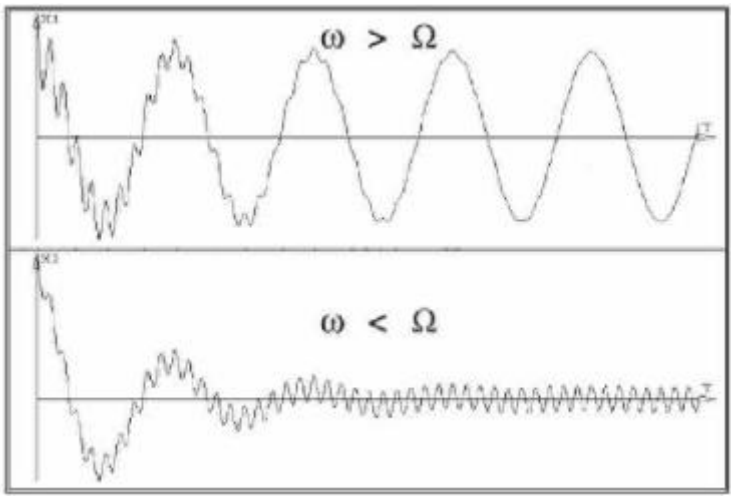

Figure 2:6 Superposition of natural and excitation frequency [7]

Figure 2:6 clarifies that depending on the excitation frequency the output oscillation has a different shape. Due to the negative exponential function, the natural frequency dies out. Afterwards the system oscillates just with the excitation frequency.

2.4 Relationship between Time and Frequency Domain

Manufactures normally announce the behavior of proportional valves by illustrating the Bode diagram in their data sheets. A Bode diagram helps to understand how the valve behaves in terms of phase and amplitude at a certain frequency. This section shall show why this is necessary to know in order to examine the valve's behavior in the time domain.

Basically, the Bode diagram consists of two different plots which is on the one hand amplitude ratio over frequency and on the other hand phase shift over frequency. In contrast to that, dynamic simulations are related to the time domain what brings out the necessity of converting one into the other to be able to extract the information needed. Therefore, the Fourier transform shall be introduced.

If an input is getting supplied to a system this signal can be transformed to frequency domain using the Fourier transform. Hence eqn. (2-25) shows the forward Fourier transform whereas (2-26) shows the inverse.

$$s(t) \circ\!\!-\!\!\bullet\, S(f) = \int_{-\infty}^{+\infty} s(t) \cdot e^{-j2\pi ft}\, dt \qquad \text{(2-25) [8]}$$

$$S(f) \circ\!\!-\!\!\bullet\, s(t) = \int_{-\infty}^{+\infty} s(t) \cdot e^{-j2\pi ft}\, dt \qquad \text{(2-26) [8]}$$

Doing that is possible due to the fact that every periodical function respectively signal can be reconstructed with a sum of sinusoids added up one after another. That allows looking at a signal in two different ways depending on the objective. Figure 2:7 below illustrates that.

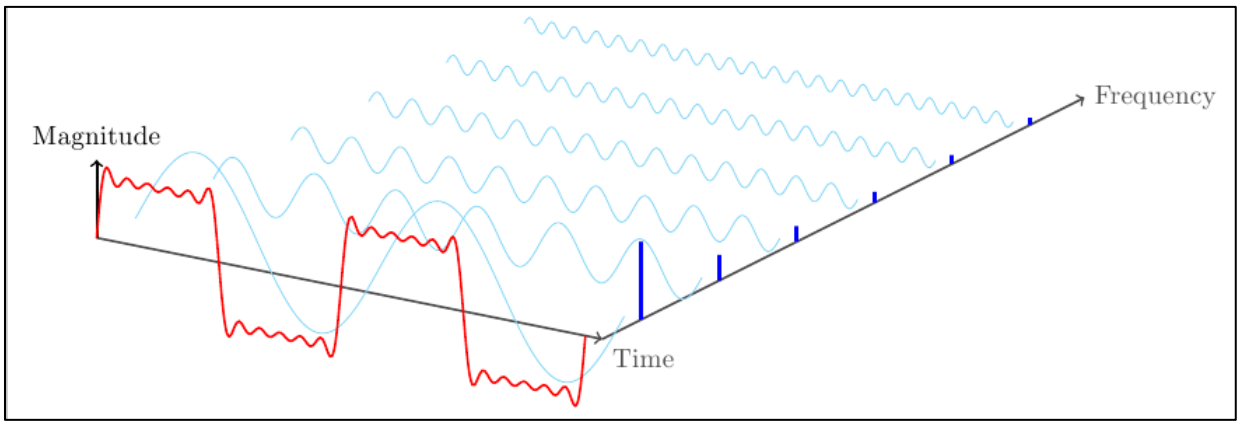

Figure 2:7 Spectrum of the Rectangle Function [9]

A magnitude plot over time and a frequency domain containing a red colored rectangle signal is shown. This rectangle signal has a specific fundamental frequency. Using a sine wave of a matching frequency and add it up with sine waves which have multiples of the fundamental frequency but less amplitude results in a rectangle signal. Exactly in the same way every signal can be produced. That is what makes the Fourier transform so essential for signal processing. A sine wave which gets supplied to a linear system always comes out as a sine wave with the same frequency. It doesn't change shape. The output signal can have a different phase or amplitude due to the systems parameters but there is always a sine wave with the same frequency coming out. Hence a signal divided into a set of different sine waves should allow processing it through the system to get the desired output signal.

Thus, it is possible looking at Figure 2:7 from a different perspective. If just the rectangle signal is known, it is necessary to identify what kind of different sine waves are contained in that signal to be able to transfer it to a system. The Fourier transform does exactly that. Thereby it is already considered that the input signal can also have a phase shift. This results in a complex number of a real cosine term and a complex sine term. Euler's formula converts that to:

$$e^{jt} = \cos(t) + j\,sin(t) \qquad \text{(2-27) [10]}$$

Using this form makes it easier to compute the complex number. This is already included in eqn. (2-25) and (2-26) as it is shown above.

Figure 2:8 below shows the relationship between phase shift and the assumption of a complex number.

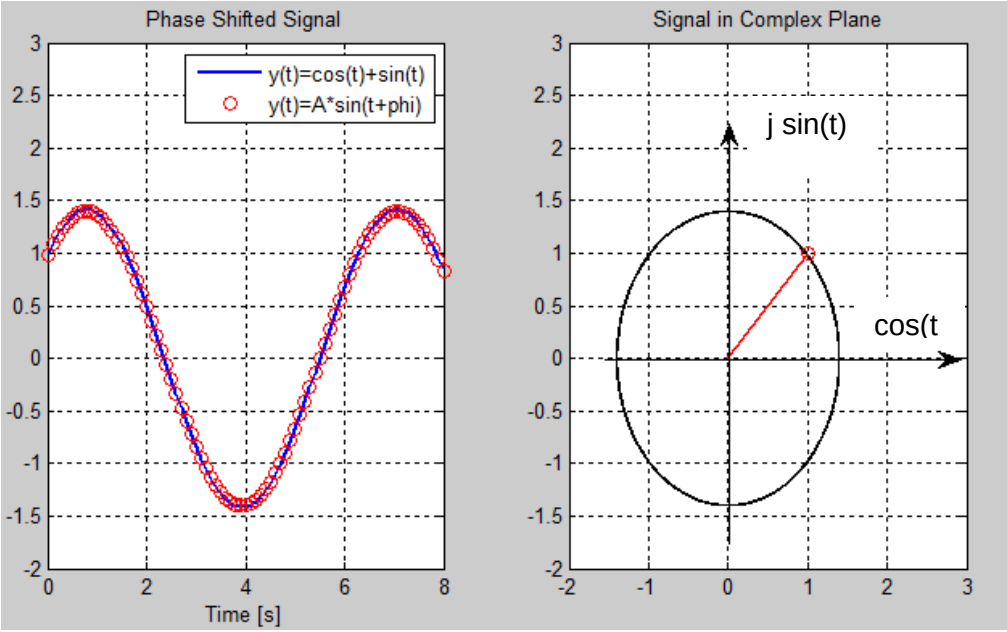

Figure 2:8 Phase Shift in Complex Plane

The left subplot shows one signal computed in two different ways. The blue line characterizes a cosine and sine wave added up together. This is equal to applying a phase shift of $\varphi = {}^{\pi}/_{4}$ to a sine wave signal. The red dotted curve illustrates that. Due to the adding up, the signal's amplitude increases which is compensated by multiplying a factor A to the red dotted curve. The right side subplot shows that relationship in the complex plane. This is the reason why it reasonable to think of a phase shift as a superposition of a cosine and sine wave.

Thereby, eqn. (2-27) can be used to transform the real and imaginary part into the Euler function. It is much easier to integrate, which is the reason why it is getting used in the Fourier transform.

If a complex signal

$$s(t) = e^{j2\pi ft} \qquad \text{(2-28) [10]}$$

is getting supplied to a LTI system, as shown below in Figure 2:9, the output can be calculated by the convolution of $s(t)$ with the system's unit impulse response $h(t)$. Referring to [1] the unit impulse response is the system's reaction of a Dirac impulse and describes the systems behavior completely. Thus the output signal $g(t)$ can be calculated for any input signal.

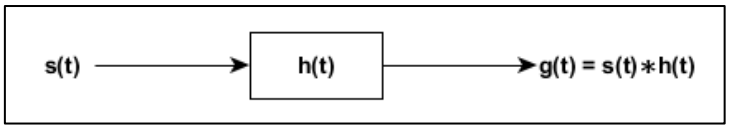

Figure 2:9 Convolution in time domain of LTI System [10]

With the convolution integral follows:

$$g(t) = \int_{-\infty}^{+\infty} h(\tau)\, e^{j2\pi f(t-\tau)}\, d\tau \qquad \text{(2-29) [10]}$$

$$g(t) = e^{j2\pi f t} \int_{-\infty}^{+\infty} h(\tau)\, e^{-j2\pi f \tau}\, d\tau \qquad \text{(2-30) [10]}$$

Eqn. (2-30) points out that the solution is a multiplication of the input signal with the convolution integral. At this point it is necessary to mention that it is not necessarily needed to have the system's unit step response. The left multiplication in (2-30) symbolizes the dynamic behavior of the system. If there is another expression available, for example the transfer function, it works exactly the same way. The transfer function just has to be transformed to the time domain. Subsequently the convolution integral method can be applied. It is important to understand though that there has to be any kind of information available which describes the dynamic behavior.

The complex convolution integral is declared as complex frequency response $H(f)$ when transferred to the frequency domain.

$$h(t) = \int_{-\infty}^{+\infty} h(\tau)\, e^{-j2\pi f \tau}\, d\tau \;\circ\!\!-\!\!\bullet\; \underline{H}(f) \qquad \text{(2-31) [10]}$$

$$\begin{aligned} H(f) &= H(f) \cdot e^{j2\pi f t} = |H(f)| \cdot e^{j\,\varphi_H(f)} \cdot e^{j2\pi f t} \\ &= |H(f)| \cdot e^{j\,(2\pi f t + \varphi_H(f))} \end{aligned} \qquad \text{(2-32) [10]}$$

The term $|H(f)|$ is the absolute value of the complex frequency response and is referred to amplitude response. The term $\varphi_H(f)$ in contrast describes the phase response of the dynamic system. Both of them are usually plotted together as a Bode diagram in the frequency domain.

So, the Bode diagram gives information about the I/O behavior of a system in terms of amplitude ratio and phase shift.

The dynamics of the system are represented by their transfer function. The transfer function is the ratio between output and input in complex variable domain. But from eqn. (2-32) can be extracted that amplitude as well as phase response are real numbers just depending on

the frequency which gets supplied to the system. For further explanations, Figure 2:10 shall be introduced.

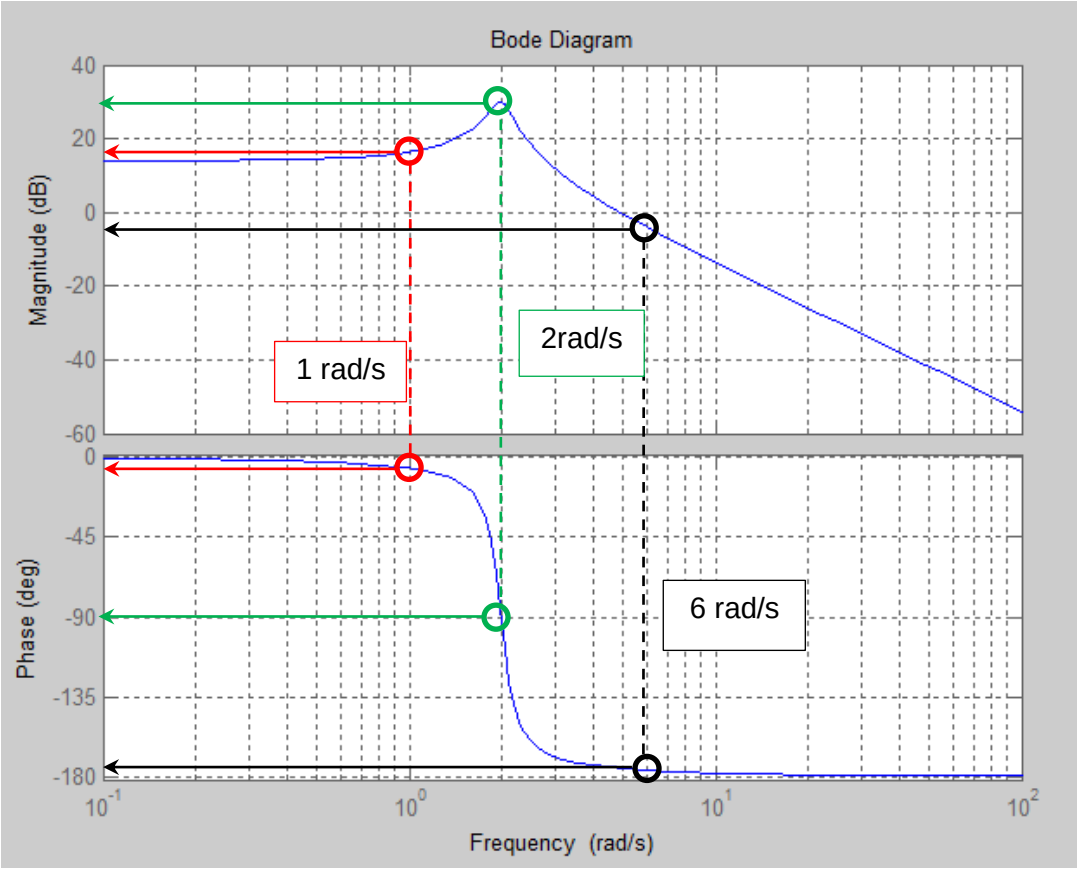

Figure 2:10 Bode Diagram of Linear Second Order System

In Figure 2:10 above a Bode diagram of a second order system shows the amplitude response in the upper and the phase response in the lower subplot over angular frequency. The systems natural undamped frequency is at 2 rad/s and due to its underdamped characteristics it has the highest amplitude ratio at exactly this frequency. Up to this frequency, the system runs in subcritical operation. The range above the natural undamped frequency is called post-critical operation. The magnitude plot is helpful in a way that it is possible to determine the output amplitudes by a given input amplitude and frequency. Therefore three different points are indicating three different states of operation.

The red circles refer to an excitation with one rad/s. At this angular frequency the system has an amplitude response of around 16.5 dB, which is equal to an amplification factor of around 6.4 regarding to the following formula:

$$A^{[dB]} = 20 \cdot log_{10}\left(\frac{A_{output}}{A_{input}}\right) \tag{2-33}$$

Thus it appears that if this system is getting excited by a force, acting periodically with 1 rad/s on the system, the input amplitude is getting increased by factor 6.4. Following the red dashed line, a phase response of -6° can be read out. These observations are valid for steady state oscillations. The following set of plots refer to the three given operation points from the Bode diagram. They show that the time domain behavior is exactly the same as it can be determined from the frequency domain.

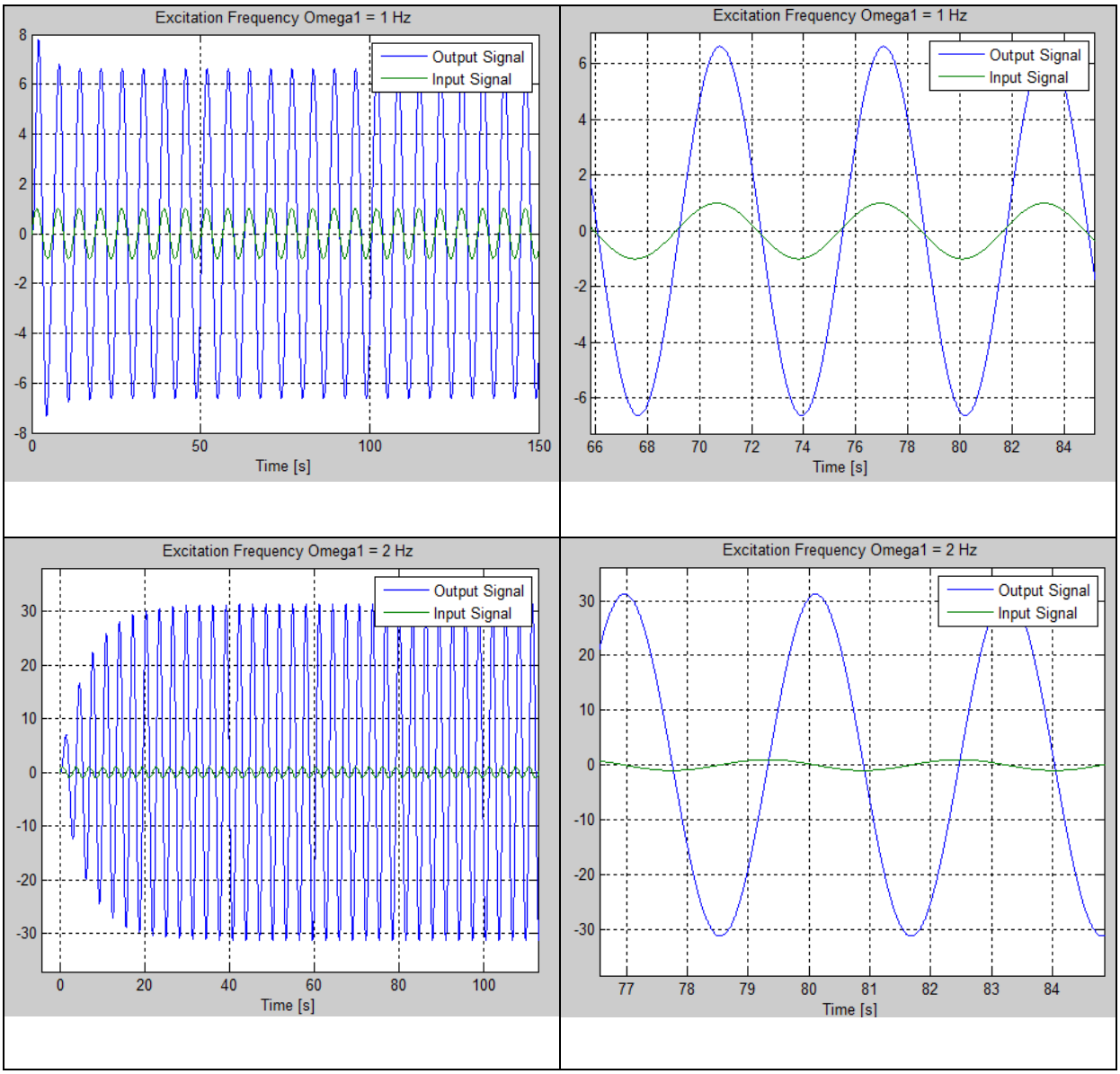

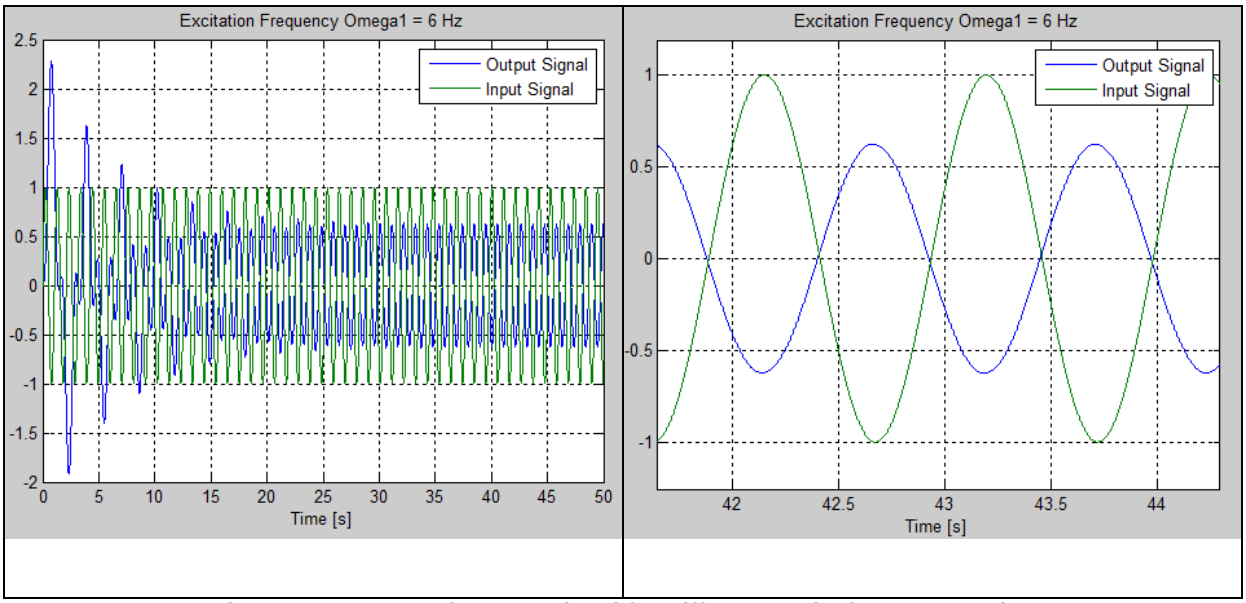

Figure 2:11 Input and Output Signal for Different Excitation Frequencies

The plots in the first row of Figure 2:11 confirm the results acquired from the Bode plot. The right plot makes clear that in steady state exactly the same amplitude can be read out as it was assumed earlier from the Bode plot. There is also the phase shift noticeable. However, it is hard to read out due to its small value. The left plot shows that both signals are fully simulated over time. According to Figure 2:6, the system's natural frequency superposes with the stimulating frequency in the beginning until the latter dies out.

The green circles in Figure 2:10 indicate natural angular frequency with the highest amplitude ratio. At this frequency the system amplifies the signal's amplitude the most. An amplitude response of 29.9 dB is equal to 31.25 output amplitude. This can be read out of the plots in the second row. Particularly well illustrated is the phase shift of -90°. The left hand side plot shows how the amplitudes rise while acting with critical frequency on the low damped system.

The black circles refer to 6 rad/s excitation frequency. Looking at the amplitude response clarifies that with a high frequency the output amplitude will be damped even more. At 6 rad/s there is already a damping behavior noticeable. A magnitude of -4.4 dB leads to an output amplitude of 0.6 which can be extracted from the Bode diagram as well. Through the phase response it is also possible to see that almost 180° of phase shift are reached. That can be confirmed by looking at the third row plots of Figure 2:11.

3 Modelling of the Circuit

The circuit which has to be modelled consists of a double acting cylinder (4), a pressure relief valve (2), a proportional valve (3), a fixed displacement pump (1) and pipe connections. It is a student training system which shows how a specific cylinder position can be controlled by using a proportional directional valve. Therefore a sensor measures the cylinder position and transfers that information to a controller. The controller compares the actual position of the cylinder with the desired position the cylinder is supposed to have. If they are not equal the controller gives an electric signal in the range from -10 V to +10 V to the proportional valve. The voltage input is the command signal which dictates the opening stroke of the proportional valve. In this case -10V refers to -100% open according to maximum spool stroke whereas +10V results in a +100% open valve. When the desired position is reached and the system is stabilized, the valve is adjusted in middle position and blocks the cylinder. That would cause high pressure and damage the system. To prevent the system from damage caused by an enormous pressure level, the pressure relief valve is used. It opens when pressure is getting beyond a certain level and allows oil to drain to the tank. An overview of the system is illustrated in Figure 3:1. The hydraulic test station is already mounted together which means the certain components are not separately accessible to measure and verify a simulation. Consequently, datasheet measurement shall be used to verify the simulation.

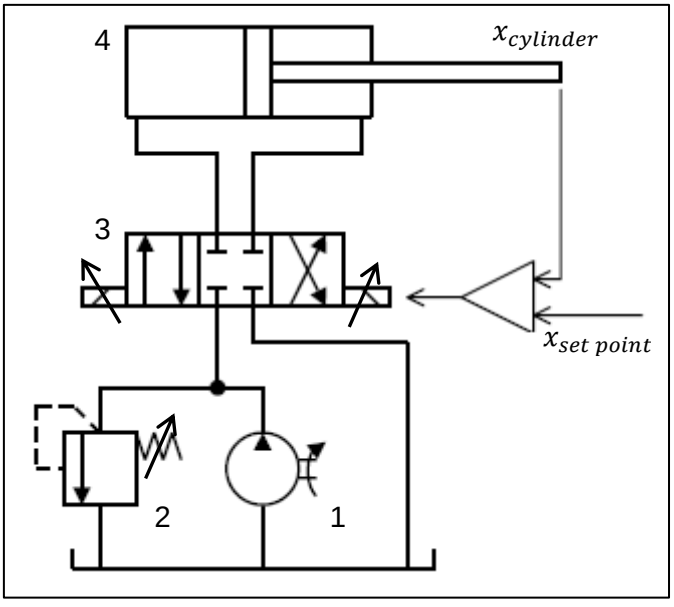

Figure 3:1 Hydraulic Circuit

4 Hydraulic Oil

To simulate a hydraulic circuit, the characteristics of the oil are necessary to determine, because of its impact on the dynamic behavior. It is not determinable which hydraulic oil is used in the circuit. For this reason the used hydraulic oil is assumed as HLP 46.

The most important properties of hydraulic oils are viscosity, density and compressibility. All these parameters depend on temperature and pressure. The consideration of temperature dependence is hard to implement and is therefore assumed to have a constant temperature. This assumption can be made because the system runs only in short time periods.

The density dependence on pressure and temperature is less than the viscosity dependence on pressure and temperature. Hence density can be assumed as a constant in practical calculations [4]. According to [11] the density was measured at 15°C and has 880 kg/m³. Other than density the viscosity changes under high pressure influence. To simplify the simulation, dynamic viscosity is assumed as a constant as well. According to [11] the kinematic viscosity is $\nu = 46\, mm^2/s$. From that follows:

$$\eta = \nu \cdot \rho \tag{4-1}$$

The compressibility of real fluids is responsible for the density-pressure-relationship. Incompressible fluids are just assumed as a model. A decreased volume due to pressure impact is characterized by following equation:

$$\Delta V = -\frac{V \cdot \Delta p}{K_b} \tag{4-2} [2]$$

The bulk modulus K for fluids is equivalent to the modulus of elasticity for solid structures.

The dependence of $\frac{\Delta V}{V} = f(p)$ is not linear which means K is not a constant. According to [12] K can be assumed to:

$$K_b(p(t)) = K_{b,max}\left(1 - e^{-n \cdot p(t)}\right) \tag{4-3}$$

Therefor K_{max} is set to $1.2 \cdot 10^9\ Pa$ [4, p. 19] whereas $n = 4.6052 \cdot 10^{-6}$. These values can be transferred to Matlab.

5 Pipes

Pipes are used to connect hydraulic components. Besides that, a pipe is an energy storage for pressure due to its capacity. When the system is in dynamic behavior, the balance equations of inflow and outflow are probably different. That means as long as the set point is not reached, the acceleration is not zero. During the dynamic process, the inflow and outflow won't be the same. When these parameters aren't equal, there will be more or less oil in a restricted capacity. That means pressure increases or decreases. According to Table 2-1 pressure is a state variable and important to characterize the dynamic behavior.
It follows:

$$\dot{p} = {}^{1}/_{C_{pipe}} \cdot [Q_{in} - Q_{out}] = {}^{1}/_{(V_{pipe} \cdot \beta)} \cdot [Q_{pump} - 0] \qquad (5\text{-}1)$$

In eqn. (5-1) pressure is location-independent. Especially in long pipes, pressure loss has to be considered. That is caused by friction between the oil flowing through a pipe and the roughness of the pipe surface. Furthermore there are position-dependent pressure losses caused by inertia forces of the accelerated oil. Approaches for that can be found in [13, p. 45]. This can be neglected because of short pipe dimensions. The system can be modelled based on (5-1).
With a volumetric flow rate of 20 l/min, a pipe diameter of 16mm and a length of 3m a pressure rate of change of $\dot{p} = 6666\ {}^{bar}/_{s}$ follows. The Simulink model is illustrated in 12.1. In the figure below, the simulation result is shown over a duration 0.1 s. It can be seen that the pressure increases linearly. The slope increases with bigger flow rate and lower capacity.

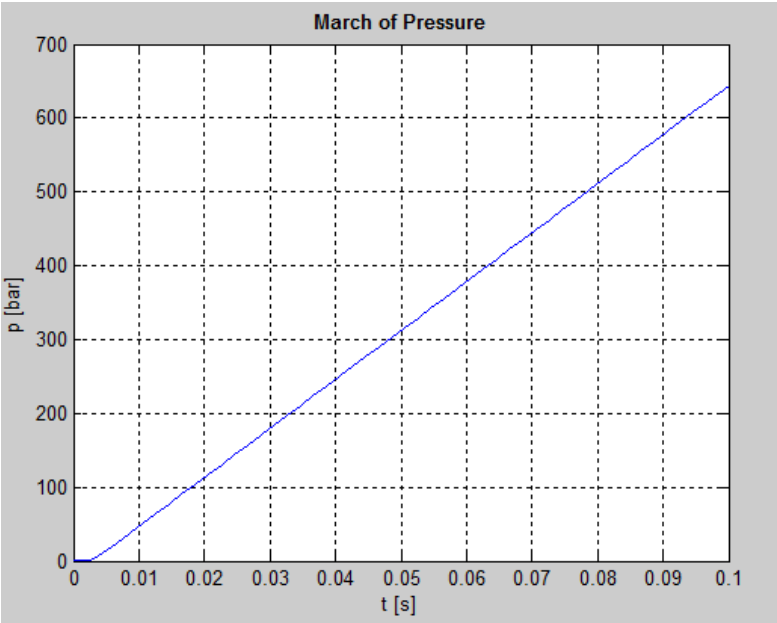

Figure 5:1 March of Pressure

6 Cylinder

In this section the theoretical considerations about the dynamic behavior of the cylinder shall be explained. Based on these considerations the model can be created and finally the results shall be discussed. In the circuit a differential cylinder with the dimension 200-100-500 is used. Thereby the piston diameter is 200mm, the rod diameter is 100mm and the stroke is 500mm.

6.1 Theoretical Equations

To determine the dynamic behavior the first step is to build a model of the system. Figure 6:1 illustrates the model of the cylinder. It is a differential cylinder with inflow and outflow port to the two cylinder chambers. For the setup shown is assumed that the piston extracts. The cylinder in the circuit is connected by pipes to the proportional directional valve. As it was discussed in the previous section, pipes act as energy storages where pressure can change over time. For the model of the cylinder, a constant pressure level in both pipes is assumed. But due to the in- and outflow ports, the pressure in both chambers can differ from the pressure in the pipes they are connected with. As long as the piston gets accelerated there is no static behavior present and the pressure levels in the chambers are not the same as in their connected pipes. When the system reached the static state the piston velocity is constant in in- and outflowing flow rate as well.

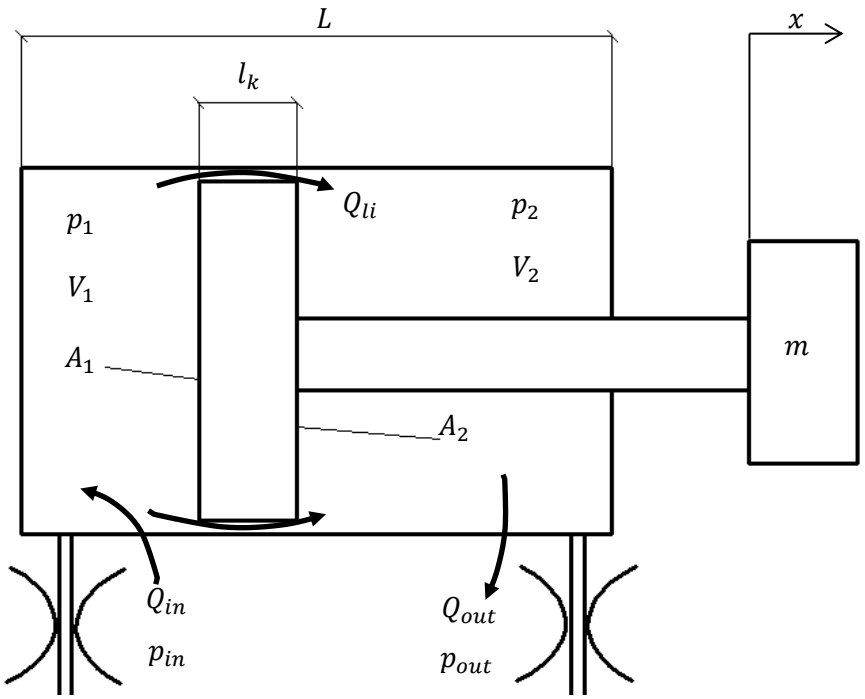

Figure 6:1 Cylinder Model

The cylinder's energy storages are the chambers and the piston mass. The chambers store fluidic energy where pressure can be obtained from. Whereas the piston mass stores kinetic energy where acceleration, velocity and displacement can be obtained from. For the derivatives of pressure p_1 and p_2 can be written:

$$\dot{p}_1 = \frac{1}{C_1}\int Q_{stor1} \tag{6-1}$$

$$\dot{p}_2 = \frac{1}{C_2}\int Q_{stor2} \tag{6-2}$$

Thereby Q_{stor1} respectively Q_{stor2} are the sums of flow rates which stream in and out of each chamber. The following equations can be written for the flow rate balances:

$$Q_{stor1} = Q_{in} - Q_{V1} - Q_{li} \tag{6-3}$$

$$Q_{stor2} = Q_{V2} + Q_{li} - Q_{out} \tag{6-4}$$

In chamber 1 Q_{stor1} characterizes the sum of in- and outflow. The only incoming flow rate is Q_{in} which depends on the restriction and the pressure difference between chamber and pipe. The inflow has to have the same amount of flow rate than the outflow. When the difference is not balanced, the pressure increases or decreases due to a constant capacity. When there is a certain flow rate Q_{in} streaming into the chamber, the same amount has to flow out. But when the pressure level remains the same, capacity has to increase. With the assumption of an almost constant bulk modulus, capacity can only increase when volume increases. For this reason flow rate Q_{V1} has to be considered in that equation. It doesn't drop out but increases the volume. Likewise, the leakage flow rate Q_{li} has to be considered as well. It results from the pressure difference between the chambers and cannot be avoided because of dimensional tolerances in the manufacturing process. A laminar flow profile is assumed in the leakage gap. From these considerations follows:

$$Q_{in} = sign(p_{in} - p_1) \cdot k_{dr1} \cdot A_{dr1}\sqrt{|p_{in} - p_1|} \tag{6-5}$$

$$Q_{V1} = \dot{x} \cdot A_1 \tag{6-6}$$

$$Q_{li} = G_g \cdot \Delta p_{12} = \frac{\pi \cdot d_m \cdot h^3}{12 \cdot \eta \cdot l_k} \cdot \Delta p_{12} \tag{6-7}$$

In the second chamber, there are the inflows Q_{V2} and the leakage Q_{li}. Q_{V2} is caused by piston movement similar to Q_{V1}. For a correct balance equation, the outflowing leakage from chamber one has to be considered as an inflow for chamber two. It follows:

$$Q_{out} = sign(p_2 - p_{out}) \cdot k_{dr2} \cdot A_{dr2} \sqrt{|p_2 - p_{out}|} \tag{6-8}$$

$$Q_{V2} = \dot{x} \cdot A_2 \tag{6-9}$$

For the capacities can be written:

$$C_1 = \frac{K_b(p)}{V_1} = \frac{K_b(p)}{V_{1,0} + x \cdot A_1} \tag{6-10}$$

$$C_2 = \frac{K_b(p)}{V_2} = \frac{K_b(p)}{V_{2,0} - x \cdot A_2} \tag{6-11}$$

The volumes $V_{1,0}$ and $V_{2,0}$ are the particular dead volumes. Both of them are assumed as 1% of the total piston volume.

In the next step the balance equation of the forces shall be determined. Therefore all relevant forces have to be considered.

$$m\ddot{x} = F_1 - F_2 - F_{fr} - F_L \tag{6-12}$$

With:

$$F_1 = p_1 \cdot A_1 \tag{6-13}$$

$$F_2 = p_2 \cdot A_2 \tag{6-14}$$

F_L is the load force and F_{fr} represents the friction force. Friction results when the piston displaces in the sleeve. This happens due to the contact between piston and the cylinder wall. Thereby the influence of static, dynamic and viscous frictions has to be considered in the same way. Viscous friction is caused by the leakage gap between cylinder wall and piston. According to [13, p. 54] the influence of friction has to be considered especially in feedback systems. For instance, when the static friction is very high, the system is not able to act on small pressure differences. Firstly, static friction has to be overcome. For high piston velocities a huge extract of energy or a high damping can be a result. The exact advance projection is not possible. For this reason, the friction force is measured on the real system. Different pressure differences at diverse speeds have to be collected for only one direction of movement. With that set of data, the coefficients of a regression polynomial can be determined in a way that the polynomial fits the real measured behavior. Thereby, the objective is to determine the dimension of these forces. During the simulation, certain values can be varied to obtain better results. When high accuracy is needed, a polynomial for each direction of movement has to be created. Another approach is illustrated in eqn. (6-15). According to [13, p. 54] the friction force on a piston can be characterized as following:

$$F_{fr} = sign(\dot{x}) \left[F_{df} + F_{sf} \cdot e^{-\frac{|\dot{x}|}{T_V}} \right] + k \cdot \dot{x} \tag{6-15}$$

With: F_{df} - dynamic friction

F_{sf} - static friction

T_V - decay constant

k - coefficient of viscous friction

The term of static friction decays exponentially with increasing velocity. The part of viscous friction is constant and proportional to velocity. Due to the assumption of a laminar flow profile in the leakage gap, factor k can be determined as following:

$$k = A \cdot 32 \cdot \frac{\eta \cdot l_k}{{d_m}^2} \tag{6-16}$$

Due to the fact that it is not possible to measure the friction force of the real cylinder, eqn. (6-15) shall be used. The static and dynamic friction forces shall be determined based on normal force. The normal force of the piston is 330N. The friction coefficients are μ_{sf} = 0.12 and μ_{df} = 0.05. From that follows:

$$F_{sf} = \mu_{sf} \cdot F_N \tag{6-17}$$

$$F_{df} = \mu_{df} \cdot F_N \tag{6-18}$$

6.2 Modelling with Simulink

Based on the theoretical equations from the previous section, the model is created in Simulink. It is assumed that the proportional valve has already reached a fixed position. Consequently the pressure levels in the input and output pipe are assumed to be constant. The Simulink model of the actuator is shown in Figure 6:2 below. Equations (6-5) to (6-7) characterize the input in the left chamber. Pressure builds up and the piston extends. Similar considerations can be made for the right piston chamber. To model the march of pressure, eqn. (6-1) respectively (6-2) is used. Pressure p_1 and p_2 are each modelled in a subsystem. The capacity is modelled in a subsystem as well. It changes with a different spool position. The maximum spool position was determined to 0.49m. The input for the capacity subsystems is the limited velocity. The limited velocity also gets computed separately. Two switch-case blocks are used to set the velocity to zero when the spool position is out of range of motion. All subsystems are illustrated in 12.2.

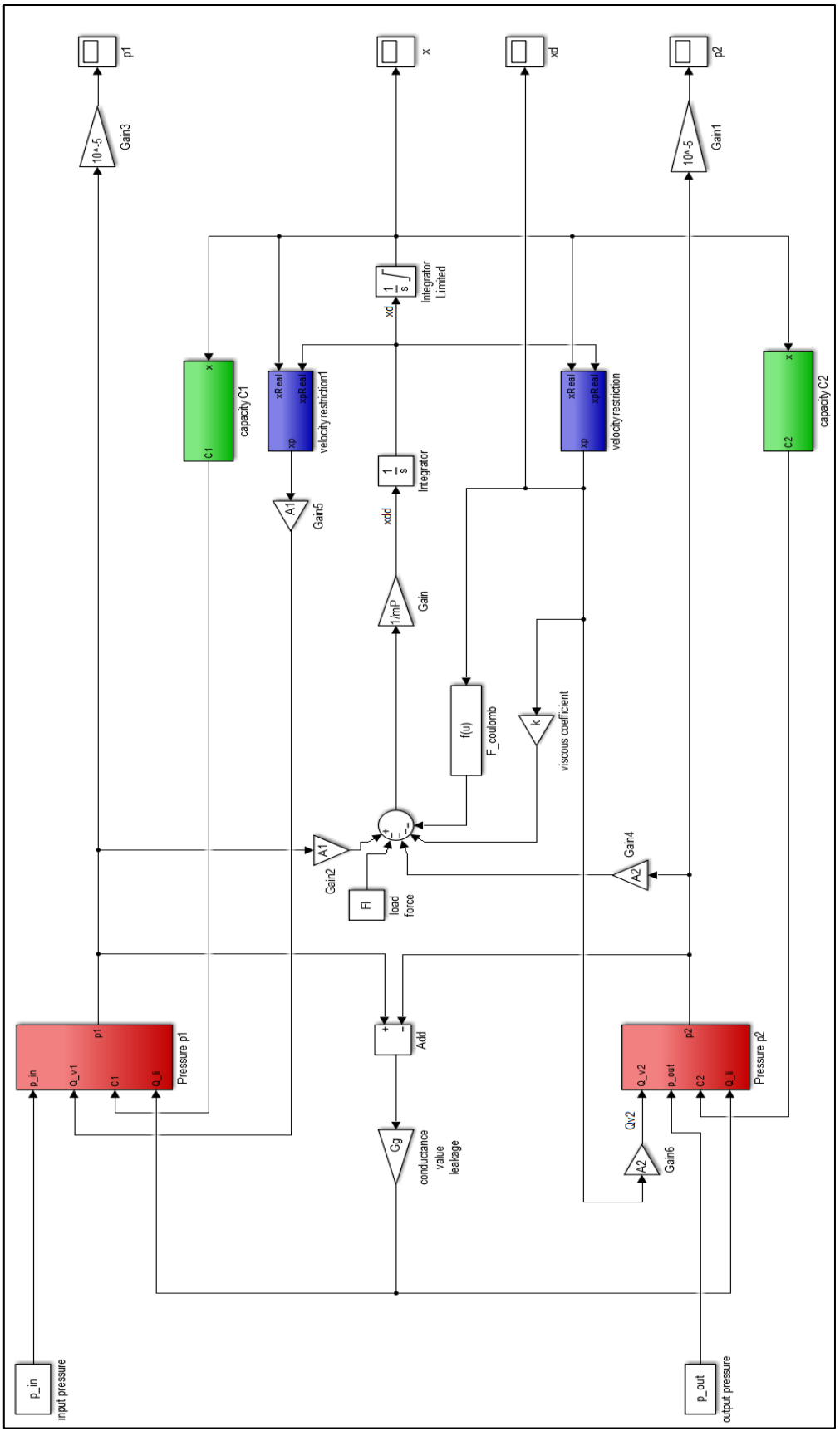

Figure 6:2 Double Acting Cylinder Simulink Model

6.3 Results

When oil pours into the chamber V_1, the piston extracts with a constant velocity until it reaches the ending position. The spool displacement can be seen in the following figure. At the beginning, the piston is at zero position. The plot points out that after reaching the final position, the spool keeps that position.

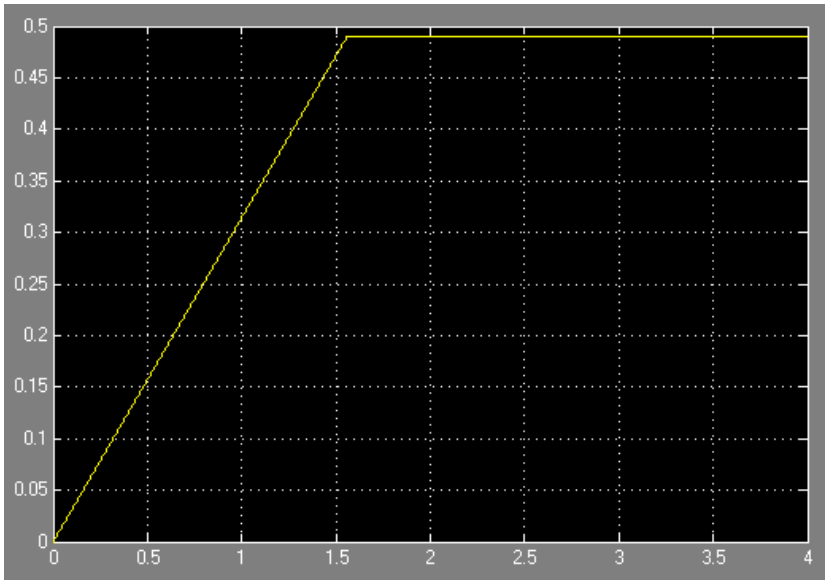

Figure 6:3 Piston Displacement

7 Pressure Relief Valve

In this section the function, theoretical modelling and simulating of the pressure relief valve (PRV) used in the circuit shall be explained. As already mentioned in section 2.2, pressure relief vales are one main group of hydraulic valves. But they can be subdivided in pressure relief, pressure reducing, differential pressure and pressure ratio valves [4, p. 152]. In the circuit, the direct operated pressure relief valve “DBD NG10” is used which is produced by Bosch Rexroth AG. It is direct operated because pressure has a straight connection to the spool to act against the spring. The pressure relief valve acts in the hydraulic circuit as a security element and protects especially the pump from too high pressure levels. For this reason there is a pressure relief valve mounted parallel to the pump in every hydraulic circuit.

7.1 Theoretical Considerations

According to 2.1, a schematic shall be used to determine all the forces and volumetric flow rates which influence the system. From Figure 7:1 below the main functionality of the direct operated pressure relief valve can be obtained. The main set up is an inner spool which is pushed by a spring against a closing edge. On the other side acts the circuit pressure p_2 on surface A. When circuit pressure is below opening pressure the spool does not move. Pressure p_1 and p_2 are the same. When the pressure increases above opening pressure, the spool displaces to the right side and oil can drain into the tank with flow rate Q_{DR}. Thereby the pipe system has a certain capacity which is constant. When oil flows through the opening surface A_{DR} there is less stored volumetric flow rate due to draining. According to Table 2-1, that implies that the pressure level decreases.

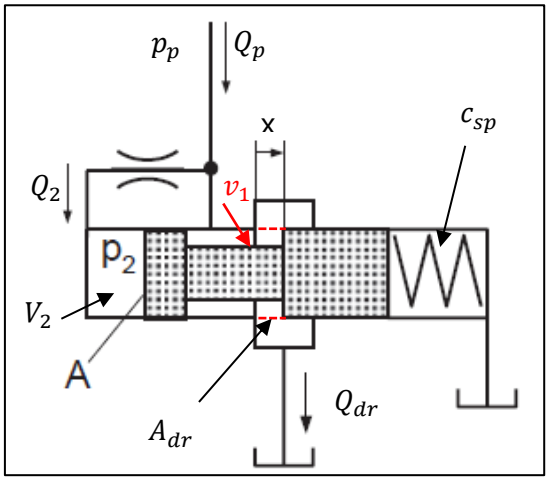

Figure 7:1 Schematic Pressure relief Valve [2, p. 251]

The system has three energy storages and four state variables. Fluidic energy is stored in volume V_2 where the state variable pressure p_2 can be obtained from. The second energy storage is the mass of the spool itself which stores kinetic energy when the dynamic motion

starts. This storage is connected to the state variable spool acceleration $\ddot{x}$. From acceleration the other state variables spool velocity $\dot{x}$ and displacement x can be determined. Also connected to state variable displacement is the spring which stores potential energy. Now, the equations for all energy storages shall be determined to obtain the state variables needed.
Firstly, the state variable p_2 shall be determined. According to Table 2-1 the following expression can be found:

$$\dot{p}_2 = \frac{1}{C_2} \int Q_{stor} \tag{7-1}$$

The capacity C_2 can be determined to

$$C_2 = V_2 \cdot \beta_b \tag{7-2}$$

where β_b is the reciprocal bulk modulus of the hydraulic oil and V_2 the volume which can change when spool displaces.

$$V_2 = V_2 + x \cdot A \tag{7-3}$$

The stored volumetric flow rate in volume V_2 is the difference between outflow and inflow. When there is more incoming flow rate than flow rate going out, the pressure starts to increase. For the considerations of the pressure relief valve the volume V_2 has to be treated as a volume. But this can only be related to the PRV itself. This volume is not incorporated in the considerations of the whole circuit because it is just too small. For the considerations of the whole circuit the PRV is just seen as an open-loop control element to release pressure level when needed.
The stored volumetric flow rate can be written as following:

$$Q_{stor} = Q_2 - Q_{V2} \tag{7-4}$$

with

$$Q_{V2} = \dot{x} \cdot A \tag{7-5}$$

$$Q_2 = \frac{\pi \cdot d_m \cdot h^3}{12 \cdot \eta \cdot l} \Delta p = G \cdot \Delta p = G \cdot (p_p - p_2) \tag{7-6, [4, p. 62]}$$

To flow into volume V_2 the oil has to pass a resistance which is assumed as a thin leakage gap. Following that assumption it can be concluded that the flow rate in that gap is laminar which makes it independent from velocity. It only depends on the geometrics and the pressure difference between incoming pressure p_p and p_2. The geometrics can be summed up to resistance factor G.
The overall balance for the flow rates through the valve can be obtained when dynamic motion is assumed. The drain flow rate Q_{dr} and Q_2 in summation has to be the same as what comes into the valve.

$$Q_p = Q_2 + Q_{dr} \tag{7-7}$$

In the next step the static, dynamic and balance equations to obtain the state variable displacement, velocity and acceleration shall be found. According to Figure 7:1 the static balance equation can be obtained to:

$$p_2 A = F_{p2} = F_{sp}(x) \tag{7-8}$$

with the spring force $F_{sp}(x)$ of:

$$F_{sp}(x) = c_{sp}\,(x - x_{init}) \tag{7-9}$$

When the pressure force in chamber V_2 overcomes $F_{sp}(x)$ the valve spool opens. The volumetric flow rate Q_{DR} can be determined to:

$$Q_{dr} = \sqrt{\frac{1}{\zeta}} \cdot \sqrt{\frac{2}{\rho}} \cdot A \cdot \sqrt{|\Delta p|} = k_{dr}\, A_{dr} \sqrt{p_p} \tag{7-10}$$

In (7-10) is assumed that the tank pressure is equal to reference pressure. When the spool displaces and enables Q_{dr} to flow through, dynamic behavior takes place. Caused by the dynamic displacement of the spool, friction force F_{fr} and flow force F_{fr} act against the opening motion. The flow force has a significant impact on the dynamic behavior of hydraulic valves in general. Most valves are designed as linear spool valves with several controlling edges. When the spool starts to open, the inflowing oil exerts radial and axial forces to the spool. The higher the differential pressure between the two valve ports, the higher the oil's velocity is. When the velocity increases the flow force increases as well because flow force can be determined by using the principle of linear momentum. By assuming oil enters the valve through an annular gap, the controlling edge deflects the oil in a way that it impacts the spool under a certain angle ε. That causes a flow force which is aligned with the closing direction. As already mentioned, that flow force has radial and axial components. The radial components act with the same absolute value on the circumference and become zero. Whereas the axial components can be obtained for steady flow to:

$$F_{ff} = \rho \cdot Q_{dr} \cdot v_1 \cdot \cos(\varepsilon_1) = \rho \cdot \frac{{Q^2}_{dr}}{A_{dr}} \cdot \cos(\varepsilon_1) \tag{7-11}$$

For unsteady flow the dynamic flow force term

$$F_{ff,dyn} = \rho \cdot \mathrm{l} \cdot \frac{dQ_{dr}}{\mathrm{dt}} \tag{7-12}$$

can be added but according to [4, p. 78] it is relatively small compared to the static term. Hence only the static flow term in (7-11) shall be used. Another important effect to determine is the friction force. The spool is installed in sleeve and is directly in contact with it. Due to manufacturing tolerances there are small gaps between spool and sleeve which are filled

with leakage oil. Thus, boundary lubrication is present in the system. Friction always depends on the direction motion. It always acts in opposite direction. To determine the friction force the same approach as in 6.1 shall be used.

$$F_{fr} = sign(\dot{x}) \left[F_{df} + F_{sf} \cdot e^{-\frac{|\dot{x}|}{Tv}} \right] + k \cdot \dot{x} \quad \text{(7-13, [13, p. 54])}$$

After determining all the relevant forces the dynamic behavior can be expressed to

$$m\ddot{x} = F_{p2} - F_{sp}(x) - F_{fr}(\dot{x}) - F_{ff}(x, p_2) \quad \text{(7-14)}$$

Eqn. (7-14) points out that only the pressure force F_{p2} acts on the spool in opening direction. The spring force F_{sp}, friction force F_{fr} and flow force F_{ff} act towards closing direction. From that perspective, the pressure relief valve characteristic can be obtained. F_{sp} represents a static offset for the valve to open while F_{fr} is an almost constant value and not absolutely necessary for the qualitative characteristic. But the flow force is even more relevant. It shows a quadratic relationship to F_{ff}. If the flow rate through the valve increases, the flow force increases quadratically. It can be concluded that the pressure level has to increase as well to maintain that drain flow rate to the tank. That behavior can be observed when looking at the characteristic curves given by the manufacturer.

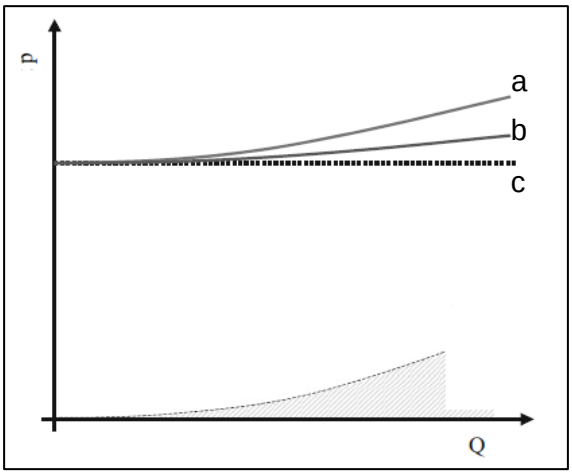

Figure 7:2 Qualitative Pressure Relief Curves

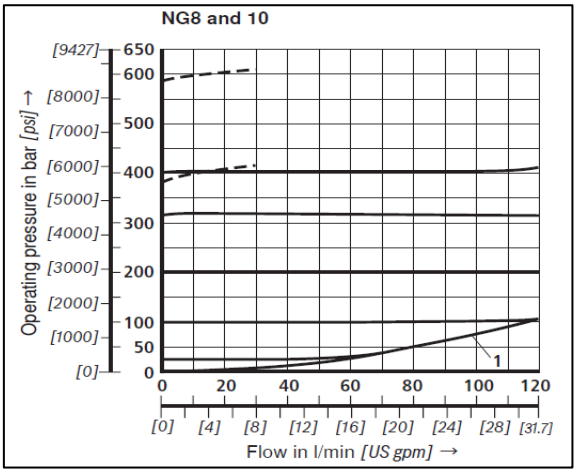

Figure 7:3 PRV Curves from Datasheet

Figure 7:2 shows the qualitative characteristics of a direct-operated (a) and a pilot-operated (b) pressure relief valve. As a comparison, curve c shows an ideal behavior. Figure 7:3 shows the real valve curves for different levels pressure levels. It is illustrated that the flow force influence is almost not present for high pressure levels. At low pressure levels (curve 1) almost without non static pressure offset it is remarkably good noticeable that the flow force plays the main role. Below curve 1, no operation is possible.

Finally, a block diagram can be drawn to determine the connection of all presented equations. Figure 7:4 illustrates the qualitative block diagram which is built on the found relation-

ships. As it is shown in the block diagram, there are the parameters volumetric flow rate Q_p as well as pressure p_p getting into the system. The outputs are the drain flow rate to the tank Q_{dr} and the spool displacement x. All other values are either fixed because of geometrics or getting computed during the simulation.

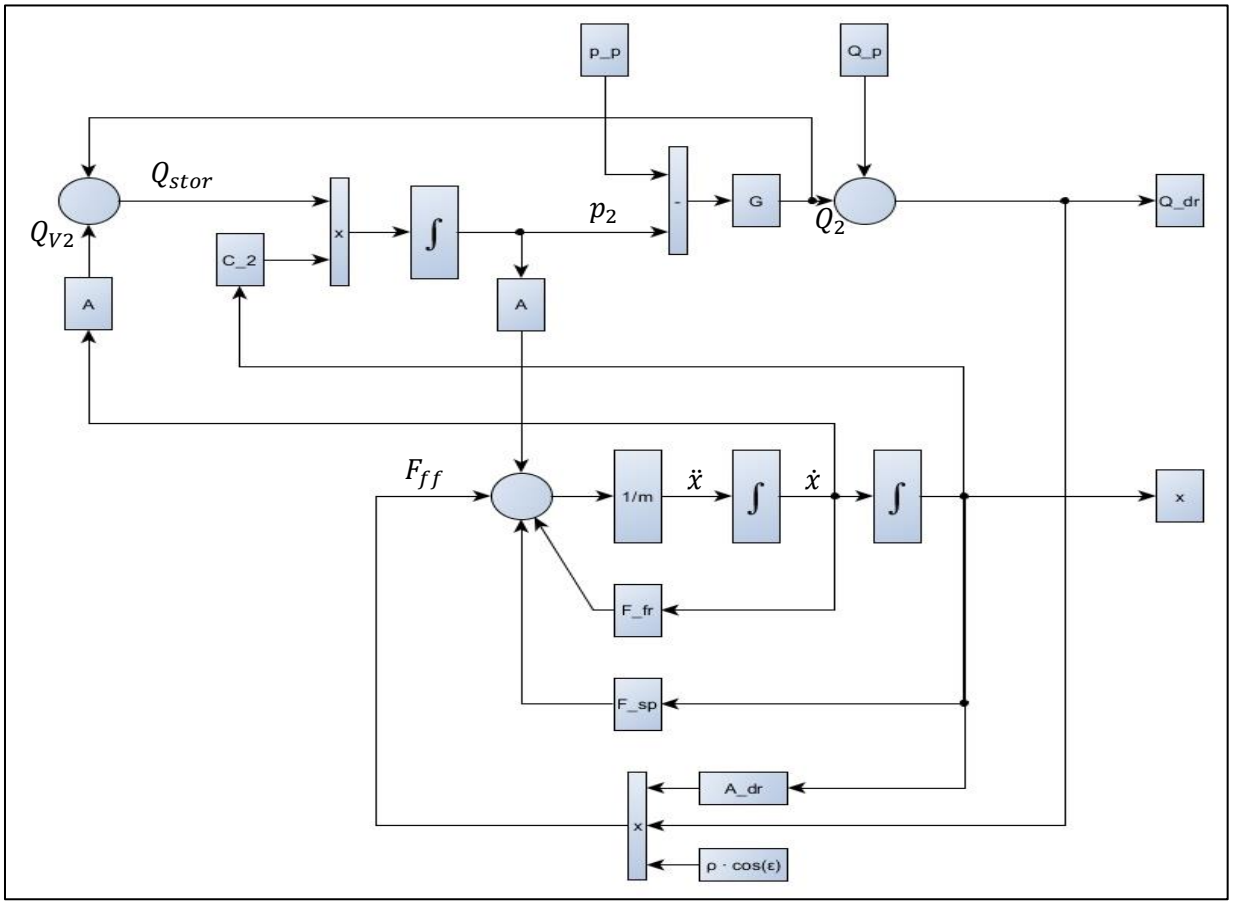

Figure 7:4 Block Diagram PRV

7.2 Pressure Relief Valve Model with Matlab/Simulink

As a basis for modelling the pressure relief valve with Matlab/Simulink, the block diagram in Figure 7:4 shall be used. All parameters needed shall be obtained from the manufacturer's datasheet [14]. However, the datasheet doesn't provide all information explicitly. But based on the provided dimensions of the cartridge valve's assembly drawing and the dimensions given from the housing, missing parameters can be assumed.

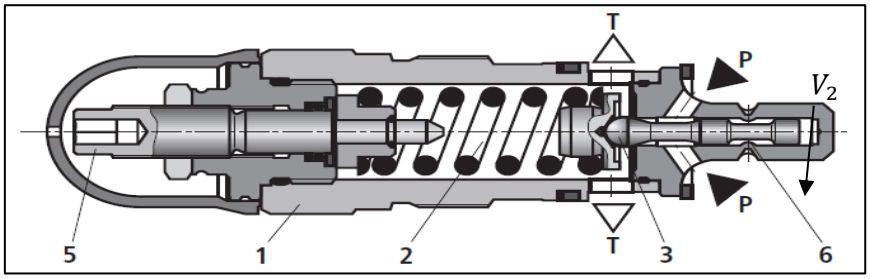

Figure 7:5 Assembly Drawing Pressure Relief Valve [14]

The assembly drawing shows that the real valve is designed as a poppet valve with cone seat. The letters P and T indicate the pump and tank connection. To restrict the displacement, the spool is limited by a stopper (6). The spool acts in a sleeve against the spring (2) with a hemisphere (3).

This design is slightly different compared to the assumptions in the previous section. First of all there is no designed flow passage which directly connects pressure port P with chamber V_2. The oil may flow as leakage into chamber V_2 to build up pressure and act against the spring. The operating direction of the flow force has to be assumed differently as well. Due to the design, it points in the same direction as the oil pressure force $p_2 A$.

When the poppet valve spool starts to move, it releases a certain area between the spool cone and the sleeve. Through this area oil can flow to the tank. The dimensions of the spool to determine that area as well as the leakage gap size shall be obtained by using following figures and tables. The PRV itself is designed as a cartridge valve which has to be screwed into the valve housing. The housing contains ports to connect pressure and tank pipe. The letters P and T shall symbolize these ports. However, the manufacturer gives detailed dimensions about the threaded hole where the cartridge valve has to be screwed into the housing. Figure 7:6 and Figure 7:7 illustrate the cartridge valve as well as their housing. Furthermore, Table 7-1 and Table 7-2 contain the relevant dimensions according to these figures.

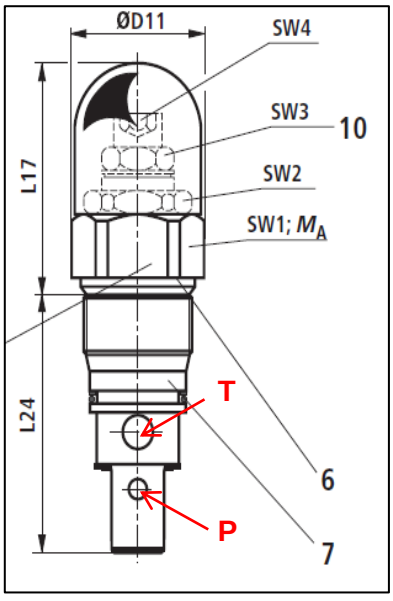

Figure 7:6 Valve Catridge

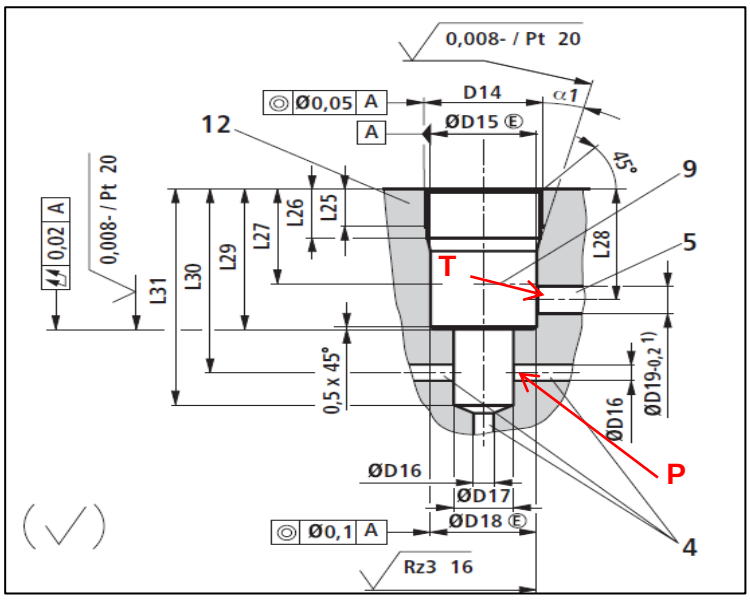

Figure 7:7 Dimensions Valve Housing

Table 7-1 Valve Housing Dimensions (I) [14]

NG	ØD11	ØD12	ØD13	L17	L18	L19	L20	L21	L22	L23	L24
6	34 *[1.34]*	60 *[2.36]*	–	72 *[2.83]*	11 *[0.43]*	83 *[3.26]*	28 *[1.10]*	20 *[0.79]*	–	–	64.5 *[2.54]*
10	38 *[1.50]*	60 *[2.36]*	–	68 *[2.68]*	11 *[0.43]*	79 *[3.11]*	28 *[1.10]*	20 *[0.79]*	–	–	77 *[3.03]*
20	48 *[1.89]*	60 *[2.36]*	–	65 *[2.56]*	11 *[0.43]*	77 *[3.03]*	28 *[1.10]*	20 *[0.79]*	–	–	106 *[4.17]*
30	63 *[2.48]*	–	80 *[3.15]*	83 *[3.26]*	–	–	–	–	11 *[0.43]*	56 *[2.21]*	131 *[5.16]*

Table 7-2 Valve Housing Dimensions (II) [14]

NG	D14	ØD15	ØD16	ØD17	ØD18	ØD19
6	M28 x 1.5	25H9 *[0.9843$^{+0.002}$]*	6 *[0.24]*	15 *[0.59]*	$24.9^{+0.152}_{-0.2}$ *[0.9803]* $^{[+0.006]}_{[-0.00786]}$	12 *[0.47]*
10	M35 x 1.5	32H9 *[1.2598$^{+0.0024}$]*	10 *[0.39]*	18.5 *[0.73]*	$31.9^{+0.162}_{-0.2}$ *[1.2559]* $^{[+0.0064]}_{[-0.0079]}$	15 *[0.59]*
20	M45 x 1.5	40H9 *[1.5748$^{+0.0024}$]*	20 *[0.79]*	24 *[0.95]*	$39.9^{+0.162}_{-0.2}$ *[1.5709]* $^{[+0.0063]}_{[-0.0079]}$	22 *[0.87]*
30	M60 x 2	55H9 *[2.1654$^{+0.0029}$]*	30 *[1.18]*	38.75 *[1.53]*	$54.9^{+0.174}_{-0.2}$ *[2.1614]* $^{[+0.0069]}_{[-0.0079]}$	34 *[1.34]*

NG	L25	L26	L27	L28	L29	L30	L31	α1
6	15 *[0.59]*	19 *[0.75]*	30 *[1.18]*	36 *[1.42]*	45 *[1.77]*	56.5±5.5 *[2.22±0.217]*	65 *[2.56]*	15°
10	18 *[0.71]*	23 *[0.91]*	35 *[1.38]*	41.5 *[1.63]*	52 *[2.05]*	67.5±7.5 *[2.66±0.295]*	80 *[3.15]*	15°
20	21 *[0.83]*	27 *[1.06]*	45 *[1.77]*	55 *[2.17]*	70 *[2.76]*	91.5±8.5 *[3.60±0.335]*	110 *[4.33]*	20°
30	23 *[0.91]*	29 *[1.14]*	45 *[1.77]*	63 *[2.48]*	84 *[3.31]*	113.5±11.5 *[4.47±0.453]*	140 *[5.51]*	20°

From the difference of length L31 and L29 (NG10), the spool length can be estimated to 30 mm by also using the assembly drawing for comparison. The inner diameter D17 characterizes the outer diameter of the sleeve where the spool is acting in. D17 for a size 10 valve is 18.5 mm. By using proportional relations from the assembly drawing, the spool diameter can be estimated to 8 mm. Further dimensions can be estimated as following:

Table 7-3 Spool Dimensions

spool length	l_S	30 mm
spool diameter	d_S	8 mm
cone length	l_C	5 mm
hemisphere diameter	d_{HP}	10 mm
flow passage length	l_{FP}	5 mm
maximum displacement	x_{max}	4 mm

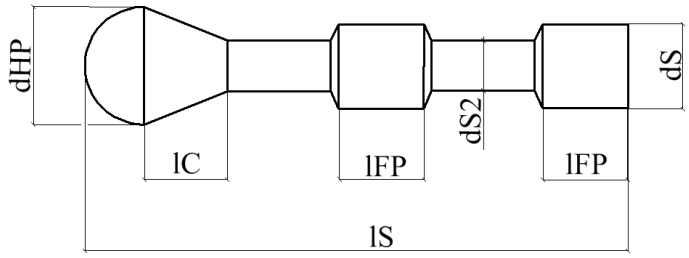

Figure 7:8 Spool Dimensions

Given the dimensions and the density of steel, the spool mass can be estimated to 0.04 kg. The height h of the leakage gap is not available from the datasheet. It is assumed to be

0.1mm. For this reason, the mean diameter d_m has a value of 8.1mm. Both values are necessary to compute the conductance value of the leakage flow rate.

Now, the flow area A_{dr} shall be determined. It has to be identified what size the area has depending on the spool position. Firstly, the cone angle φ shall be determined by using the estimated spool dimensions. With angle φ the distance Δx can be calculated using trigonometric relations. That results in a circular ring area with an upper diameter d_S and a lower diameter of $d_S - (2 \cdot \Delta x)$. This is illustrated in Figure 7:9 below.

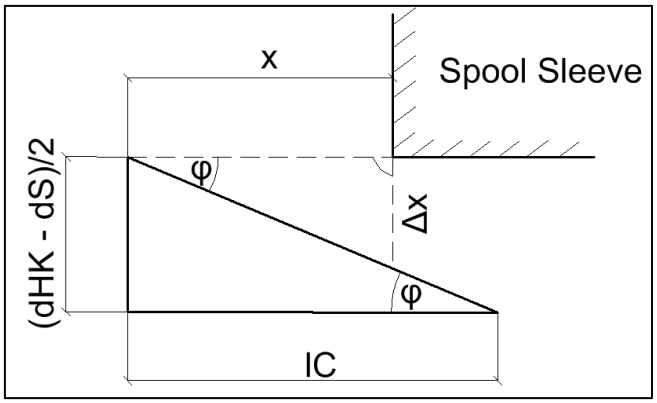

Figure 7:9 Diameter Dimensions

With:

$$\varphi = tan^{-1}\left(\frac{(d_{HP} - d_{S2})}{2} \Big/ l_C\right) \tag{7-15}$$

$$\Delta x = \tan(\varphi) \cdot x \tag{7-16}$$

$$A_{dr} = \frac{\pi}{4} \cdot \left({d_S}^2 - (d_S - 2 \cdot \Delta x)^2\right) \tag{7-17}$$

In the next step the spring force shall be determined. There is no information about the spring constant or preload displacement in the datasheet. Thus it has to be assumed. According to the static balance equation (7-8) the pressure force has to overcome the preloaded spring force to open the valve. The opening system pressure is supposed to be 200 bar. But there is no way computing the spring force without having spring constant or preload displacement. For this reason the spring constant is assumed to be 100000 N/m. The resulting preload displacement for 200 bar can be calculated to 10.1mm.

It is assumed that ρ and ζ are constant values. That is a rough assumption because ζ depends on differential pressure and the Reynolds number which depends on velocity. Due to the fact that the velocity can change while the valve opens and closes, ζ also varies. The flow coefficient α has been assumed to 0.7. The density of the oil is set to a constant value of 880 kg/m³.

Finally, static and dynamic friction forces shall be determined to use equation (7-13,) in the simulation. With the use of the normal force and the static and dynamic friction coefficient they can be determined. The spool as well as the sleeve where it is acting in is fabricated from steel. Manufacturing tolerance causes leakage which results in lubricated friction. From that follows:

$$F_{sf} = \mu_{sf} \cdot F_N \tag{7-18}$$

$$F_{df} = \mu_{df} \cdot F_N \tag{7-19}$$

According to [15] the friction coefficients can be estimated to μ_{sf} = 0.12 und μ_{df} = 0.05. The decay constant T_V is assumed to be 0.1 according to [16]. The viscous friction coefficient k is determined to 0.1 as well. In order to that all parameters are obtained and can be stored in Matlab. The initializing file is listed in 12.3.

Then the system can be modelled in Simulink. The whole model of the PRV is shown in the appendix under 12.4. Due to the fact that there is no direct flow passage into chamber V_2, this volume is no longer treated as an energy storage for pressure. It is assumed that the volume is already filled with oil. When the system pressure at port P increases, pressure acts on volume V_2 and the spool diameter because of the leakage gaps. When the pressure overcomes the needed opening pressure the valve opens. When the valve opens, it can be concluded that the spool moves and because of that V_2 increases on $\dot{x} \cdot A_S$. It is assumed that the same amount of oil has to flow as leakage into the chamber. That means both flow rates are equal.

The increase of pressure at port P is modelled by a constant pump flow rate which streams into a specified pipe capacity of one meter length. The initial pressure level in that pipe is zero bar differential pressure.

The flow force acts in opening direction and has to be fed back with a positive sign. The reason is that the oil comes into the valve with an angle of 45° as it is shown in the assembly drawing. According to that the horizontal component of that momentum force points in opening direction.

To ensure that the spool has the same limited displacement barriers of $0\,mm \leqslant x \leqslant 4\,mm$, a restriction hast to be modelled. Moreover, it has to be ensured that velocities only getting fed back when the spool is acting between these boundaries. Outside of these boundaries, the velocity has to be zero.

To simulate the displacement restriction, an integration block with saturation limits is used. It has velocity on the input which is getting integrated over time. But on the output side it only generates values in the limits of zero to four millimeters. And so the output can immediately be used for computing the flow area A_{dr}.

To simulate the velocity, the subsystem ‘restriction’ is used. It is shown in Figure 7:10 below.

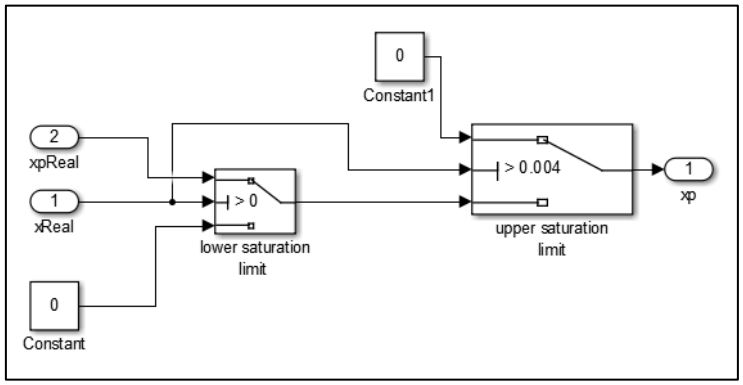

Figure 7:10 Limiting Velocity

The first switch block checks if the displacement is higher than zero. If it is less than zero, velocity gets set to zero. If it is higher, the displacement gets transferred to the second switch block. Here, the upper boundary limit gets checked. If it is higher than 4mm, the velocity is limited to zero as well.

The simulation of the flow force is executed in a subsystem too. The flow force has to be computed from the current flow area and the pressure p_p. Also the current drain flow rate Q_{dr} has to be computed.

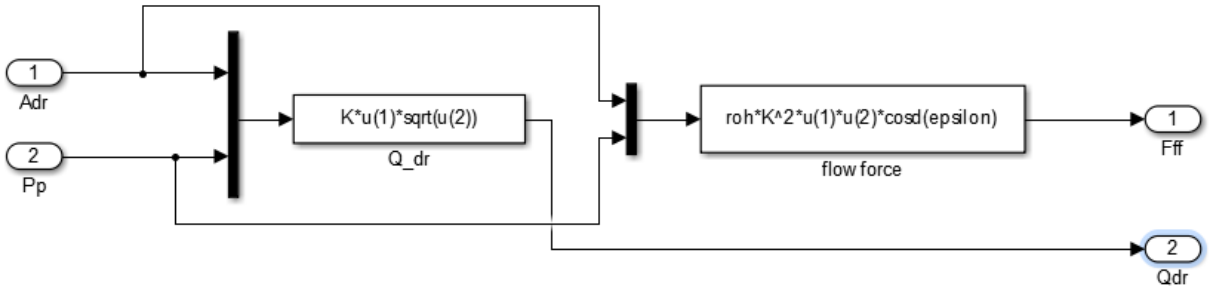

The flow force gets simulated as follows:

$$F_{ff} = \rho \cdot \frac{Q^2{}_{dr}}{A_{dr}} \cdot \cos(\varepsilon_1) = \rho \cdot \frac{(K \cdot A_{dr} \cdot \sqrt{p_p})^2}{A_{dr}} \cdot \cos(\varepsilon_1) = \rho \cdot {K_b}^2 \cdot A_{dr} \cdot p_p \cdot \cos(\varepsilon_1) \quad (7\text{-}20)$$

7.3 Results

To analyze the system, it is essential that the pressure and flow rate behavior is simulated over time. The spool position is interesting as well. To have a good view on the behavior, the system gets simulated with three different pump flow rates of 20, 40 and 100 l/min. These are illustrated in the following figures.

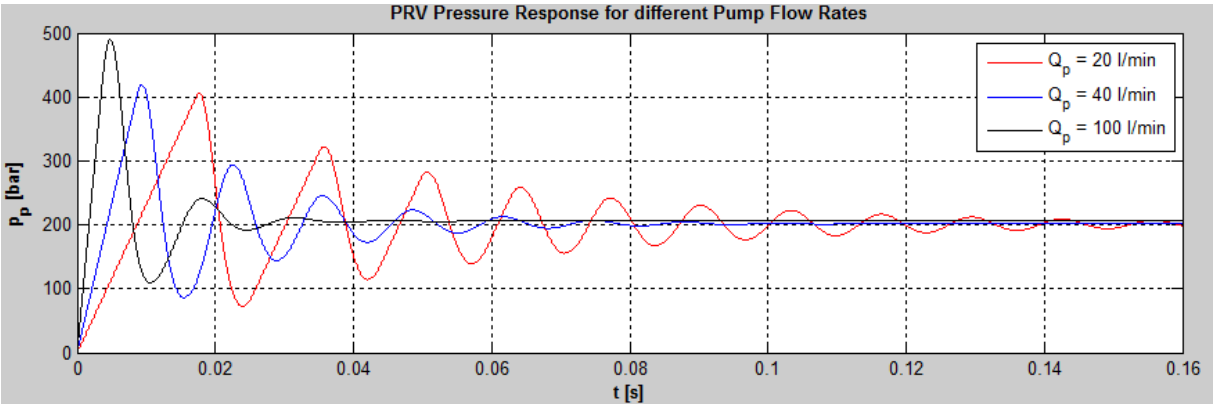

Figure 7:11 PRV Pressure Response

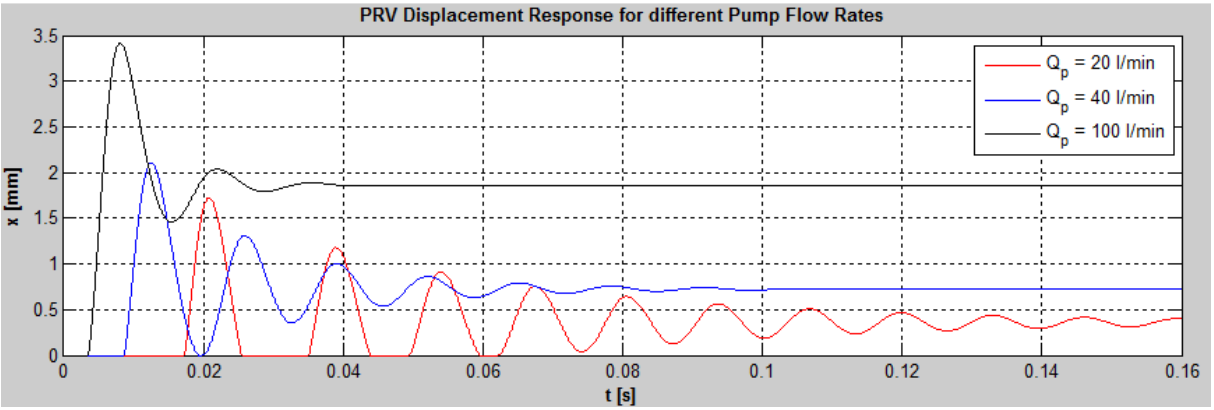

Figure 7:12 PRV Displacement Response

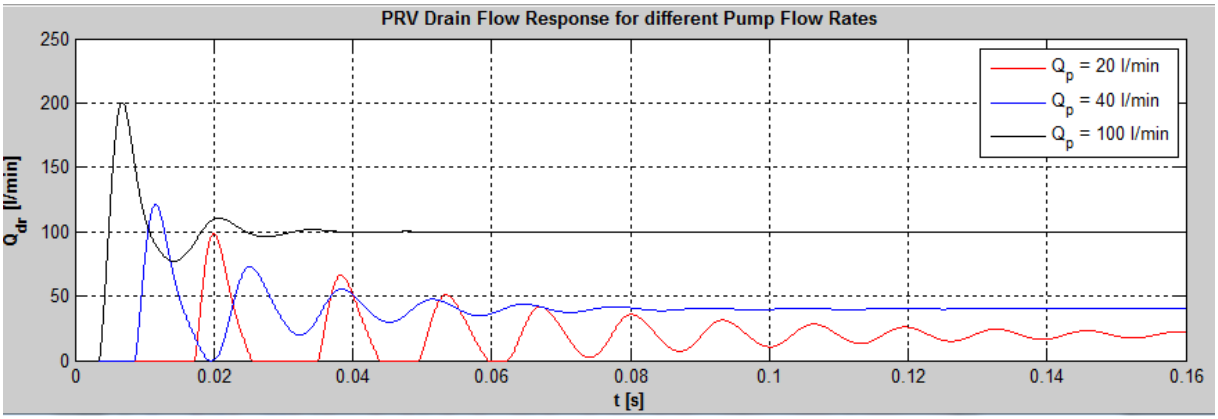

Figure 7:13 PRV Drain Flow Response

It can be seen that it is difficult to design a PRV which stabilizes quickly for a huge band of different flow rates. Figure 7:11 illustrates that the pressure level increases faster when the

pump flow rate is higher. This is caused by the fact that a high flow rate can fill a certain volume faster as a low flow rate can do. Due to the mechanical inertia, the system needs some reaction time even when the opening pressure is reached. Thus the pressure increases very rapidly for a short moment. At this pressure peak moment, the system reacts by opening the valve rapidly as well. This can be seen in the plots. When the pressure is the highest the spool position is at the highest, displacement as well. For all pump flow rates the system stabilizes at a point where the drain flow rate is equal to the pump flow rate.

Due to the fact that many assumptions had to be made and the simulation results can't be compared to any measurement curves, the static characteristic curve can be used as an alternative. It can be modelled by using an exponential function with PT1 behavior.

$$p_{static} = p_{open} - p_{open} \cdot e^{-Q/T} + c \cdot Q^2 \tag{7-21}$$

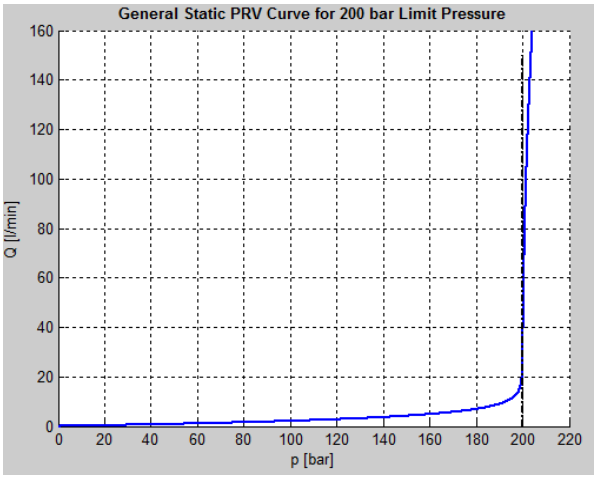

Figure 7:15 General Static PRV Curve

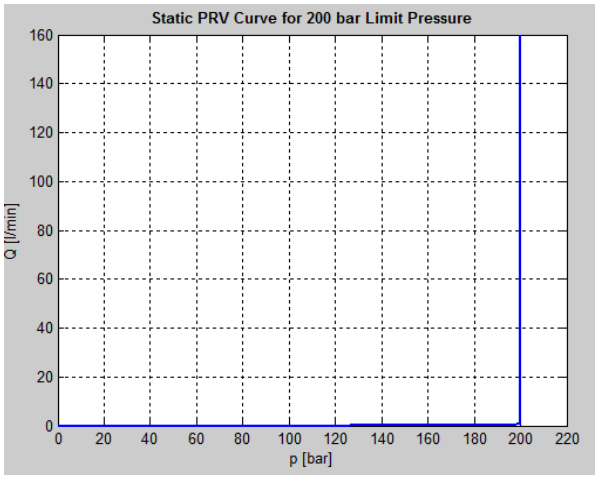

Figure 7:14 Real Static PRV Curve

The general static curve shows the behavior pretty good. It has to reach the opening pressure point very fast even at low flow rates and has to be stabile over a huge band of flow rates. The quadratic dependence on the flow rate can be seen as well. In the right figure, the real static curve is illustrated. The decay constant is set to 0.1 and the factor c is determined to 10^{-7}.

8 Proportional Directional Control Valve

In this section the modelling of the proportional directional valve shall be described. For creating a dynamic simulation the valve behavior can be divided into a dynamic and static part. The dynamic part provides information about how fast the valve is able to react on a step response. That means how fast the spool can react to a certain input signal. The static behavior provides information about the flow and pressure characteristics at a certain spool position.

With reference to the signal sequence, first the characteristics of the dynamic system shall be introduced. Afterwards the static behavior shall be determined. In [17] this approach was applied to the proportional valve KBSDG4V-3 designed by Eaton Vickers. The obtained results matched the real frequency characteristics pretty well. However, the dynamic behavior of the used proportional valve 4WRSE-10 by Bosch Rexroth has slightly different dynamic characteristics. It doesn't show any amplitude gain behavior at certain frequencies, unlike the Vickers valve.

However, this approach shall be applied to the used valve to test its applicability and to obtain the same good results.

8.1 Dynamic Model

Modelling the dynamic behavior by using basic theoretical foundation would lead to imprecise results due to the complexity of the valve. For this reason a different approach shall be applied. The non-linear frequency response data given by the manufacturer shall be used because they represent the proper dynamic behavior of the valve. That implies that this approach provides specific results only relating to that valve type. It doesn't provide general results for different types of valves.

Figure 8:1 shows the curves extracted from the datasheet. It measures the amplitude response as well as the phase angle for three different normalized input signals of ±10%, ±25% and ±100% of maximum spool stroke. Due to the fact that the data is valid for positive and negative spool position, symmetrical valve behavior can be suggested.

There are measured data over the whole displacement range of the spool. That provides a good understanding of the real valve behavior which makes these curves appropriate to build a simulation on.

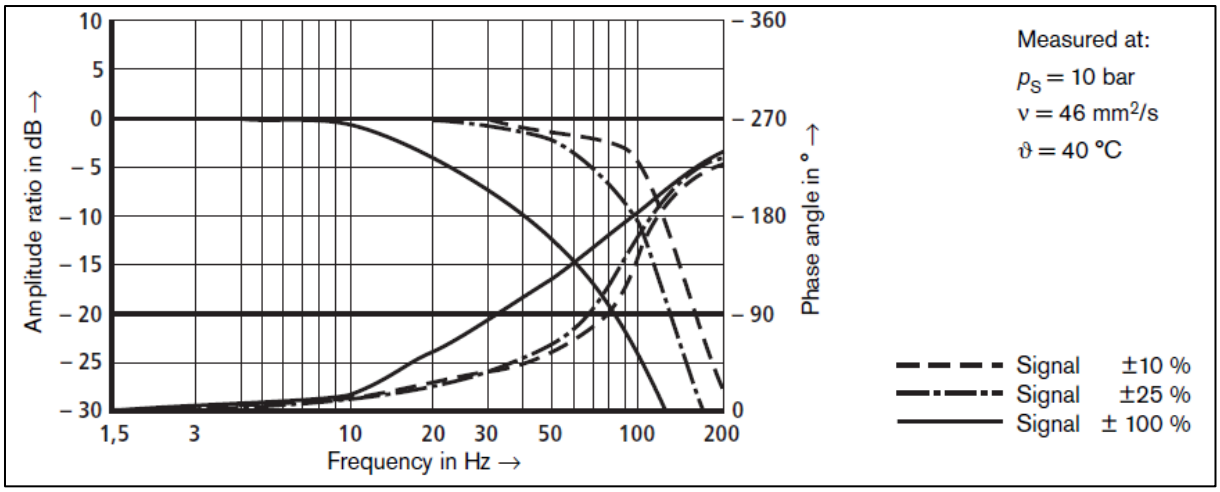

Figure 8:1 Amplitude and phase response curves [5]

A Simulink model which represents the data curves shown above has to be implemented. Due to the non-linearity, the valve shows different output behavior when fed with different amplitudes on the input. The Simulink model needs to have this particular characteristic as well. It is supposed to provide different dynamic behaviors for different inputs in only one model. According to [17] a linear second order system shall be used which has to be optimized to obtain the needed behavior. Otherwise the non-linearity couldn't be realized. As already mentioned, the valve characteristics are equal for positive and negative spool displacement. It also can be assumed that the real valve has limitations for velocity and acceleration because they cannot be infinitely big. According to the same behavior in positive and negative direction the velocity and acceleration limitations have to be equal for both directions too. It also has to be considered that the curves are not measured absolutely but normalized to the maximum spool stroke. Therefore, there is no need for a stationary gain factor because it is equal to one.

In the following procedure shall be explained how the linear second order model has to be modified to obtain a non-linear model. At this stage shall be pointed at the mechanical second order model of a spring-mass-damper oscillator in Figure 2:4 which is the foundation. Cutting the system free leads to the equation of motion with general input analog to (2-17):

$$m\ddot{x} + d\dot{x} + cx = F \cdot \cos(\omega t) = F(t) = u(t) \tag{8-1}$$

To be able to create the Simulink model, eqn. (8-1) has to be transposed for the highest derivative of x. That leads to:

$$\ddot{x} = \frac{u(t)}{m} - \frac{d}{m}\dot{x} - \frac{c}{m}x = K\omega_n^2\, u(t) - 2\zeta\omega_n\dot{x} - \omega_n^2\, x \tag{8-2}$$

According to (8-2) the model in Simulink can be created as following:

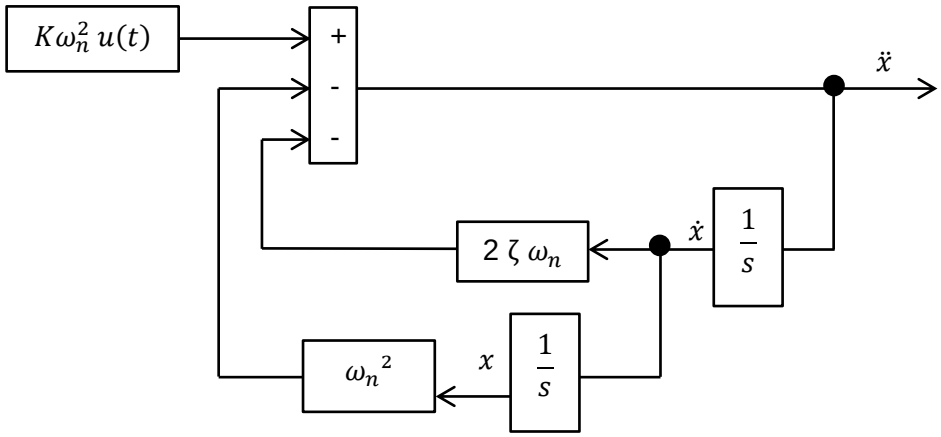

Figure 8:2 Linear Second Order Model

In contrast, the following figure below shows the model which was created in [17, p. 247]. Compared to Figure 8:2, it is reshaped and extended by saturation blocks. There is also no stationary gain factor on the left which confirms former explanations. Also noticeable is the delay block which is used to obtain the phase lag. The rest of the model is used to achieve the amplitude response behavior.

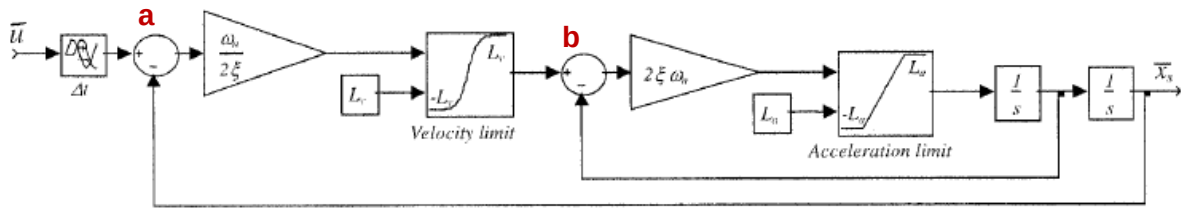

Figure 8:3 Non-Linear Valve Model

Now it shall be discussed how the non-linear model was created. Therefore, balance equations can be created on the summation points “a” and “b” in Figure 8:3. Doing so leads to:

$$a = \bar{u} - \bar{x}$$
$$b = a\frac{\omega_n}{2\zeta} - \dot{x} \qquad (8\text{-}3)$$

Additionally the acceleration can be written as:

$$\ddot{x} = b \cdot 2\zeta\omega_n \qquad (8\text{-}4)$$

With substituting “a” and “b” from (8-3) in (8-4) and expanding them, acceleration can be written as following:

$$\ddot{x} = u(t)\omega_n^2 - 2\zeta\omega_n\,\dot{x} - \omega_n^2\,x \qquad (8\text{-}5)$$

By comparing the coefficients of equation (8-2) and (8-5), it can be determined that both equations are equal except the gain factor K.

The model in Simulink is created with general variables as it is shown in Figure 8:3. This model shall be fit to the measurement curves from the manufacturer. Therefore the data points have to be available in Matlab. If the model is simulated with certain initial values there is an error resulting between the measurement points and the simulation values at any frequency of the three amplitude responses. This is due to the fact that the chosen initial values most likely don't represent the dynamic behavior. But there have to be values for the Simulink model which minimizes the error between measurement and simulation. Additionally, these values represent the best dynamic behavior the model can achieve. The fact that the error deviation is strongly connected to the model parameters leads to the conclusion that the error sum at each measuring point has to be minimal to obtain good parameters for the model. This leads to an optimization problem. To solve optimization problems, Matlab offers various functions which optimize target values with different kinds of implemented algorithms. The optimization function used in this work is "*fminsearch*" which optimizes non-linear problems without using derivatives. It is based on the Nelder-Mead simplex algorithm [18]. To execute the simulation, initial values are necessary. That influences the simulation duration considerably when far from the final values. Hereafter shall be described how the implemented optimization algorithm works.

The calculation of amplitude and phase has to be done separately. Thereby the phase shift is acquired by using a pure time delay. The rest of the model is used to compute the amplitude response. The following flow chart in Figure 8:4 only refers to the amplitude response computation.

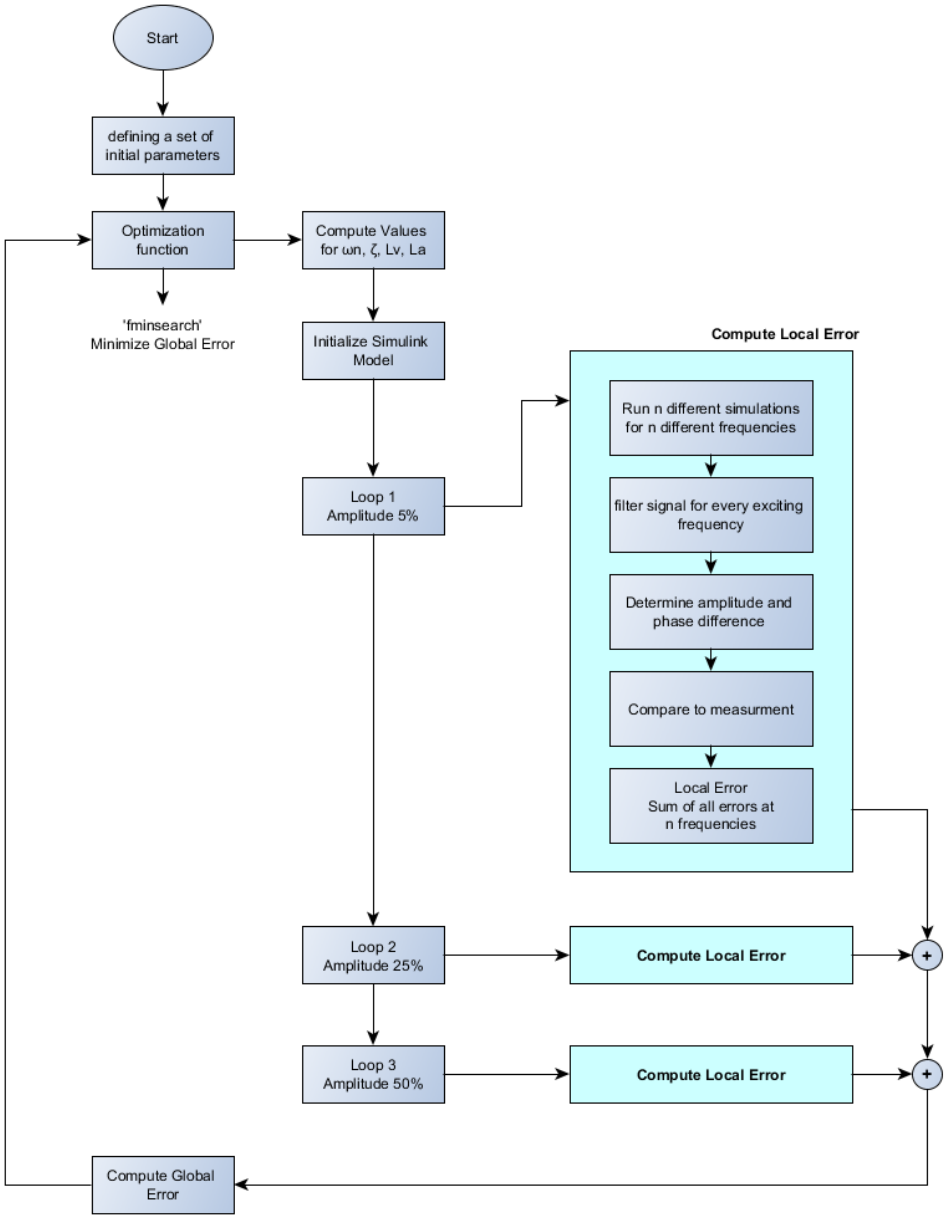

Figure 8:4 Optimization of Dynamic Model

Firstly the initial values for ω_n, ζ, L_v und L_a have to be determined. These initial values are passed to the optimization function. The optimization function manipulates the initial values due to the result of the target function. In this case, the target function is the sum of all squared error deviations. For the first iteration step the system has to be simulated completely to achieve a target function value for the initial values. Based on their inner algorithm *fminsearch* decides which initial value has to be manipulated and how much. Next the model can be simulated again and the impact on the target function can be examined.

When the optimization function changed the initial values, they were passed to the Simulink model. As illustrated in Figure 8:4, the simulation is divided into three parts. This is due to the three different input amplitude curves. The result of each of these blocks is the sum of all

local squared errors from measurement to simulation point at a certain frequency. According to [17] the global error is computed as following:

$$F_{global} = 4 \cdot F_{local,10\%} + F_{local,25\%} + F_{local,100\%} \tag{8-6}$$

The local error deviation $F_{local,10\%}$ is weighted with a factor of 4. This is why the valve operates most of the time around the middle position to adjust the flow rate very precisely when controlling an actuator position. Hence it is necessary to put more effort in a good approximation of that curve.

To compute the local error, a few steps are important. Firstly, amplitude response measurement data at different frequencies is needed. These have to be extracted from the datasheet. The used measurement data is illustrated in 12.5. When the Simulink model is supplied with a sinusoidal signal, nonlinearities occur due to the saturation blocks. The saturation blocks are essential to fit the model to the non-linear curves but they complicate the optimization as well. Because of the saturation blocks, the output signal can contain other frequencies in their spectrum. These harmonics cause an unstable amplitude behavior because of their superposing with the exciting frequency. That makes it impossible to obtain a steady oscillation behavior. But according to 2.4 that is necessary to compute the amplitude response. For this reason, the simulated output signal has to be filtered for the certain exciting frequency. Following the filtering the output signal is supposed to have steady amplitude. Consecutively the amplitude ration of output to input at every exciting frequency can be computed by using eqn. (2-33). That result can be additionally compared with the measurement and the local error can be determined.

$$F_{local} = \sum_{i=1}^{n} \left(A_{measur}(f(i)) - A_{local}(f(i)) \right)^2 \tag{8-7}$$

A final solution for the solution vector is found when the optimization function determined a minimum for the target function. In that case the solution vector values for ω_n, ζ, L_v und L_a can be passed to the Simulink model and the phase shift can be obtained by optimizing the time delay. The procedure is similar to the amplitude optimization. The measurement data to compare the optimization result with are the phase response data points.

To filter the output signal and compute amplitude and phase response, various functions are implemented in Matlab. They need input variables and vectors to execute different computations. In the next sections they shall be described more precisely.

8.1.1 Signal Filtering

To filter the output signal, the function *calcFilteredSig* is implemented. The function requires the exciting frequency, the initial value vector and the normalized input amplitude. It returns the simulation time, the input signal and the filtered output signal as well. The syntax is following:

$$[[simTime], [inputSig], [filteredSig]] = \boldsymbol{calcFilteredSig}(f_{in}, [\omega_n, \zeta, L_v, L_a], A_{in}) \tag{8-8}$$

Depending on the excitation frequency, the sampling frequency is set to a certain value. The higher the excitation frequency, the higher the sampling frequency has to be. Otherwise it is possible to have aliasing which occurs when the sampling frequency is too low. As the transformation to the frequency domain is performed with FFT, only sampling frequencies of the basis two are used. Furthermore, the total number of measurement points is computed with an exponential function of the basis of two as well. Performing the FFT the signal vector has to have the length of an exponential function to the basis of two anyway. Otherwise the signal vector is filled with zeros. That can cause high frequencies. The following table shows which sampling frequency corresponds to which excitation frequency.

Table 8-1 Sampling Frequency

Excitation Frequency [Hz]	f_S *[Hz]*
$\mathrm{f} \leqslant 4$	2^{12}
$4 < \mathrm{f} \leqslant 10$	2^{13}
$10 < \mathrm{f} \leqslant 40$	2^{15}
$40 < \mathrm{f} \leqslant 80$	2^{16}
$80 < \mathrm{f} \leqslant 160$	2^{17}
$\mathrm{f} > 160$	2^{18}

Having the sampling frequency the sampling step size can be determined:

$$t_S = {}^{1}/_{f_S} \tag{8-9}$$

The number of sampling points is determined to 2^{16}. From the total number of sampling point and the step size, the simulation time can be computed. Both, simulation time and step size, are passed to Simulink as well. The computation of an FFT is not possible when using a variable step size. The simulating options have to be changed to fixed step size. Then, the Simulink model can be simulated. Now the output signal which is determined by the Simulink model can be transformed with FFT. Due to the FFT algorithm, a reflecting spectrum results at the Nyquist frequency. For this reason is it sufficient to plot only half the spectrum until Nyquist frequency. The Nyquist frequency is half of the sampling frequency. Due to subsequent computation steps, the spectrum has to be normalized by its maximum value. In this

case the maximum value is represented by the excitation frequency. Following figures illustrate the output signal of the Simulink model for the simulation values of $\omega_n = 1000\,rad/s$, $\zeta = 0.8$, $L_v = 50$ und $L_a = 50{,}000$. The excitation frequency is set to 180 Hz. In this case the signal is sampled with 2^{12} Hz which leads to a Nyquist frequency of 2048 Hz.

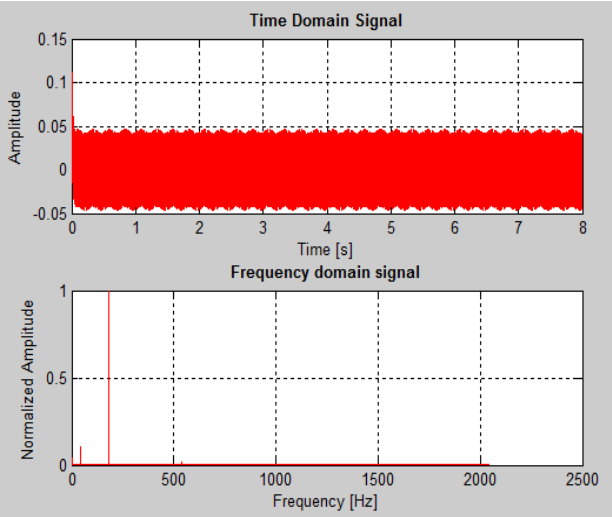

Figure 8:5 Time and Frequency Domain (I)

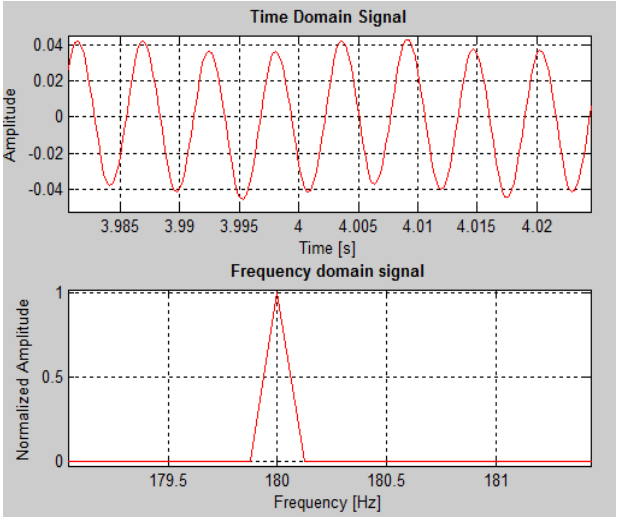

Figure 8:6 Time and Frequency Domain (II)

In Figure 8:5 and Figure 8:6 the unfiltered output signal is illustrated in time and frequency domain. As it is shown in the time domain plot, there is a superimposition present in the signal. The frequency domain plot confirms that suggestion. The excitation frequency of 180 Hz is dominated in the signal. But due to the nonlinear saturation blocks other frequencies are present as well. It is recognizable that there are frequencies of 45 Hz and 540 Hz contained too. Without applying a filter routine, no amplitude response can be determined. Figure 8:6 provides a closer look on the time and frequency domain. It is obvious that the amplitudes are quite unstable. The frequency plot shows that the spectrum is normalized by the maximum amplitude at 180 Hz.

The signal shall be bandpass filtered. Analog bandpass filter techniques were tried but their characteristics are inappropriate for this problem. Analog filters got unstable very quickly when the bandpass filter got too narrow. Therefore, a digital FIR filter is used. To design the filter, the cutoff frequencies have to be normalized on Nyquist frequency. It is determined that:

$$\omega_{2,1} = {}^{2 \cdot f}/_{f_S} \pm 0.0001 \qquad (8\text{-}10)$$

Furthermore, the filter order is determined to 5000 in denumerator and 1 for the numerator. Now, the filter is used to exclude the interfering frequencies. The result is illustrated in the following figures.

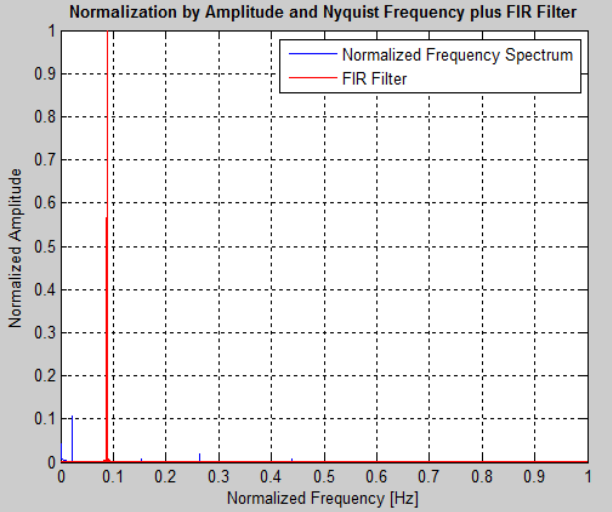

Figure 8:8 Filtering in Frequency Domain (I)

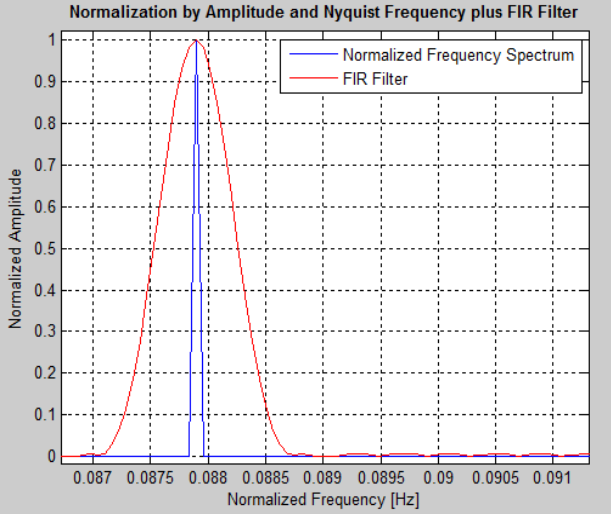

Figure 8:7 Filtering in Frequency Domain (II)

According to the plots in the figures above, it can be seen that the FIR filter provides good results. Even interfering frequencies which are close to the excitation frequency can be filtered out very well due to the high order and the narrow cutoff frequencies.

Finally, the filtered output signal shall be inverse transformed to time domain. As it is shown in Figure 8:9 and Figure 8:10, the harmonics could be excluded completely from the former signal. Therefore the signal can be used to determine the amplitude and phase shift.

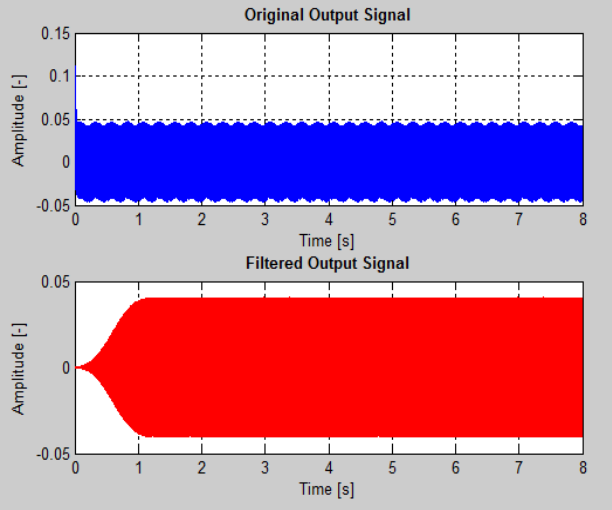

Figure 8:9 Filtered Signal in Time Domain (I)

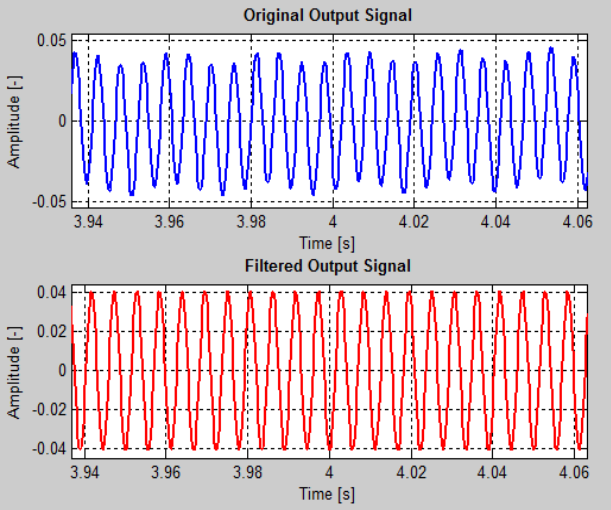

Figure 8:10 Filtered Signal in Time Domain (II)

8.1.2 Finding Intersection

To determine amplitude and phase response, the output signal has to be analyzed precisely. The amplitude response can only be computed when steady oscillation behavior is reached. That is explained in detail in section 2.4. Now the objective is to determine the intersections of the output signal. Between these intersections positive and negative half-waves are located. The half-waves necessarily contain amplitudes. When the amplitudes and areas underneath the curve of two consecutive half-waves are nearly the same, steady oscillation is reached. For this reason the intersections are important for integration limits. Furthermore, they are needed to compute the phase shift between output and input signal.

A function has been created to detect all time steps in which a zero-crossing occurs in the signal. Therefore the signal value vector and the time vector have to pass to the function. The syntax is described below.

$$\left[[vecZero], [vecZeroPos], [vecZeroNeg], [tZeroPos], [tZeroNeg]\right] = \boldsymbol{calcZeroCrossings}([signal\ values], [time]) \tag{8-11}$$

With:
- $vecZero$ ⟶ Vector with all intersection
- $vecZeroPos$ ⟶ Vector with only positive intersections
- $vecZeroNeg$ ⟶ Vector with only negative intersections
- $tZeroPos$ ⟶ Time span vector for positive intersections
- $tZeroNeg$ ⟶ Time span vector for negative intersections

The zero-crossings of a signal can be described in two different ways. Before the signal is intersecting the x-axis it can be positive or negative. Therefore, the terms ‘positive zero-crossing’ and ‘negative zero-crossing’ shall be introduced. When the signal intersects from positive to negative, a positive zero-crossing can be detected. When the function has a negative value before intersecting the x-axis, a negative zero-crossing can be detected. This is illustrated in Figure 8:11 below.

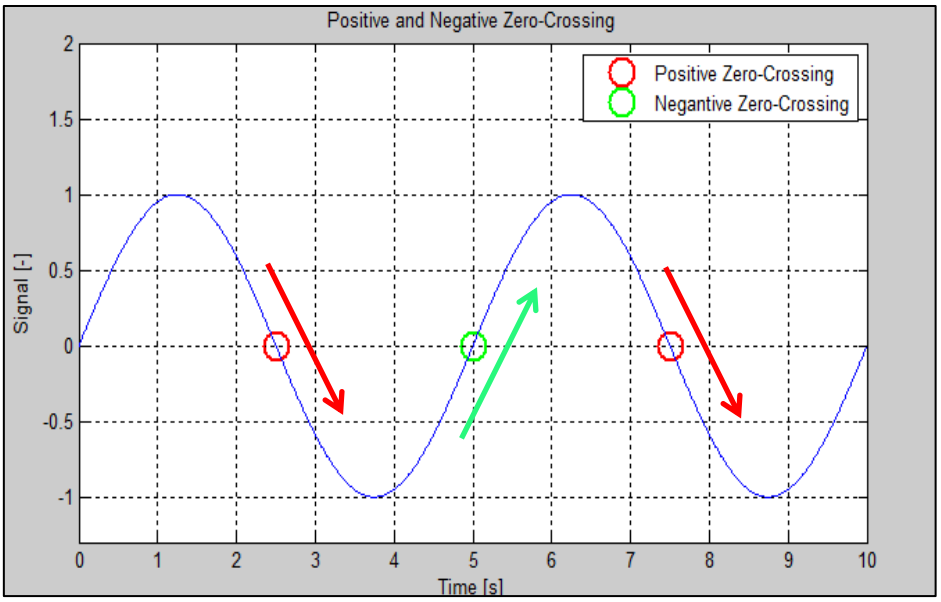

Figure 8:11 Positive and Negative Intersections

In this way the function is sorting the positive and negative zero-crossings out of the signal and stores their relating time values. Depending on if they are positive or negative, the values get stored in vector „*vecZeorPos*“ or „vecZero*Neg“*. The column numbers where the zero-crossings are located in the time vector are stored into the vectors “*vecZero*”, “*tZeroPos*” and “*tZeroNeg*”. Vector “*vecZero*” contains all the column positions of both zero-crossing types. Whereas “*tZeroPos*” and “*tZeroNeg*” just contains the positive and negative ones. The flow chart in Figure 8:12 below illustrates the procedure of the function.

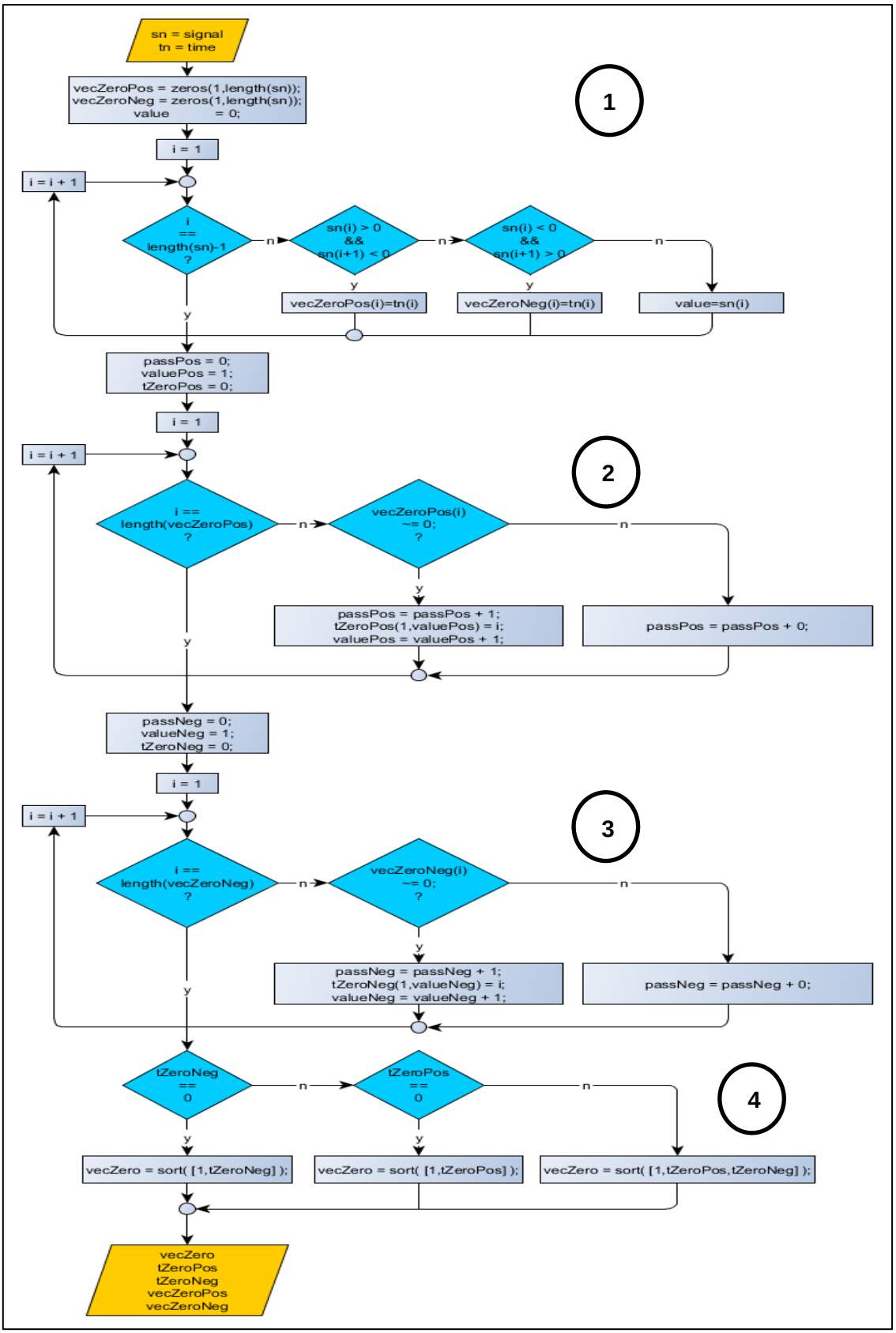

Figure 8:12 Computing Intersection Values

At first it has to be looped through signal vector, checking at any position if the current value is bigger than zero and if the following is less than zero. If so, it detects a positive zero-crossing and adds this time to the vector *vecZeroPos*. The same procedure is applied for negative zero-crossing with switched operators (①).
Then, it has to be checked how many positive and negative zero-crossings occurred. Total number of both get detected and stored in *passPos* respectively *passNeg*. Then the function loops through the vector *vecZeroPos* and checks if the current value is not equal to zero. If so, the value gets stored in vector *tZeroPos* otherwise the counter increases (②).
To determine the negative zero-crossing, the same procedure as it is described in ② has to be applied. The positions get stored in *tZeroNeg* (③).
Finally, the all zero-crossings get stored in one vector one after another (④).

8.1.3 Determining Zero-Matrixes

Building up zero-matrixes is important because Matlab does not fill up an array with an inconsistent number of vectors by itself. But especially in the beginning, when the natural frequency interferes with the excitation frequency, the resulting frequency can vary. That means one period in the beginning can have more discrete measured data points. This is why the length of the different vectors for all the half-waves is going to be different as well. To bring them all together a zero matrix is needed. The *calcZeroMatrixes* function has the task of producing zero matrixes for the positive and negative half-waves. They were designated as *posMat* and *negMat*. Therefore, it has to be known at which time point a zero-crossing occurs and how many positive and negative half-waves are contained in the signal. For this reason *calcZeroMatrixes* also uses the outputs from *calcZeroCrossings* which is described in the previous section.

$$\begin{aligned}&\left[[posMat],[negMat],[lMat],[l]\right]=\\&\boldsymbol{calcZeroMatrixes}(switcher,[vecZero])\end{aligned} \tag{8-12}$$

With:
- $posMat$ ⟶ Zero matrix for positive half-waves
- $negMat$ ⟶ Zero matrix for negative half-waves
- $lMat$ ⟶ Row dimension of *posMat* and *negMat*
- l ⟶ Time span vector for positive intersections
- $switcher$ ⟶ Boolean value which indicates if the first value in the signal is positive (1) or negative (0)
- $vecZero$ ⟶ Vector with all intersection

The column number of the zero matrix has to have the same length as the number of data points measured for the longest half-period. The number of rows depends on the number of

positive and negative half-waves contained in the signal. After building up these two matrixes, they can be filled up with the data points detected from the output signal. Every row is supposed to contain the data points for one half-wave, but in the end just the maximum value is of importance.

Furthermore, it is important to know if the signal starts with a positive or a negative value. For this reason, the second value of the signal is checked whether it is bigger than zero or not. The first value of the signal cannot be used for checking purposes because it will be zero due to the reaction time the system needs. What kind of different signal sequences are possible is shown in Table 8-2 below. The first value at t = 0s is considered as a zero-crossing, although it is not falling below zero. This exception has to be made otherwise the first half-wave cannot be considered.

Table 8-2 Signal Characteristic

	Even number of zero-crossings	***Odd number of zero-crossings***
Signal starts in positive range	① 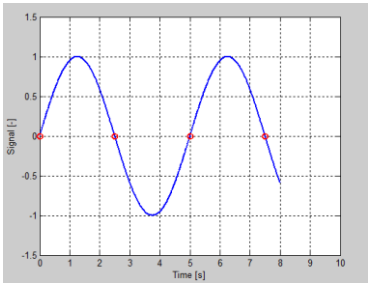	② 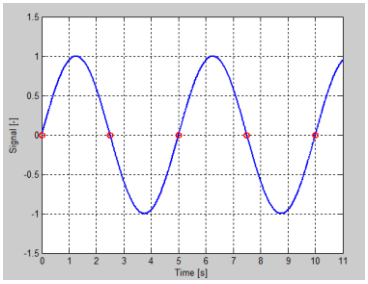
Signal starts in negative range	③ 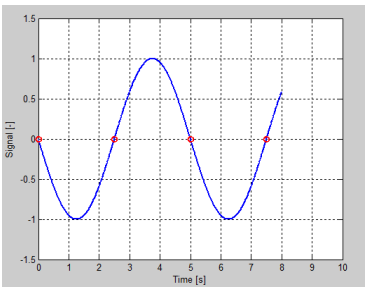	④ 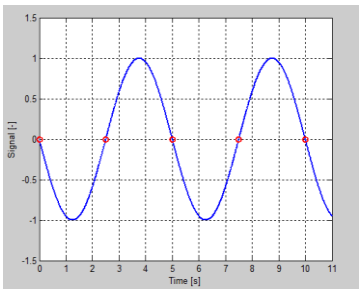

Table 8-2 points out that it is important to know how many zero-crossings the output signal has and if it starts in the positive or negative range. Comparing the two signals ① and ④ shows the difference. Signal ① has four zero-crossings and starts in positive range whereas Signal ④ contains five zero-crossings and starts in negative range. That means signal ① would need a 2xm matrix for positive half-waves and 1xm for negative half-waves. Signal ④ would need a 2xm matrix for both. This has to be taken into account for the implementation of zero matrixes. Out of the four different constellations result four different calculation methods. Hence the four following charts point out explicitly how many positive respectively negative half-waves are contained in the signal at a certain number of zero-crossings and starting range.

①

Table 8-3 Column Dimension Case 1

i	*number of zero-crossings*	*number of columns*	
		positive	*negative*
1	2	1	0
2	4	2	1
3	6	3	2
4	8	4	3
5	10	5	4

From the chart above the calculation method for the number of rows needed in *posMat* and *negMat* can be deduced:

- total number of columns for positive half-waves matrix = number of crossings – i
- total number of columns for negative half-waves matrix = number of crossings – (i – 1)

②

Table 8-4 Column Dimension Case 2

i	*number of zero-crossings*	*number of columns*	
		positive	*negative*
1	3	1	1
2	5	2	2
3	7	3	3
4	9	4	4
5	11	5	5

⟶ total number of columns for positive half-waves matrix = number of crossings – (i + 1)

⟶ total number of columns for negative half-waves matrix = number of crossings – (i + 1)

③

Table 8-5 Column Dimension Case 3

i	*number of zero-crossings*	*number of columns*	
		positive	*negative*
1	2	0	1
2	4	1	2
3	6	2	3
4	8	3	4
5	10	4	5

⟶ total number of columns for positive half-waves matrix = number of crossings – (i + 1)

⟶ total number of columns for negative half-waves matrix = number of crossings – i

④

Table 8-6 Column Dimension Case 4

i	***number of zero-crossings***	***number of columns***	
		positive	***negative***
1	3	1	1
2	5	2	2
3	7	3	3
4	9	4	4
5	11	5	5

⟶ total number of columns for positive half-waves matrix = number of crossings – (i + 1)

⟶ total number of columns for negative half-waves matrix = number of crossings – (i + 1)

Firstly the function creates four arrays with the content of Table 8-3 to Table 8-6 which makes them available in the Matlab Workspace. These tables have to be implemented in Matlab as arrays. According to their table number they are named *mat1*, *mat2*, *mat3* and *mat4*. How the function builds them is illustrated in Figure 8:13 below.

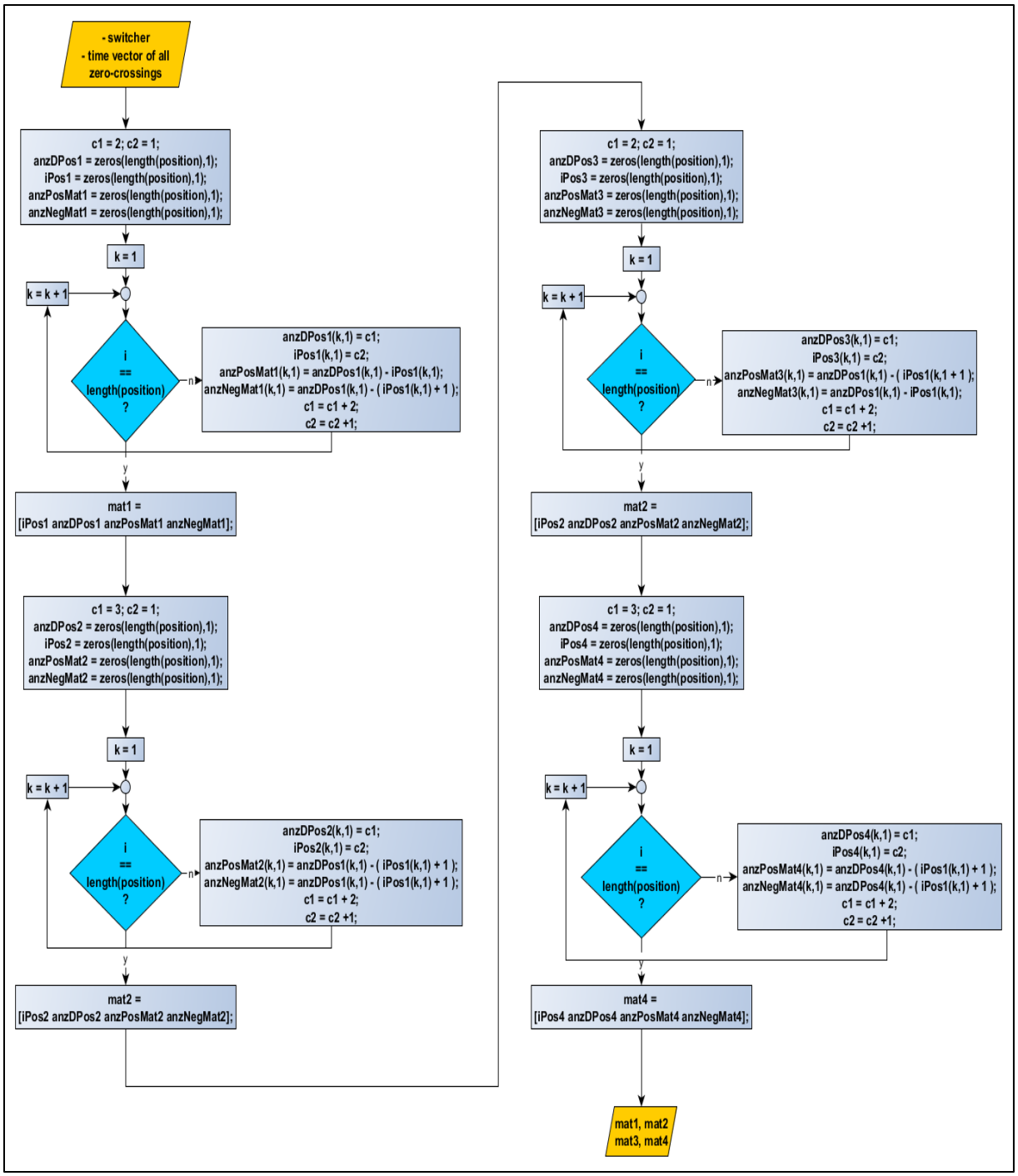

Figure 8:13 Flow Chart of Computing Signal Characteristic Arrays

During the functions further procedure the maximum number of columns *lMat* is calculated. Due to the fact that vector *vecZero* contains all the position numbers of the output signal, it just has to be calculated how many data points are in between one zero-crossing to another. These numbers get stored in vector *l*. The maximum value of this vector is then equal to the row number *lMat*. This procedure is implemented with a for-loop and is illustrated by Figure 8:14 in the flow chart below.

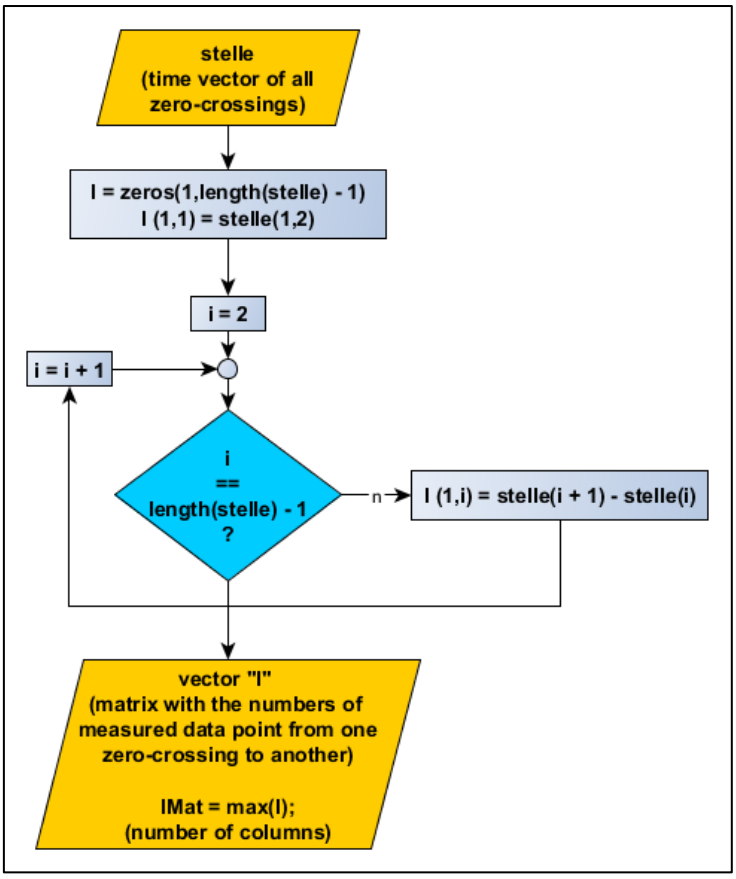

Figure 8:14 Flow Chart of Computing the Row Dimension

During the last part of the function, two switch-case loops firstly determine which type of output signal has to be evaluated. The outer switch-case loop, which is represented by the red box in Figure 8:15 below, checks for the value of “switcher”. It can either be positive (1) or negative (0) and represents the starting range.

Afterwards *anzD* (abbr. number of intersection) is used to find out if the number of zero – crossings is even or odd. Then a for-loop is used to loop through the second column of the array *mat1*, *mat2*, *mat3* or *mat4* and check whether the current value is equal to the total number of zero-crossings or not. If so, *mat1* to *mat4* can easily be used to read out the rows for *posMat* and *negMat* needed. If not, the counter “i” is getting increased by one.

Finally, the dimensions for *posMat* and *negMat* are fixed and the zero-matrixes can be built. Figure 8:15 below illustrates the described procedure.

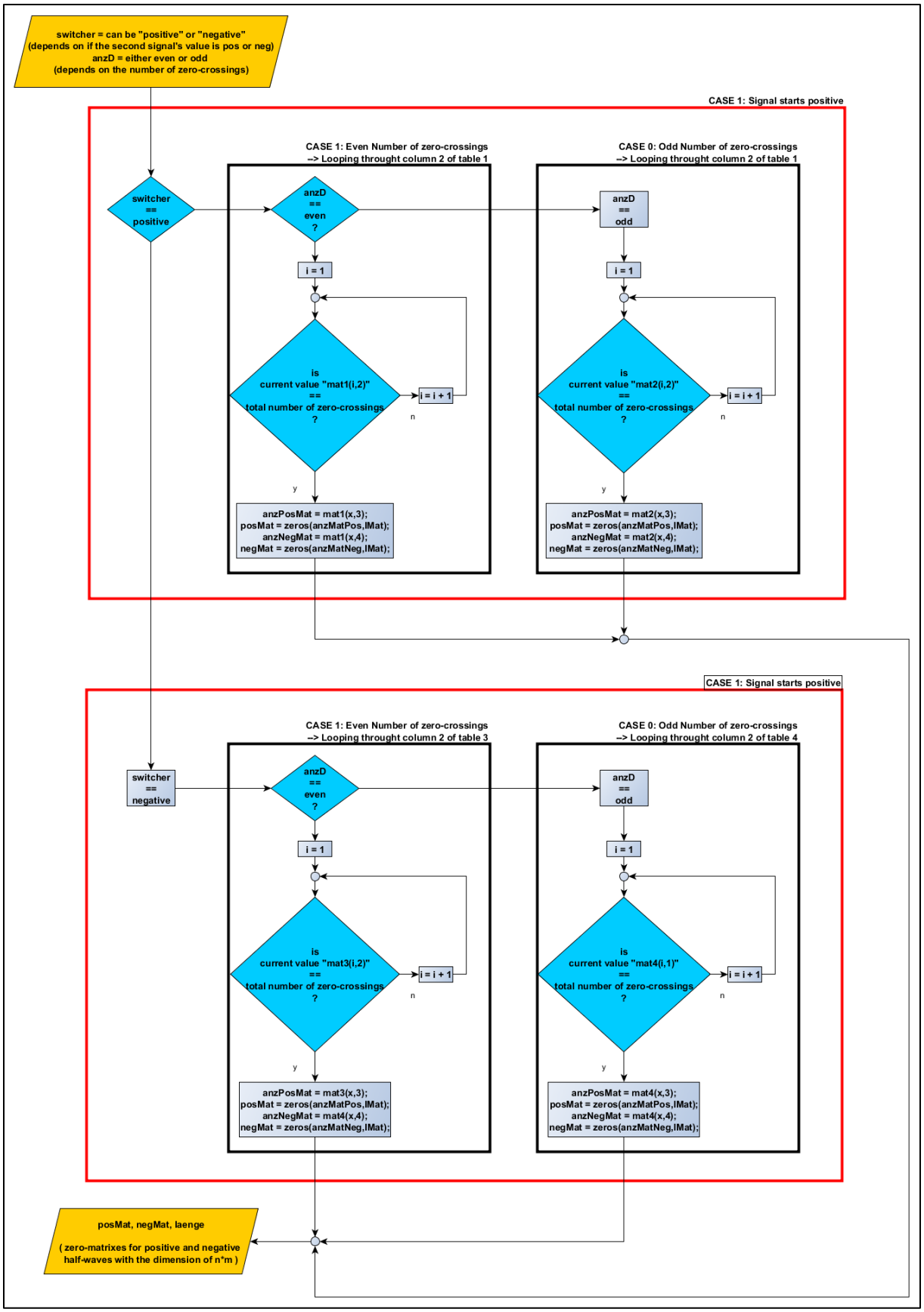

Figure 8:15 Flow Chart of Computing Zero Matrixes

8.1.4 Compute Amplitude and Phase Shift

This function computes the steady-state amplitude of a dynamic system's output signal. It also determines the phase shift compared to the dynamic system's input signal. The syntax is as following:

$$[amplitude, phase] = \boldsymbol{calcAmpPhs}([time], step\ size, [input\ signal], [output\ signal]) \quad (8\text{-}13)$$

This function firstly calls the described two functions "*calcZeroCrossings*" and "*calcZeroMatrix*". These provide the information about the intersection and zero-matrixes to fill in values. Firstly the function identifies how many data points are available between the first two intersections. That provides the information how many columns from the first row are needed. The next step is to find out which values from the output signal are necessary to extract and to put there. This information is contained in vector "*vecZero*" (cf. calcZeroCrossings) which contains the positions of all zero-crossings in the output signal.

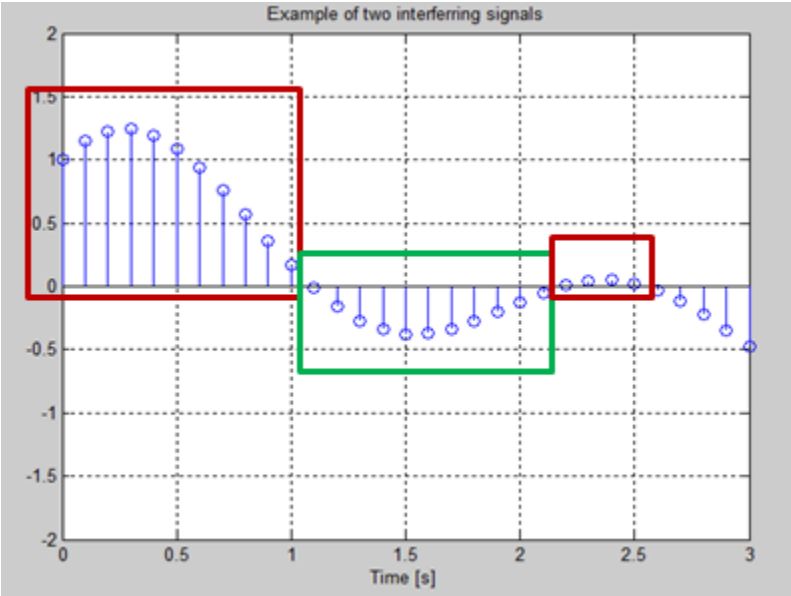

Figure 8:16 Superposed Signal

Therefore the function reads out the positions of the first and second intersection. Then, all values between those positions get read out and transferred to the first row of "*posMat*" or "*negMat*". Now the function fills up both matrixes alternately with exactly the same procedure. A simple example below shows how the algorithm is detecting a given signal and filling up both zero-matrixes. The first positive eleven values (left red box in Figure 8:16) get stored in the first row of *posMat*. Then, the negative data points marked with the green box are supposed to get stored in the first row of "negMat". Finally the last four values are added to the second row of "posMat". Due to the smaller number of data points the remaining columns are already filled with zeros.

That is exactly what the matrixes in Matlab Workspace are indecating. This is shown in Figure 8:17 and Figure 8:18.

posMat

2x11 double

	1	2	3	4	5	6	7	8	9	10	11
1	1	1.1471	1.2277	1.2419	1.1938	1.0908	0.9434	0.7637	0.5652	0.3616	0.1659
2	0.0062	0.0417	0.0491	0.0251	0	0	0	0	0	0	0
3											

Figure 8:17 Positive Matrix Array

negMat

1x11 double

	1	2	3	4	5	6	7	8	9	10	11
1	-0.0102	-0.1575	-0.2693	-0.3420	-0.3751	-0.3714	-0.3361	-0.2770	-0.2032	-0.1249	-0.0520
2											
3											

Figure 8:18 Negative Matrix Array

The next step is to loop through all the columns row by row to find the highest value per row which is the amplitude for one half-wave. All amplitudes are stored in vector “maxWertPos” (cf. maximum positive value).

The algorithm is now able to compare one amplitude with the following to detect when the difference between them is acceptably small and the steady state oscillation is reached. But the matching of amplitudes is not the only criteria. Furthermore, the area underneath two consecutive half-wave with the same sign has to be almost identical. As shown in Figure 8:19, two consecutive amplitudes with the same sign can be almost equal without reaching a steady oscillation yet. For this reason, an integration between two intersection points has to take in account as well.

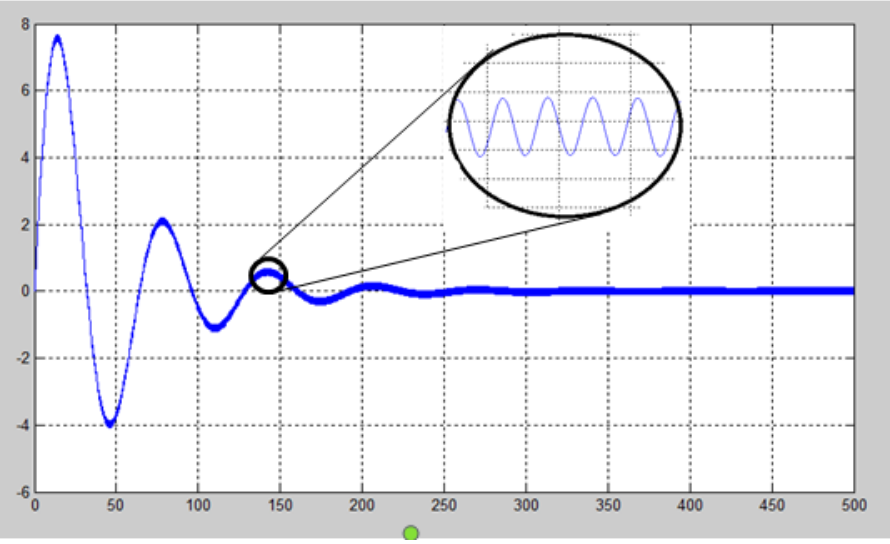

Figure 8:19 Checking for Steady-State Amplitude Behavior

To be able to compare the amplitudes and calculate the integrals, the algorithm has to check for the bigger amplitude first. That can be either the current amplitude or the one for the next iteration step.

Therefore, the function detects for each iteration step which amplitude is bigger, sets that amplitute to 100% and calculates the maximum deviation possible. This deviation can be at most 0.05% less then the bigger amplitude, otherwise the function continues. If the difference is in between acceptable boundaries, the zero-crossings get detected depending what position the bigger amplitude has. The zero-crossings are important as boundaries for the integral. The two different possibilities are illustrated for a better understanding in the figures below.

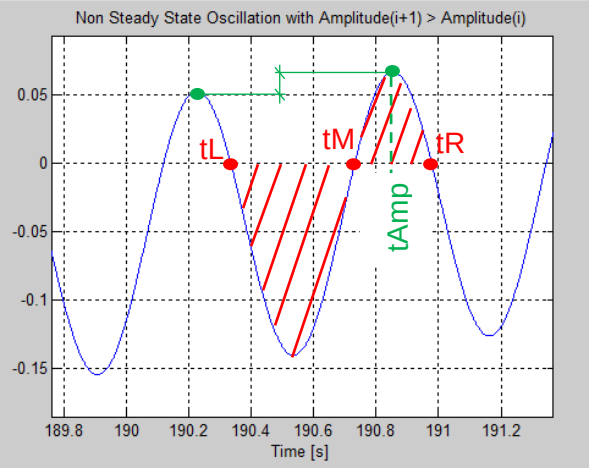

Figure 8:21 Non-Steady-State Oscillation (1)

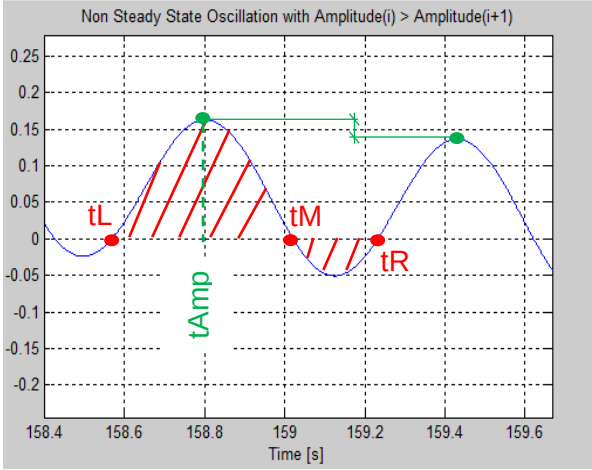

Figure 8:20 Non-Steady-State Oscillation (2)

As shown in Figure 8:20 and Figure 8:21, there are the time values tL (cf. time left), tM (cf. time middle) and tR(cf. time right) to set the integration boundaries. They depend on the time where the amplitude gets detected. This time is illustrated as tAmp in the figures above. Then, two integrals can be computed. It is either:

$$A_{i+1} > A_i: \quad y_{pos} = \int_{tM}^{tR} output\ signal\ (t)dt$$
$$y_{neg} = \int_{tL}^{tM} output\ signal\ (t)dt \qquad (8\text{-}14)$$
$$\rightsquigarrow \quad diff = |y_{pos}| - |y_{neg}|$$

$$\text{or } A_i > A_{i+1}: \quad y_{pos} = \int_{tL}^{tM} output\ signal\ (t)dt$$
$$y_{neg} = \int_{tM}^{tR} output\ signal\ (t)dt \qquad (8\text{-}15)$$
$$\rightsquigarrow \quad diff = |y_{pos}| - |y_{neg}|$$

The bigger absolute result of y_{pos} and y_{neg} is then set to 100%. If the difference *diff* is smaller then 0.05% from the absolute value, the steady state oscillation is reached and the steady state amplitude at the time step "*tAmp*" is found.

Now the phase shift can be calculated. As already mentioned in section 2.4, the phase shift in the time domain is a time delay from output to input signal. Thus function „calcZeroCrossings" computes the zero-crossings of the input signal first. Based on the fact where the bigger amplitude is located – right-hand sided or left-hand sided – there is a different way of calculating the phase shift. To calculate the phase shift, only the positive zero-crossings matter. In case of $A_{i+1} > A_i$ time *tR* is important. For the other case time *tM* has to be used.

If *tR* or *tM* is computed, the function loops through the input vector searching for the last zero-crossing time befor *tR* or *tM.* From that difference it is now possible to calculate the phase shift according to the following steps.

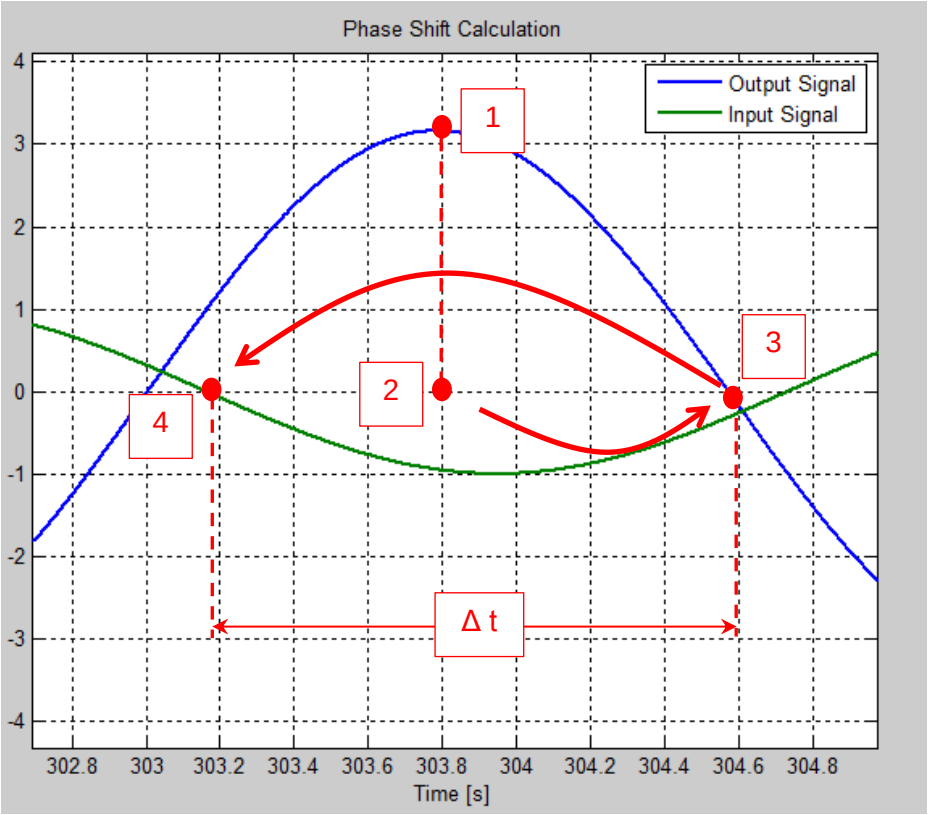

Figure 8:22 Computation of Phase Shift

The figure above illustrates the computing steps in detail. The output signal is blue, the input signal is green and the steps of calculation are illustrated in red. The first step is to calculate the steady state amplitude. During the second step the matching time is sorted out and afterwards the subsequent time of the next positve zero-crossing of the output signal.

In the fourth step the function loops through the input signal vector and detects the next zero-crossing following. At this point the time gets extracted and the difference between time at point three and four can be calculated.

$$\longrightarrow t\ at\ position\ 3\ \equiv\ t_{OUT}$$

$$\longrightarrow t\ at\ position\ 4\ \equiv\ t_{IN}$$

$$\rightsquigarrow \Delta t = t_{OUT} - t_{IN} \tag{8-16}$$

$$\rightsquigarrow \varphi^{[°]} = {}^{\varphi^{[rad]}\ \cdot 180°}/_{\pi} = 2 \cdot \pi \cdot f \cdot \Delta t \cdot {}^{180°}/_{\pi} = 360° \cdot f_{IN} \cdot \Delta t \tag{8-17}$$

Due to the fact that the system always oscillates at least with the same phase but never with a leading one, this computing method can also be applied to systems with a phase shift of almost 360°. The datasheet of the proportional valve indicates that the maximum phase shift is 270°.

The Figure 8:23 below shows four different sine waves with a phase shift up to 270 °. As the figure illustrates, there is no problem to apply this function to systems with less then 360° phase shift.

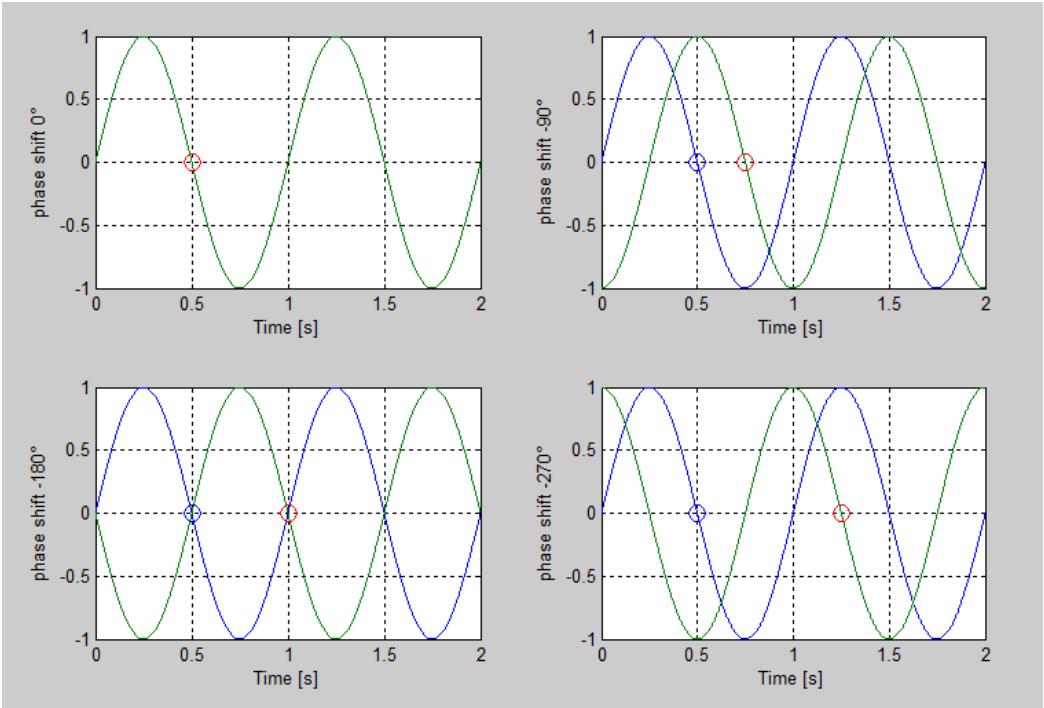

Figure 8:23 Influence of Phase Shift

After finishing the computation, function *calcAmpPhs* transfers the values of steady state amplitude and phase to the Workspace which makes them accessible for further calculations.

8.1.5 Optimization

The implemented functions from section 8.1.2 to 8.1.4 shall be used to optimize a linear second order transfer model. The parameters for the gain factor K, damping factor ζ and eigen angular frequency ω_0 were initially set. For a general linear second order system, following term is valid:

$$G(s) = \frac{K \cdot {\omega_0}^2}{s^2 + 2\zeta\omega_0 s + {\omega_0}^2} \tag{8-18}$$

$\curvearrowright$

$$A(\omega) = |G(j\omega)| = \frac{K \cdot {\omega_0}^2}{\sqrt{({\omega_0}^2 - \omega^2)^2 + (2\zeta\omega_0\omega)^2}} \tag{8-19}$$

with:
$$K = 5$$
$$\zeta = 0.8$$
$$\omega_0 = 50$$

Therefore, the system can be simulated over a wide range of frequencies. Now, the simulation data can be used as measurement points. For this reason a general second order system can be optimized for these data points. The following figure points that out. Two optimization computations have been executed. Thereby the maximum number of iterations is set to 30 and 80. Only filtering is not necessary due to the linearity of the transfer function.

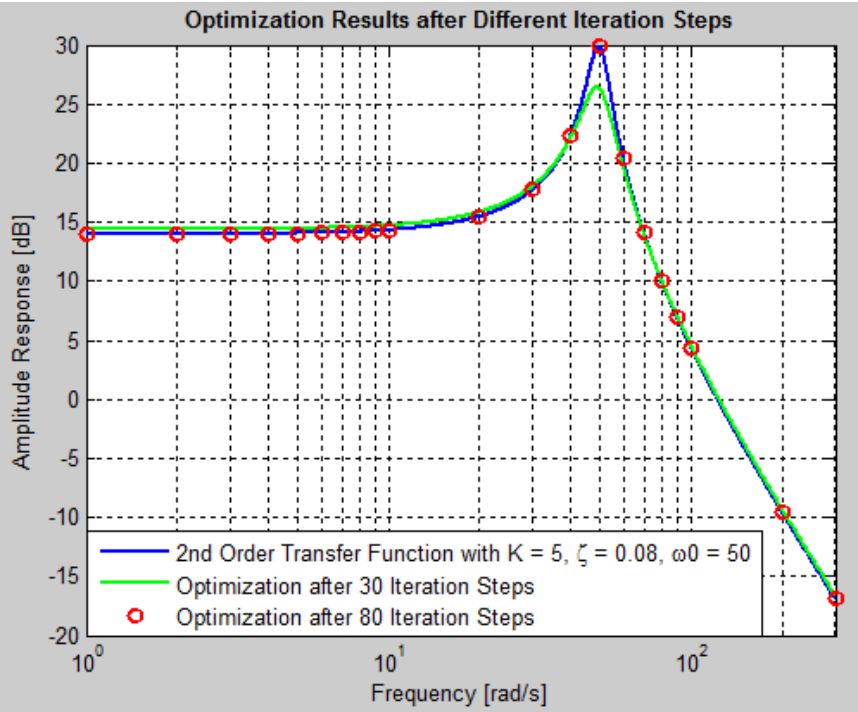

Figure 8:24 Optimization Results Linear System

The figure points out that after 30 iteration steps a good approximation can be already seen. Sorely the area around the natural angular frequency is not good approximated. There are slight deviations recognizable. The simulation results for an optimization after 80 iteration

steps are illustrated in red. It can be seen that there is a very good approximation noticeable. This confirms that the implemented functions work properly.

Now, nonlinear optimization shall be applied. At first, the saturation characteristic to limit the velocity has to be found. This approach as well as the implemented function from the previous section shall be used to run an optimization of the proportional valve used in [17]. Comparing the results helps to verify a correct implementation. Afterwards the approach shall be applied to the proportional valve 4WRSE-10.

The Simulink model in Figure 8:3 does not have two general limiting blocks with a sudden saturation. [19, p. 187] reveals that a smooth saturation for velocity limitation combined with a sudden saturation for acceleration limitation minimizes the target function the most. For this reason, the smooth saturation shall be obtained by using an exponential function with negative exponent similar to a step response behavior of a PT1 element. The general equation to determine the step response behavior is shown in eqn. (8-20) below.

$$a(t) = K\left(1 - e^{-\frac{t}{T_V}}\right) \tag{8-20}$$

The value K represents the final gain value the function is reaching to. T_V is the time constant which indicates the time the function needs to reach 63% of the final value. The following figure illustrates the desired behavior the saturation block is supposed to have. From the figure the values for the final value and the time constant shall be determined.

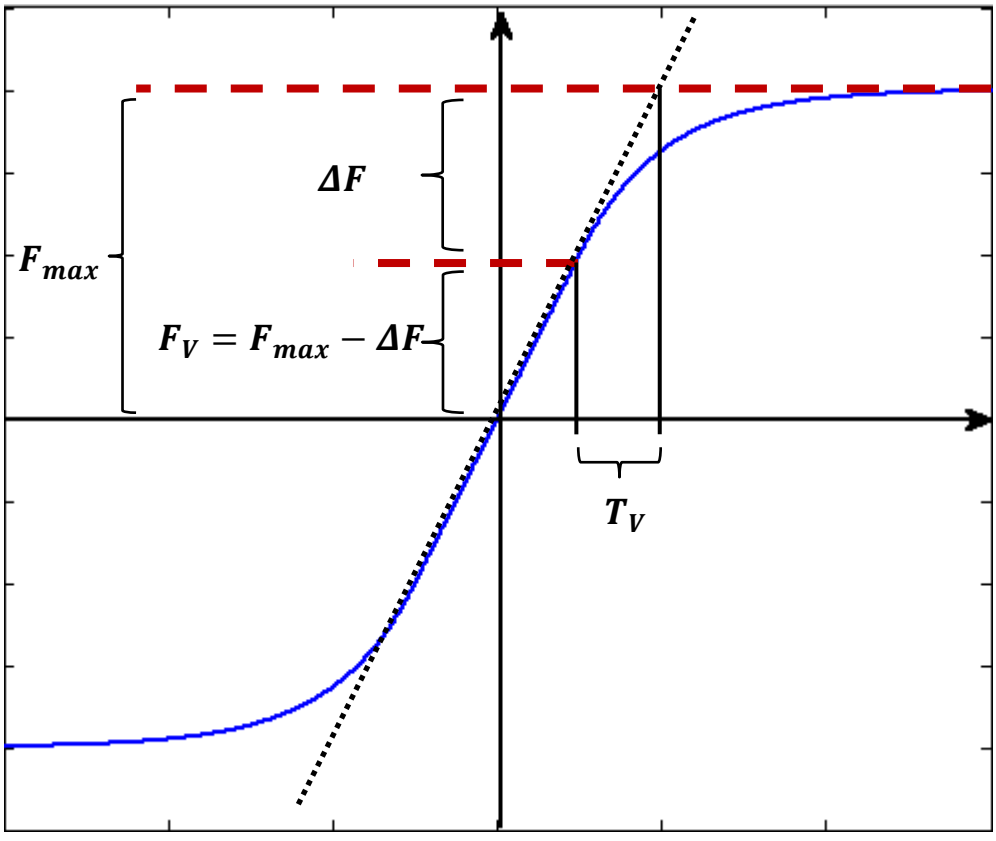

Figure 8:25 Determination of Velocity Saturation Parameters

According to Figure 8:25 the final value the function has to reach is F_{max}. The saturation block does not limit incoming values if they are less than F_V. Within the limits of $\pm F_V$ the input is equal to the output. The value of ΔF is determined to $0.5F_{max}$. Ratio equations can be used to determine the needed parameters.

$$\frac{T_V}{T_V + (F_{max} - \Delta F)} = \frac{F_{max} - \Delta F}{F_{max}} \tag{8-21}$$

$\sim$

$$T_V = {F_{max}}^2 / _{\Delta F} + \Delta F - 2F_{max} \tag{8-22}$$

With $\Delta F = 0.5F_{max}$ follows:

$$T_V = {F_{max}} / _2 \tag{8-23}$$

from that follows:

$$F_{out} = \begin{cases} F_V + \Delta F\left(1 - e^{-\frac{F_{in}+F_V}{K}}\right) : F_{in} \geqslant F_V \\ F_{in} \quad : -F_V < F_{in} < F_V \\ -F_V - \Delta F\left(1 - e^{\frac{F_{in}-F_V}{K}}\right) : F_{in} \leqslant F_V \end{cases} \tag{8-24}$$

In [19, p. 183] is mentioned that the saturation function is based on arc tangent function. This approach has a slightly lower slope than using (8-25). Thus it takes longer to settle at the final value.

The equation in (8-26) can be implemented in the Simulink model. The complete model is illustrated in section 12.7. In the following procedure the nonlinear Simulink model shall be optimized for the proportional valves KBSDG4V-3 (Vickers) from [17] and 4WRSE-10 (Bosch Rexroth). Thereby the optimization result for the KBSDG4V-3 valve can be compared to those in [17]. That allows to verify the implemented functions working together with the non-linear Simulink model.

The results were slightly different from those in [17]. Finally, the obtained values are:

Table 8-7 Optimization Results for Vickers Valve

Optimization Results	*Optimization Results from* [17, p. 246]
$\omega_0 = 950.73\ rad/s$	$\omega_0 = 1007\ rad/s$
$\zeta \ = 0.4823$	$\zeta \ = 0.48$
$L_v \ = 179.95\ s^{-1}$	$L_v \ = 125\ s^{-1}$
$L_a \ = 70{,}840.4\ s^{-2}$	$L_a \ = 81184\ s^{-2}$

Figure Figure 8:26 illustrates the simulation results of the Simulink model for these obtained values compared to the measurement curves. The plot demonstrates that the obtained val-

ues provide a good approximation to the measurement curves. Only for the amplitude curve of 25% of the maximum spool stroke a slight deviation at 80 Hz is noticeable. By comparing the results from [17, p. 246] it can be seen that only the approximation for the amplitude ratio of 25% is slightly better. There is no increasing amplitude ratio present at 80 Hz. This can be caused by the approach of the saturation function. Another aspect is that the measurement data is just measured from the datasheet and not from the manufacturer itself. This can be imprecise and can cause inconsistent curve characteristics. Additionally it affects the optimization quality as well.

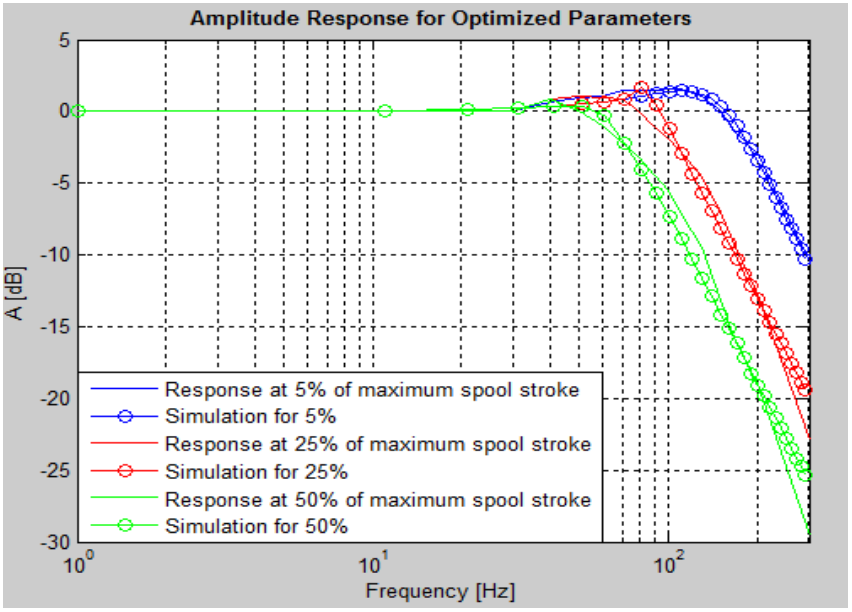

Figure 8:26 Amplitude Response KBSDG4V-3 (I)

For comparison, the obtained parameters from [17] (Table 8-7) get passed to Simulink Model. The results are illustrated in Figure 8:27. It can be seen that there is a very good approximation for the amplitude ratios of 5% and 25%. But the simulated curve of 50% has a slightly bigger deviation.

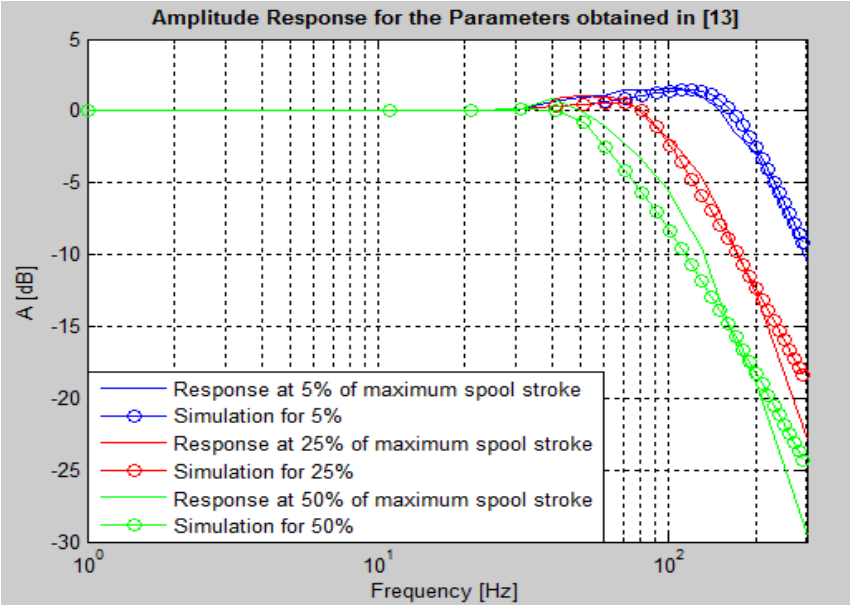

Figure 8:27 Amplitude Response KBSDG4V-3 (II)

The obtained results provide a good approximation compared to the results obtained in [17]. Therefore, it can be concluded that the implementation of the nonlinear Simulink model as well as their belonging function is correct. With this verification the optimization shall be applied to the Bosch valve 4WRSE-10. The optimization result for the parameters is:

$$\omega_0 = 336.7663\, rad/s$$
$$\zeta = 0.4542$$
$$L_v = 77.14\, s^{-1}$$
$$L_a = 128{,}700\, s^{-2}$$

These parameters can be used to plot the amplitude responses together with the measured data. In Figure 8:28 can be seen that the deviation from simulation to measurement is quite large. Only the Amplitude curve for 100% spool stroke has an acceptable approximation.

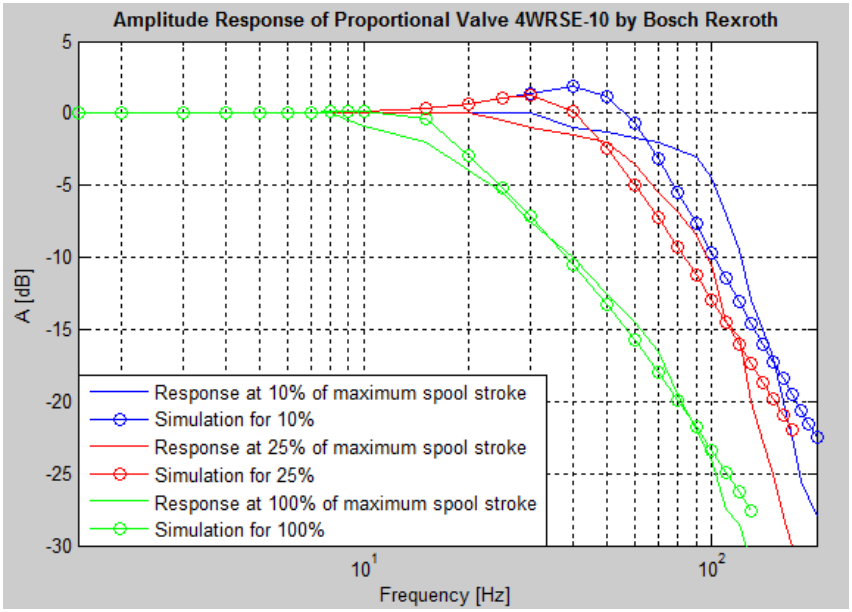

Figure 8:28 Amplitude Response 4WRSE-10

The target function stabilized at a value of 1020.38 which is $F_{target} = 1020.38$, being quite large. For a good approximation the target function value is supposed to be between 5 and 40. Different sets of initial values have been tried to exclude local minimum solution. These are shown in the following Table 8-8.

Table 8-8 Initial Values for Optimization of 4WRSE-10

	ω_0 $[rad/s]$	ζ $[-]$	L_v $[s^{-1}]$	L_a $[s^{-2}]$	$Abort\ Iteration$ $at\ step$	F_{target}
$[x_{init1}]$	900	0.5	100	90,000	140	1052
$[x_{init2}]$	70	1	200	50,000	135	1073
$[x_{init3}]$	625	900	70	10,000	142	1020.38

As Table 8-8 illustrates, the different sets of initial values lead all to the same result. The target function stabilizes at a value of around 1050.

The results for the proportional valve 4WRSE-10 are not as satisfying as those for KBSDG4V-3. It can be assumed that the reason is the missing amplitude incensement. The curves of 4WRSE-10 indicate that there is no excitation frequency where the output amplitude gets amplified. The results for KBSDG4V-3 show that the implemented functions work pretty well. In [19] several Simulink model approaches had to be tested to find an appropriate model. A different approach for the Simulink model leads to better results more probably.

8.2 Static Model

Besides the dynamic behavior it is also necessary to determine the static behavior of the proportional valve. The static behavior describes the relationship between flow rate and pressure loss. The valve can be looked at as a built-in part. Built-in parts are components which get assembled in the pipe system of a hydraulic circuit. This can be fittings, nozzles, orifices, valves or filters. Thereby every built-in part has its own friction factor characteristics ζ. The friction factor describes the relationship between pressure loss Δp_{Loss} and flow rate Q. But there is no universal approach to pre-calculate pressure loss depending on the flow rate for every built-in part. Besides straight pipes the exceptions are nozzles and orifices. The other components have a higher complexity of geometrics which makes a theoretical approach difficult.

A general approach provides Bernoulli's law:

$$p + \rho\, g\, h + \frac{1}{2}\rho\, v^2 = const \qquad \text{(8-27) [4]}$$

By applying balance eqn. (8-27) from the input to the output of a given component under consideration of pressure loss follows:

$$p_1 = p_2 + \frac{1}{2}\rho\, v^2\zeta = p_2 + \frac{1}{2}\rho\, \frac{Q^2}{A^2}\zeta \qquad \text{(8-28)}$$

The dynamic pressure at in- and output as well as the static pressure height terms can be set to zero. Under this consideration the flow rate can be determined by solving (8-28) as following:

$$Q = \sqrt{\frac{1}{\zeta}}\, A \sqrt{\frac{2}{\rho}}\, \sqrt{|\Delta p|} = G\, \sqrt{|\Delta p|} \qquad \text{(8-29)}$$

Eqn. (8-29) consists of two factors which are hard to calculate. Factor A represents the area the valve provides for the oil to flow through. This area depends on the spool position. The size of the area directly affects the value of pressure loss factor ζ.

In return, the pressure loss depends on the Reynolds number which is a function of flow rate. But the flow rate has to be calculated. And so in the following procedure an approach shall be introduced to determine the conductance value G which indirectly determines the pressure loss factor ζ as well. But the prerequisite of this approach is to have explicit information of the valve such as measurement possibilities or datasheet information which is the same thing. Figure 8:29 below illustrates the general shape. According to [17] the conductance value G is now referred to pseudo-section function. With the help of Figure 8:29 all parameters needed to obtain the correct pseudo-section behavior shall be found.

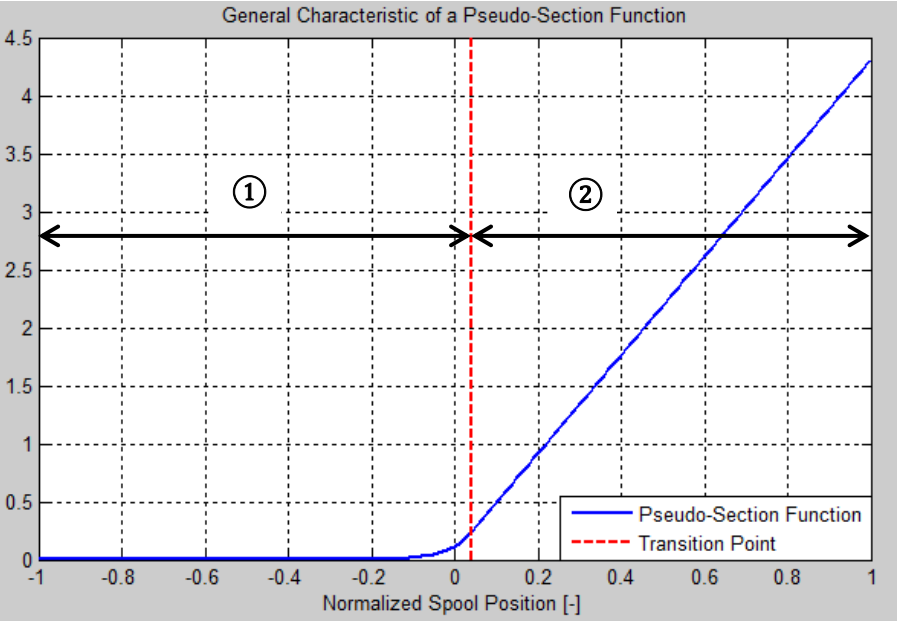

Figure 8:29 Pseudo-Section Function of Spool Position

As Figure 8:29 illustrates, there are two sections over the spool displacement which have a different behavior. Both are connected at the transition point. At a spool position from $-1 \leqslant \bar{x}_s \leqslant x_t$ the valve blocks that port aside from a small amount of leakage. But if the spool is almost reaching the transition point, a strictly non-linear behavior is noticeable. This is due to fabrication tolerances and cannot be avoided completely. By looking at the figure it becomes clear that it is necessary to know where the transition point is located in relation to the normalized spool position. Why the spool position has to be normalized is going to be explained later throughout this section.

If the spool displacement exceeds the transition point, a strictly linear behavior is noticeable. This is the main characteristic of a proportional valve. From these considerations it appears that there have to be found two functional equations for section ① and ② as well as for the transition point x_t. Section ① can be approximated as follows:

$$A\,(-1 \leqslant \bar{x}_s \leqslant x_t) = a\,e^{b\,\bar{x}_s} \tag{8-30}$$

Thereby the exponential function approximates the behavior around the transition point very good and also provides small values when the spool position is low. This represents the effect of leakage. The parameters a and b are used to adjust the function to the valve's characteristics. Section ② can be approximated by using a linear function with a small offset:

$$A\,(x_t < \bar{x}_s \leqslant 1) = c \cdot \bar{x}_s + d \tag{8-31}$$

To determine these parameters, the following approach according to [17] shall be used. The first step is to build a model of the proportional valve with all flow rates and differential pressures included. This is shown in Figure 8:30.

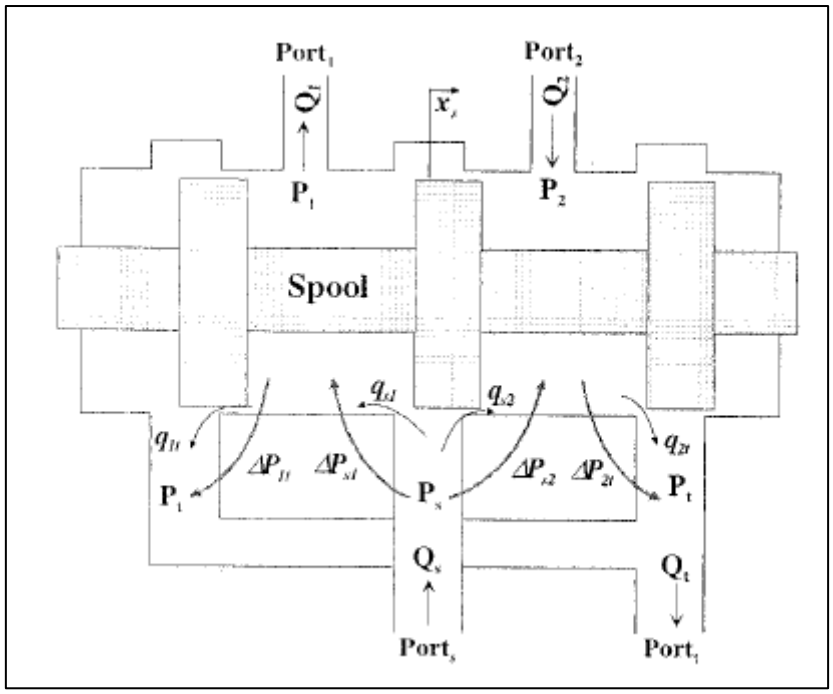

Figure 8:30 Static Spool Position Model [17]

According to Figure 8:30 there are different flow rates in and out of the valve. In this setup it can be assumed that $Port_1$ is connected to the cap end of an actuator while $Port_2$ is connected to the rod end. If a certain flow rate is supplied by the pump, oil flows in the cap chamber under high pressure and the piston extends. The extended piston replaces a certain volume in the rod chamber due to its displacement. That produces a flow rate through the valve to the tank with a lower pressure level. The outcome is a pressure difference between the two chambers of the valve. Therefore, the incoming flow rate generated by the pump splits up in leakage flow rate q_{s2} and q_{s1}. Thereby q_{s2} flows to the low and q_{s1} to the high pressure chamber as shown in (8-32).

$$Q_s = q_{s1} + q_{s2} \tag{8-32}$$

The flow rate Q_1 which extends the piston is the difference between q_{s1} and the loss due to leakage to the tank:

$$Q_1 = q_{s1} - q_{1t} \tag{8-33}$$

The flow rate Q_2 has to be the sum of the flow rate coming from the actuator and the leakage from the high pressure chamber:

$$Q_2 = q_{2t} - q_{s2} \tag{8-34}$$

Finally, the flow rate Q_t which goes back to the tank has to be

$$Q_t = q_{1t} + q_{2t} \tag{8-35}$$

From Figure 8:30 emanates that if the spool starts to move in positive or negative direction there are two control sections open. The other two are closed. According to [17] high perfor-

mance proportional valves are usually designed with matched and symmetrical control orifices. That means there might be four different control edge areas but they have the same geometry. Consequential, only one pseudo-section function has to be specified. But it is relevant that two of them are closing for positive spool displacement whereas the others opening. That leads to:

$$A_{s1} = A_{2t} = A_P(\bar{x}_s) \tag{8-36}$$

$$A_{s2} = A_{1t} = A_N(\bar{x}_s) \tag{8-37}$$

From that knowledge the inner valve flow rates can be specified to:

$$q_{s1} = sgn(\Delta p_{s1})\, A_P(\bar{x}_s) \sqrt{\Delta p_{s1}} \tag{8-38}$$

$$q_{s2} = sgn(\Delta p_{s2})\, A_N(\bar{x}_s) \sqrt{\Delta p_{s2}} \tag{8-39}$$

$$q_{1t} = sgn(\Delta p_{1t})\, A_N(\bar{x}_s) \sqrt{\Delta p_{1t}} \tag{8-40}$$

$$q_{s1} = sgn(\Delta p_{2t})\, A_P(\bar{x}_s) \sqrt{\Delta p_{2t}} \tag{8-41}$$

According to [17], the most important operating point is the central spool position because servo-systems usually operate near this region most of the time. To determine the correct static spool behavior depending on the spool position, several gain factors have to be introduced. Linear gain factors help to obtain how the displacement infects the system. Important gain factors for proportional valves are pressure and flow gain as well as the influence due to leakage. Hereafter shall be explained how certain gain factors can be estimated, which information have to be extracted from the manufacturers data sheet and how this is useful to obtain the values of the pseudo-functions needed.

▪ *Pressure Gain*

Instead of using an absolute gain, the pressure gain is notated relatively based to the supplied pressure at $Port_S$. Thus, the pressure gain can be understood as the derivative of relative load pressure to spool position.

$$\overline{K}_{p0} = \left. \partial \frac{\Delta p_L}{p_S} \middle/ \partial\, \bar{x}_s \right|_{\bar{x}_s=0} \tag{8-42}$$

The relative load pressure is the ratio of pressure difference between $Port_1$ and $Port_2$. Taking a look to the datasheet reveals out that the manufacturer provides exactly this measured characteristic.

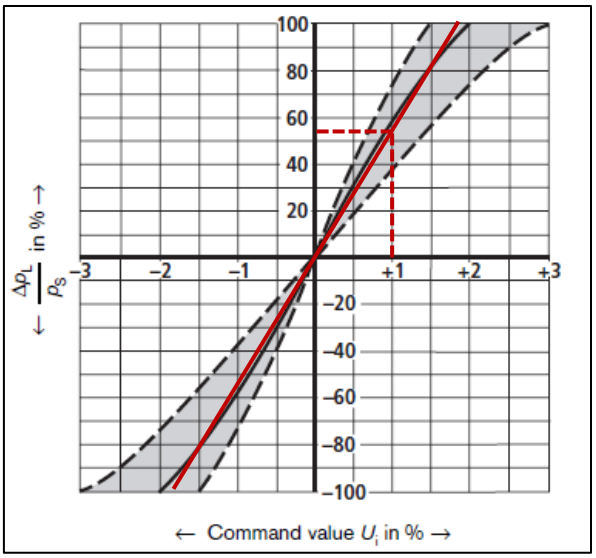

Figure 8:31 Pressure Characteristic Curve

The characteristic curve shows the almost linear behavior of relative load pressure in relation to the command value. The command value measured is not the spool position as Eqn. (8-42) might suggest. On the one hand this is due to the fact that the displacement isn't measurable under normal conditions because it is sealed in the housing. On the other hand the proportionality between input voltage and spool displacement helps to solve this problem. But it is necessary to normalize the values because a normalized change in voltage can automatically be transferred to a normalized spool displacement which likewise results in an almost linear pressure response.

From that perspective the pressure gain $\overline{K}_{p0}$ can be determined to 55.

▪ *Flow Gain*

To obtain the flow gain $\overline{K}_{q0}$ the derivative of the load flow under zero load pressure at the middle position has to be determined. The flow gain is also a linear estimated factor to predict the flow rate through the valve in relation to the displacement around the middle position.

$$\overline{K}_{q0} = \left.\frac{\partial Q_L}{\partial \bar{x}_s}\right|_{\bar{x}_s=0} \tag{8-43}$$

Figure 8:32 illustrates the measured flow curves for two nominal flows of 25 l/min and 75 l/min at a nominal differential pressure of $p_n = 10\ bar$. The used valve type 4WRSE corresponds to 25 l/min nominal flow. It is shown that the characteristic is almost perfectly linear. For this reason the derivative at every point is almost equal. This leads to $\overline{K}_{q0} = 25\ l/min$.

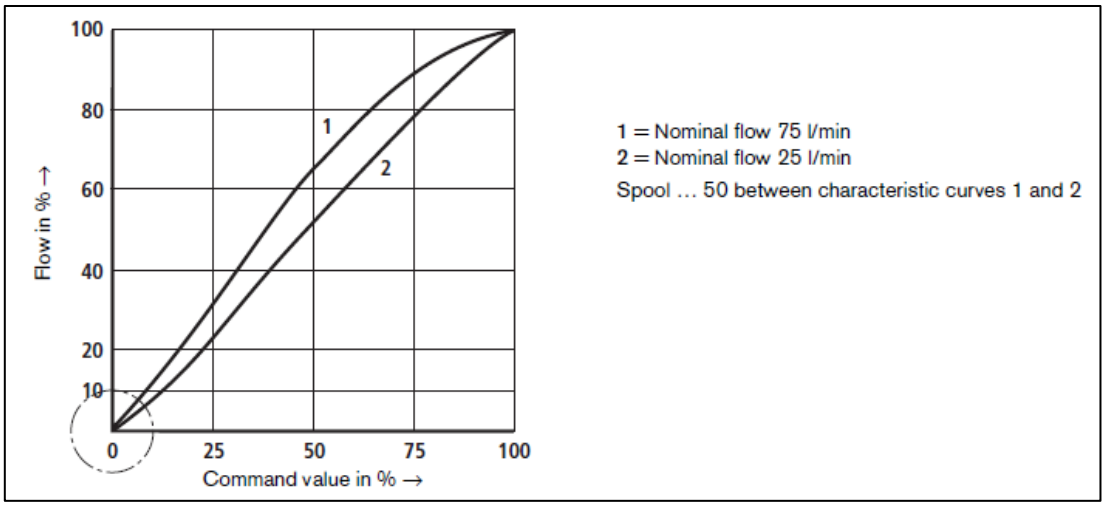

Figure 8:32 Flow Characteristic Curve

▪ Leakage Flow

By looking at Figure 8:33 the leakage flow rate q_{lk0} at central spool position can be obtained to $0.75\,l/min$ at a supply pressure $p_s = 100\,bar$. In genera,l leakage flow curves are only measured at central spool position. This is due to the fact that the valve acts most frequently around this position. Additionally, in middle spool position the overlap of all the leakage gaps is the shortest.

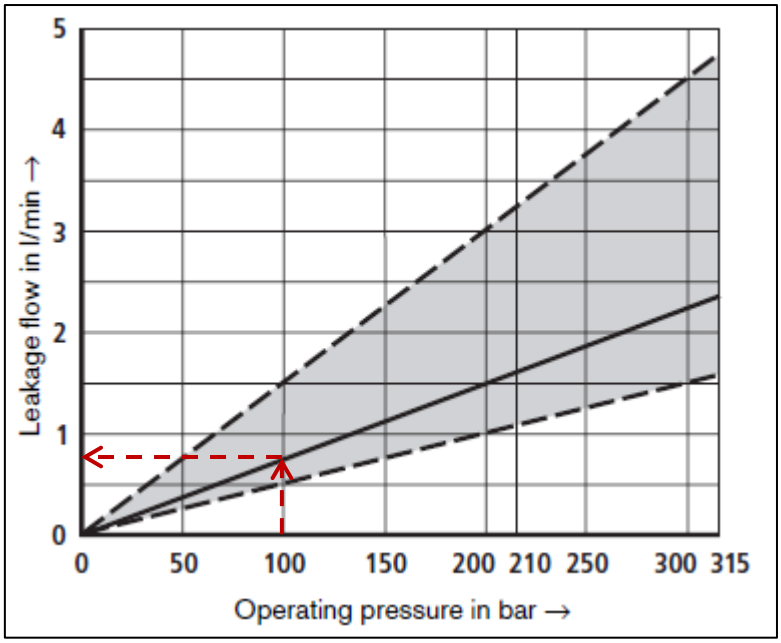

Figure 8:33 Leakage Flow

After extracting all important gain factors from the datasheet, the pseudo-section functions can be determined. According to [17] the functions for $A_n(\bar{x}_s)$ and $A_p(\bar{x}_s)$ can be calculated as follows:

$$A_n(\bar{x}_s) = \begin{cases} \gamma\, e^{-\frac{k\,\bar{x}_s}{2}}, & -x_t \leqslant \bar{x}_s \leqslant 1 \\ -\alpha\,\bar{x}_s + \beta, & -1 \leqslant \bar{x}_s < -x_t \end{cases} \tag{8-44}$$

$$A_p(\bar{x}_s) = \begin{cases} \alpha\,\bar{x}_s + \beta, & x_t \leqslant \bar{x}_s \leqslant 1 \\ \gamma\, e^{\frac{k\,\bar{x}_s}{2}}, & -1 \leqslant \bar{x}_s \leqslant x_t \end{cases} \tag{8-45}$$

Subsequently the values for each parameter of α, β, γ, k and the transition point x_t have to be found. The equations (8-44) and (8-45) describe the combined behavior of the conductance value depending on the spool position. Thereby the parameters in (8-44) and (8-45) build a connection with the gain factors determined by the datasheet.

$$k = \bar{K}_{p0} \tag{8-46}$$

$$q_{lk0} = \gamma\sqrt{2\,p_s} \tag{8-47}$$

$$\bar{K}_{q0} = k\,\gamma\sqrt{\frac{p_s}{2}} \tag{8-48}$$

$$\begin{aligned} \alpha\,x_t + \beta &= \gamma\, e^{\frac{k\,x_t}{2}} \\ \alpha &= \gamma\,\frac{k}{2}\,e^{\frac{k\,x_t}{2}} \\ Q_n|_{\bar{x}_s=1} &= (\alpha\,\bar{x}_s + \beta)\sqrt{p_n}\big|_{\bar{x}_s=1} \end{aligned} \tag{8-49}$$

At first k has to be calculated. As it is shown in (8-46), k is equal to the pressure gain at middle position. Depending on the application γ can either be estimated by using eqn. (8-47) or (8-48). This is due to the fact that the model can adjust only two parameters at the same time. Finally, the set of non-linear equations in (8-49) has to be solved.

The obtained values:

- $q_{lk0} = 0.75\ l/min$
- $\bar{K}_{p0} = 55$
- $p_s = 100\ bar$
- $p_n = 10\ bar$
- $\bar{K}_{q0} = 25\ l/min$
- $Q_n = 25\ l/min$

were computed with Matlab's built-in function $fsolve$. Following values could be determined:

- $\mathrm{k} = 55$
- $\beta = -0.21153$
- $\gamma = 0.0530$
- $x_t = 0.062423$
- $\alpha = 8.1172$

which leads to following pseudo-section functions:

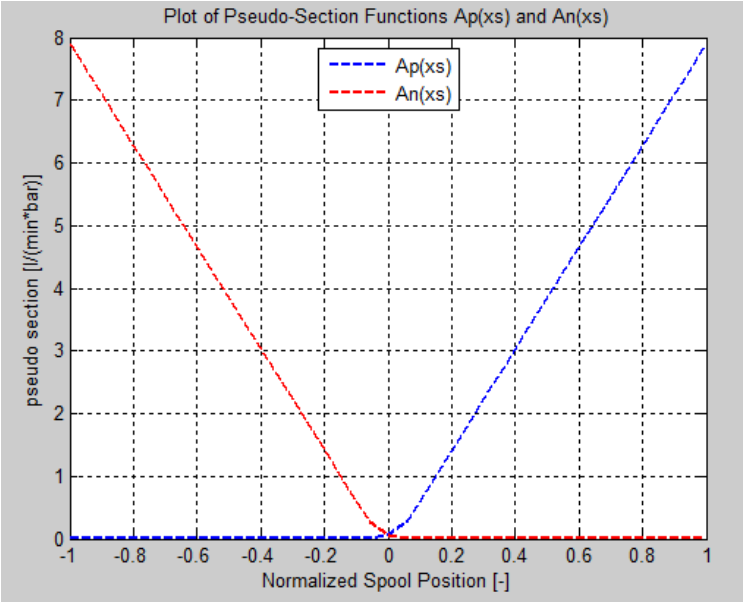

Figure 8:34 Pseudo-Section Function of Valve 4WRSE-10

8.3 Results

In this chapter simulation approaches for the static and dynamic behavior are presented. To model the dynamic behavior, a nonlinear Simulink model was implemented. The model is based on a second order linear system but with additional saturation blocks for velocity and acceleration to [17]. Because of the saturation blocks the model has to be reshaped. Due to the fact that the input amplitudes are normalized, a static gain factor is not necessarily to be implemented. To optimize the nonlinear model, several functions had to be implemented. They are used to filter the nonlinear output signal from the Simulink model for their excitation frequency, determine the intersection and needed zero matrixes to finally compute the amplitude and phase shift. Their functionality got tested by comparing the obtained results for an optimization with those from [17]. Due to a different saturation approach for the velocity limits, the results are slightly different but fully acceptable. Therefore the optimization approach is applied to the Bosch valve 4WRSE-10. It turned out that the target function stabilized around a value of 1050 for different sets of initial values. To obtain a good approximation, a target function value between 5 and 40 is desired. From that follows an imprecise approximation. Only the amplitude ratio curve for 100% of maximum spool stroke is approximated quite well. To obtain a better result, the Simulink model has probably to be adjusted most probably.

To create the static model, the characteristics of pressure and flow gain at the middle position as well as the leakage flow rate have to be determined. These parameters were obtained from the datasheet. A nonlinear system of equations had to be solved to obtain pseudo-section functions which describe the relationship between spool position and flow rate.

9 Summary and Discussion

Modelling a hydraulic system, several fundamental observations have to be made. It was shown which input and output parameters or energy storages are usual in hydraulic systems. This information is needful to determine balance equations as well as static relations to finally create a block diagram. On the one hand a block diagram helps to visualize all important factors which influence the simulated system. On the other hand it is helpful to build up a model in Simulink.

The proportional directional valve is the most important component in the circuit because of its controlling performance. Due to that its functionality was described, especially the LVDT. It was shown how the LVDT translates the input voltage into a linear spool displacement which is the main requirement for its good controlling abilities. It was pointed out that the proportional valve can be simplified to a second order spring-mass-damper system. For that reason, the dynamic behavior of forced oscillations was explained on a linear spring-mass-damper system in order to understand the dynamic behavior in a better way. It was explained that in the beginning of the oscillation the excitation frequency superposes with the natural frequency of the system. Furthermore it was shown that the natural frequency dies out over time due to the transient effect. Also the impact of a post and subcritical excitation on the oscillation characteristics was discussed. These considerations are needful to evaluate the present waveform in a time domain simulation. But usually, hydraulic valve manufacturer use frequency response curves to illustrate the dynamical behavior of their valves. To be able to understand these characteristics, frequency response plots were explained precisely. Due to the fact that the simulation is done in time domain, the connection between time and frequency domain was explained by introducing Fourier transform.

After fundamental considerations, the functionality of all circuit components together as a system in a closed loop circuit was explained. It is necessary to understand how the system works and where cutting points exist between the several parts. That helps dividing the main system into subsystems which simplifies the process of building models and simulating them due to the lower complexity.

Before subsystems can be created, an oil model needed to be developed. It was assumed that HLP 46 is used in the circuit. The viscosity, density and compressibility are the key properties of the oil. They depend from temperature and pressure. Due to the fact that the positioning unit only operates in short periods of time, the temperature influence was neglected. The density and kinematic viscosity were assumed to be constant. But for the bulk modulus a model is used which takes into account the dependence on pressure. That means a higher pressure in a certain capacity causes a higher bulk modulus.

After that, the pipe system was the first subsystem which was created. The pipes connect all the components with each other and they additionally act as pressure energy storage due to their capacity. From the dimensions and the bulk modulus model, the capacity can be determined. To simulate the march of pressure, a model of a pump producing a flow rate into a pipe system without an outlet was created. The simulation result showed a quick and linear increase of pressure in the pipe system. That increase was faster with a higher pump flow rate and a lower pipe capacity.

In the next step the hydraulic cylinder was modelled. Due to the fact that there was no datasheet with specific dimensions available, only a general model could be created. Firstly, a simplified in- and output flow rate model was created. Using this model, all energy storages and balance equations could be determined. Additionally, the dynamic balance of forces had to be incorporated. Thereby the friction force plays an important role. To characterize it properly, the approach in [13] was used. Among others this approach considers static and dynamic friction coefficients as well as a decay constant. The friction coefficients were extracted from [15] whereas it was necessary to make an assumption for the decay constant. Based on the model, a simulation of the extending piston was made. It could be shown that the piston extracts with constant velocity and when the end position is reached, it remains there.

Then, the PRV was modelled based on the dimensions from the manufacturer's datasheet. But not all dimensions or material constants which were necessary for the simulation are pointed out in the datasheet. For this reason the spool dimensions had to be estimated by the dimensions from the valve housing and the cartridge. Expecting an opening pressure of 200 bar, the spring constant was set to 100000 N/m which led to a preload displacement of 10.1 mm. Based on those assumptions, a model was created in Simulink. The behavior of the PRV for different pump flow rates in a closed pipe system was examined. It came out that the valve stabilized quicker the higher the pump flow rate was. But a higher pump flow rate also caused a higher pressure peak due to the inertia of the system. It can be concluded that the selected spring constant is well suited for the performance at high pressures. Due to the fact that the dynamic simulation is mostly based on assumptions, a static model was developed. Using a PT1 characteristic with a low time constant, the static relationship between flow rate and pressure could be simulated very well.

Finally, the proportional directional valve was modelled. Due to the non-linear characteristics, the approach had to be split up into a static and a dynamic valve model. To simulate the non-linear dynamic behavior, a second order model with velocity and acceleration saturation was used. All parameters contained in the Simulink model were variable to be able to manipulate them with Matlab's optimization function *fminsearch.* Doing so, the optimization function tries to find the best possible model parameters to minimize the error between the measured data

points given from the frequency response curves and the Simulink model. For that to realize, the non-linear model had to be simulated for several excitation frequencies. Thereby the saturation blocks cause harmonics. For that reason a filter function was developed in Matlab to exclude those. Furthermore, functions for finding intersections, determining zero-matrixes and computing the amplitude and phase shift were developed as well to create simulated frequency response curves in order to compare simulation with reality. A proper functionality of those functions was shown for an optimization of a linear second order Simulink model. Also the optimization for the non-linear hydraulic valve KBSDG4V-3 led to good results when compared to [17]. Nevertheless, the optimization for the Bosch valve 4WRSE-10 showed big deviations for the amplitude response of 10% and 25% of maximum spool stroke. This is reasoned by the Simulink model which has to be adjusted more properly to the frequency response curves of the 4WRSE-10 valve.

For the static model, pressure, flow and leakage gain as well as supply and nominal pressure had to be determined from the valve's datasheet. Thus it was possible to solve several non-linear equations for values which describe the behavior of positive and negative pseudo-section functions. These functions can be understood as conductance values which gives information about the flow rate through the valve at a certain normalized spool position. It has shown how the gain parameters can be obtained from the datasheet and how the final characteristics look like.

The methodologies and developed models were subsequently tested with manufacturer's data. The good quality of results seems to support the adopted approach.

10 Recommendations for Future Work

To pursue this work in the future, several tasks have to be complied. As it is mentioned in the previous chapter, the hydraulic cylinder's friction force model is based on assumptions which needed to be made. With this data the friction force model has to be adapted better on the real behavior. It can be achieved by changing the certain parameters such as decay constant T_V. It is necessary to mention that extending and retracting characteristic is not equal most likely.

As long as there is no measurement data available for the PRV, static characteristic shall be used.

The Simulink model for obtaining the dynamic behavior of the proportional directional valve needs to be adapted better to the curves in the datasheet. Therefore [17] provides approaches which can be useful for further considerations. Also the time constant needs to be optimized to determine the phase shift. Finally, the different models have to be connected to each other.

It will be also important in the future to validate the model the built model by comparison with a real hydraulic circuit.

11 Reference List

[1] J. Lunze, Regelungstechnik 1: Systemtheoretische Grundlagen, Analyse und Entwurf einschleifiger Regelungen, Springer, 2008.

[2] W. Dieter and G. Norbert, Hydraulik - Grundlagen, Komponenten, Systeme, vol. 6, Berlin-Heidelberg: Springer Verlag, 2015.

[3] H. Watter, Hydraulik und Pneumatik, Grundlagen und Übungen - Anwendungen und Simulation, vol. 4, Wiesbaden: Springer Vieweg, 2015.

[4] D. Will, H. Ströhl und N. Gebhardt, Hydraulik - Grundlagen, Komponenten, Schaltungen, Berlin: Springer, 1999.

[5] "Bosch Rexroth Web Page," Bosch Rexroth, [Online]. Available: https://dc-us.resource.bosch.com/media/us/products_13/product_groups_1/industrial_hydraulics_5/pdfs_4/re29067.pdf. [Accessed 15 July 2016].

[6] "National Instruments Web Page," National Instruments, [Online]. Available: http://www.ni.com/white-paper/3638/en/. [Accessed 10 July 2016].

[7] J. Dankert und H. Dankert, Technische Mechanik, Wiesbaden: Vieweg+Teubner, 2009.

[8] "University of Koblenz," [Online]. Available: https://www.uni-koblenz.de/~physik/informatik/DSV/Faltung.pdf. [Accessed 28 06 2016].

[9] "Stack Exchange," [Online]. Available: http://i.stack.imgur.com/Ofkna.png. [Accessed 23 06 2016].

[10] M. Werner, Digitale Signalverarbeitung mit Matlab, 4. ed., Wiesbaden: Vieweg+Teubner, 2009.

[11] "Cartechnik Hydrauliköle," ATR, [Online]. Available: http://www.atr.de/fileadmin/downloads/Cartechnic/Produktinfos/LM_PB_Hydraulikoel_HLP_46.pdf. [Accessed 02 07 2016].

[12] T. Pinheiro, "Conceção e pré-dimensionamento de um sistema de frenagem para um Tuned Mass Damper," Porto, 2014.

[13] P. Beater, Entwurf hydraulischer Maschinen, Berlin Heidelberg: Springer, 1999.

[14] "Homepage Bosch Rexroth," [Online]. Available: https://www.boschrexroth.com/various/utilities/mediadirectory/index.jsp?publication=NET&ccat_id=20000&remindCcat=on&pagesize=50&search_action=submit&language=de&search_query=25402&MEDIA_TYPE=Datenblatt&History=p545161&DisplayType=

pict. [Accessed 15 July 2016].

[15] "Coefficient Summary," [Online]. Available: http://www.schweizer-fn.de/stoff/reibwerte/reibwerte.php. [Accessed 28 07 2016].

[16] B. Bestmann, "Entwicklung eines Simulationsmodells für eine hydraulische Positioniervorrichtung," Hamburg University of Applied Sciences, 2005.

[17] J. A. Ferreira, F. Gomes de Almeida and M. R. Quintas, "Semi-empirical model for a hydraulic servo-solenoid valve," IMechE, 2002.

[18] "Mathworks," [Online]. Available: http://www.mathworks.com/help/matlab/ref/fminsearch.html. [Accessed 03 08 2016].

[19] J. A. F. Ferreira, "Modelacao de Sistemas Hydraulicos para Simulacao com HArdware-in-the-Loop," 2002.

[20] "MIT Official Home Page," [Online]. Available: http://ocw.mit.edu/courses/mechanical-engineering/2-003-modeling-dynamics-and-control-i-spring-2005/labs/lab3fig3.gif. [Accessed 20 June 2016].

[21] N. Hanson. [Online]. Available: http://www.cmafh.com/enewsletter/PDFs/Hydraulic_Proportional_Closed_Loop_System_Design.pdf. [Accessed 10 July 2016].

12 Appendix

12.1 Pipe Model

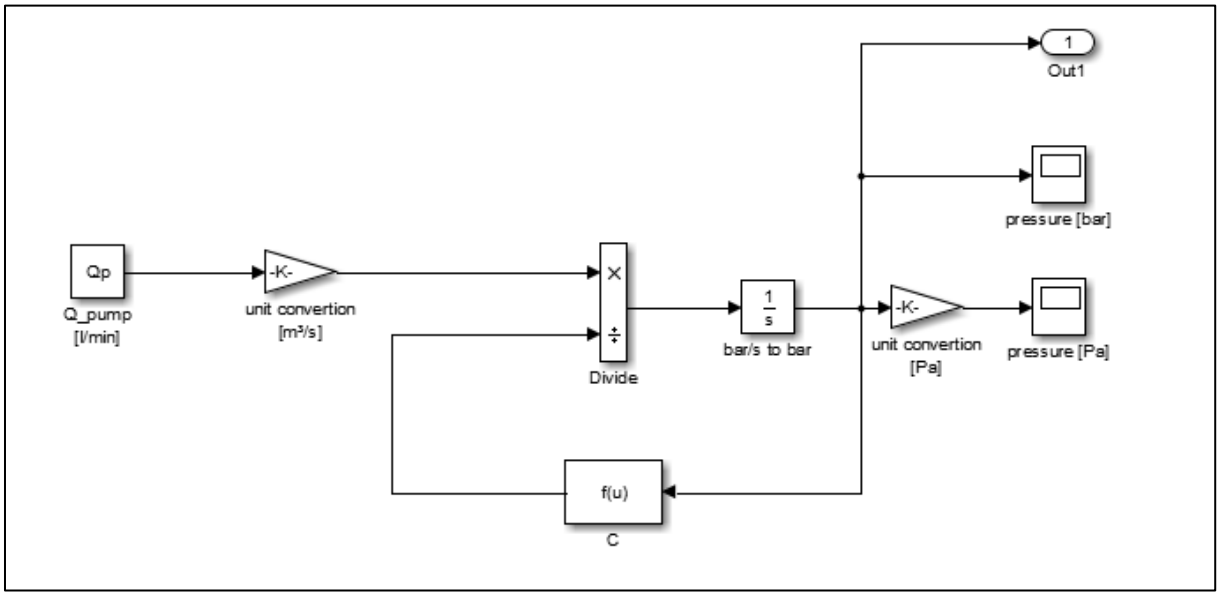

Figure 12:1 Pipe Model

12.2 Subsystems of Cylinder Model

▪ Velocity Saturation

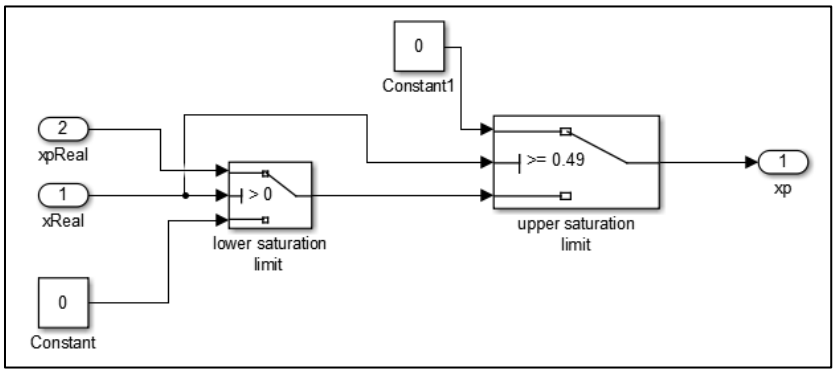

▪ Capacity C_1

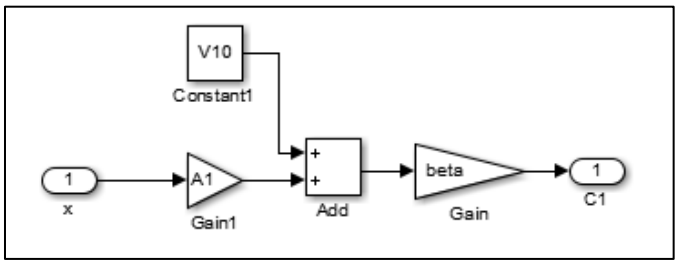

▪ Capacity C_2

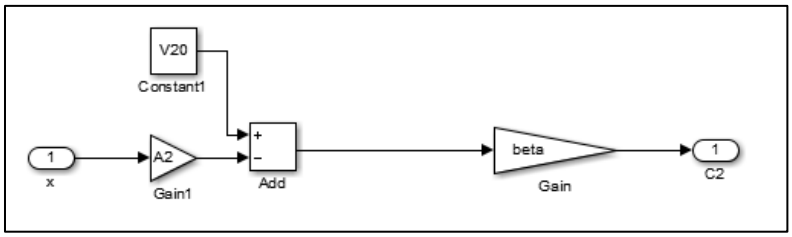

▪ Pressure p_1

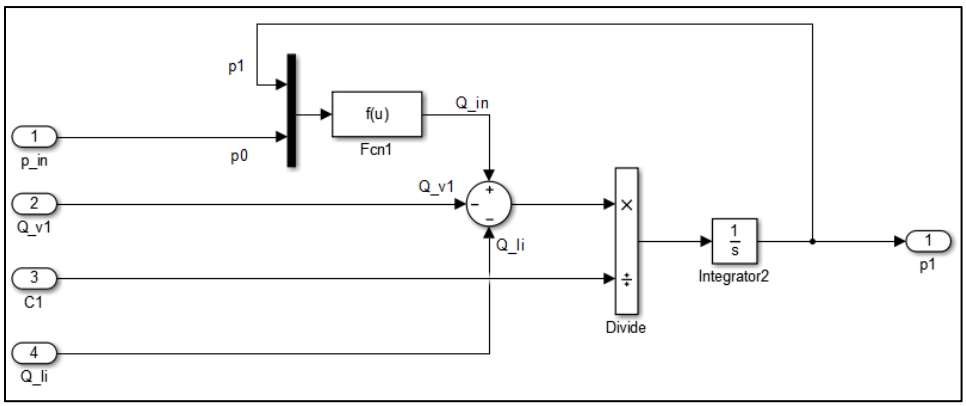

▪ Pressure p_2

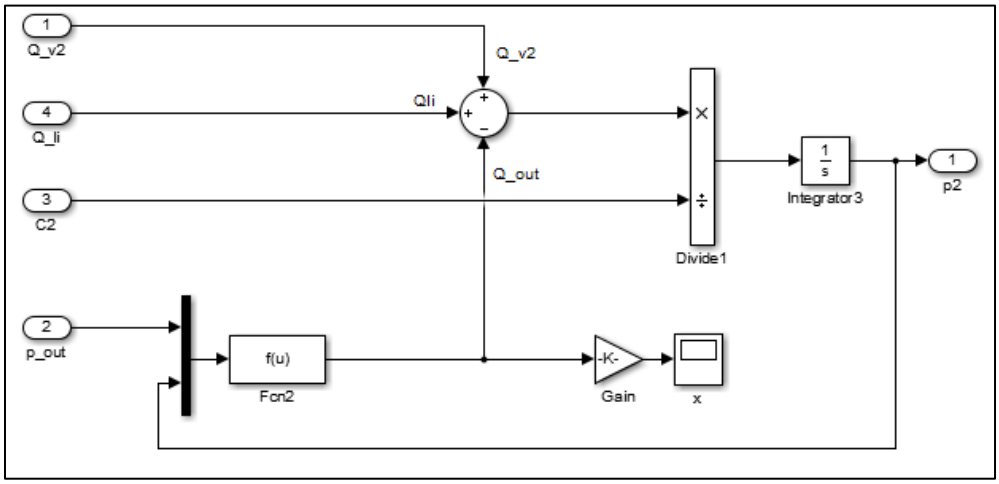
1
Q_v2
Q_v2
4
Q_li
Qli
Q_out
3
C2
Divide1
Integrator3
1
p2
2
p_out
f(u)
Fcn2
-K-
Gain
x

12.3 Initializing Data for PRV

```
%% Initialisierungsdatei DBV
clear all
close all
clc

% oil parameters
eta = 0.12; % Pa*s -> dynamische Viskosität
roh = 880;
K   = 1.4*10^4; % Kompressionsmodul Hydrauliköl
beta= 1/K;

% pipe and pump
Qp1= 15/60000;
Qp2= 35/60000;
Qp3= 60/60000;
dP = 16/1000;
lP = 1*1000/1000;
VP = pi/4*dP^2*lP;
CP = 1/(VP*beta);

% Spool dimensions
dS  = 8/1000;
dS2 = 5/1000;
AS  = pi/4*dS^2;
dHK = 10/1000;  % diameter of hemisphere
mS = 0.04;      % 40g
lC = 5/1000;
yy    = (dHK-dS2)/2;
phi   = atand(yy/lC);
epsilon = 45;

% volume chamber V2
V2 = 4*(pi/4)*dS^2;

% Leakage in spool gap
h  = 0.0001;
dm = dS+h;
lk = 10/1000;
Ggap = (pi*dm*h^3)/(12*eta*lk);

% Spring force parameters
pOpen = 200*10^5;
c     = 100000;
xInit = AS*pOpen/c;

% friction force parameters
g = 9.81;
m = 0.2;
mueG = 0.05;
mueH = 0.12;
FG   = m*g*mueG;
FH   = m*g*mueH;
Tv   = 0.1;
k = 0.1;

% flow force
alpha = 0.9;
K     = alpha*sqrt(2/roh);
```

12.4 Simulink Model of Pressure Relief Valve

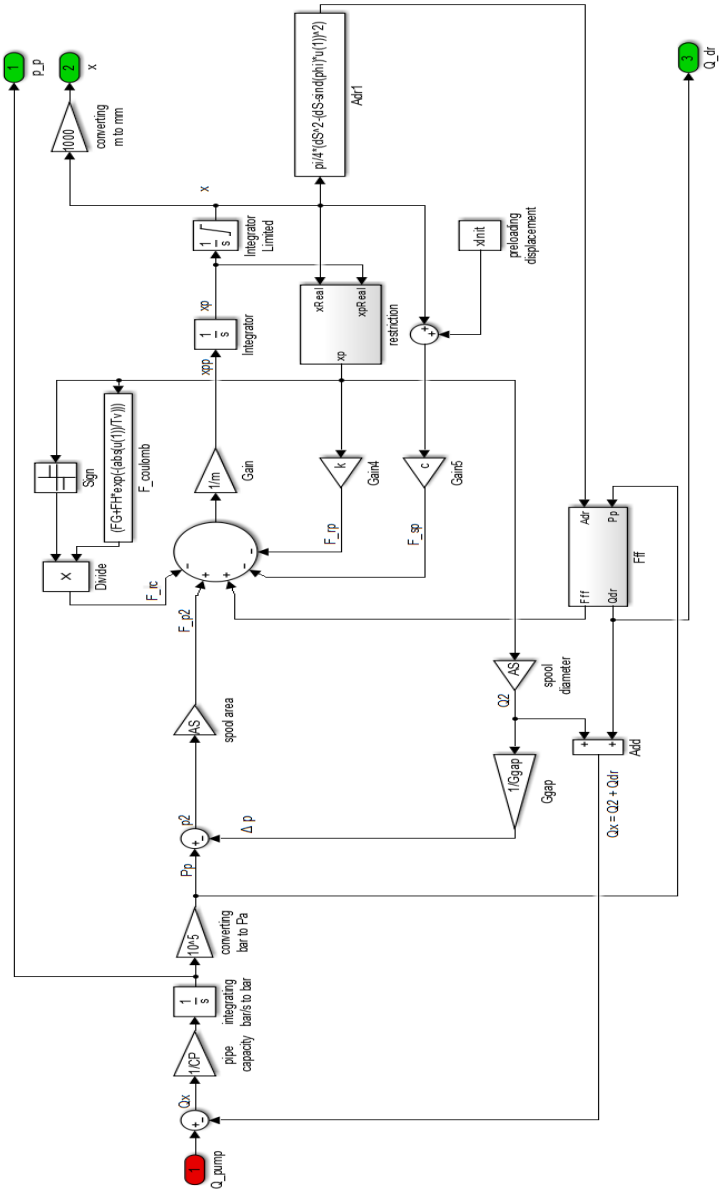

12.5 Measured Amplitude and Phase Data Points for 4WRSE-10

Frequency [Hz]	ϕ at 10% [dB]	ϕ at 25% [dB]	ϕ at 100% [dB]	A at 10% [dB]	A at 25% [dB]	A at 100% [dB]
1,5	0	0	0	0	0	0
2	-4	-4	-4,5	0	0	0
3	-6	-6	-6,3	0	0	0
4	-7	-7	-8,1	0	0	0
5	-7,5	-7,5	-9	0	0	0
6	-7,6	-7,6	-9,9	0	0	0
7	-7,9	-7,9	-9,9	0	0	0
8	-8,3	-8,3	-10,8	0	0	0
9	-8,6	-8,6	-11,7	0	0	-0,5
10	-9	-9	-12	0	0	-0,9
15	-14,5	-14,5	-31,5	0	0	-2
20	-20,7	-23,4	-54	0	0	-4
25	-26,1	-27,9	-63	0	-0,5	-5,5
30	-36	-36	-82	0	-1	-7,5
40	-44,1	-45,9	-103,5	-1	-1,5	-10
50	-54	-62,1	-124,2	-1,3	-2	-12,5
60	-67,5	-76,5	-139,5	-1,7	-3,5	-14,5
70	-76,5	-94,5	-148,5	-2	-5,5	-16,5
80	-90	-119,7	-162	-2,5	-6,8	-19,5
90	-112,5	-148,5	-175,5	-3	-8,5	-22
100	-139,5	-157,5	-184,5	-4,5	-10,5	-24
110	-171	-184,5	-193,5	-7	-14,5	-27,5
120	-184,5	-193,5	-202,5	-9,5	-15,5	-28,5
130	-198	-207	-211,5	-13	-20	-31
140	-207	-216	-216	-15	-22,8	-
150	-211,5	-220,5	-220,5	-17	-25	-
160	-216	-225	-225	-20	-28	-
170	-220,5	-229,5	-229,5	-22,5	-30	-
180	-225	-231,3	-234	-25,5	-	-
190	-225,5	-233	-238,5	-26,7	-	-
200	-226,5	-234	-243	-28	-	-

12.6 Measured Amplitude Data Points for KBSDG4V-3 Valve

Frequency [Hz]	A at 5% [dB]	A at 25% [dB]	A at 50% [dB]
1	0	0	0
2	0	0	0
3	0	0	0
4	0	0	0
5	0	0	0
6	0	0	0
7	0	0	0
8	0	0	0
9	0	0	0
10	0	0	0
20	0	0	0
30	0	0	0
40	0,7	0,9	0,9
50	1	1,1	0
60	1,1	1	-1
70	1,45	0,9	-2,2
80	1,5	-0,1	-3,2
90	1,5	-1,1	-4,5
100	1,6	-1,9	-5,5
110	1,55	-2,7	-7
130	1,1	-4,6	-9,5
150	0	-7	-13,2
170	-1,5	-9,5	-16
200	-2,9	-12,8	-19
300	-10,5	-22,9	-29,5

12.7 Simulink Model of Proportional Valve